WEST WIND LABORATORY, INC

WIND STUDY
GOLDEN GATE BRIDGE

for

HNTB

Job No. 13-03

10 June 2013

by

Jon D. Raggett, PhD, PE
President, West Wind Laboratory, Inc.

TABLE OF CONTENTS

CHAPTER A
INTRODUCTION AND OBJECTIVES

The subject of this wind study is the Golden Gate Bridge, in San Francisco, California. The bridge is a suspension bridge with span lengths of 343 m (1125.41 ft), 1280 m (4200 ft), and 343 m (1125.1 ft). The deck is a steel truss stiffened deck, with the roadway on top of the trusses, 27.43 m (90 ft) wide and 7.62 m (25 ft) deep. The plan and elevation are shown on Figure A.1.

One objective of this wind study was to determine the critical flutter wind speeds on the bridge with the proposed suicide deterrent system netting (SDS), and the proposed aerodynamic enhancements on the west side of the main span. The proposed SDS is shown on Figures A.2 and A.3. The proposed aerodynamic enhancements on the west side of the main span are shown on Figure A.4. The need for aerodynamic enhancements is described in References 5, 6, and 7. In those studies, it was determined that the modified bridge should remain stable for a 10-minute averaged, wind speed with a mean return period of 10,000 years. It was determined that, at the bridge deck elevation of 70.87 m (232.5 ft), the 10,000 year wind speeds were 44.7 m/s (100 mph) for winds from the West, and 29.06 m/s (65 mph) for winds from the East. The existing bridge, unmodified, has a critical flutter wind speed of 31 m/s (69.34 mph). The results of those stability analyses are presented in Chapter B..

A second objective of this wind study was to determine the number of wind induced oscillations of the SDS support structures, at various stress amplitudes, over the life of the structure. Vertical fluctuating wind loads on the windward side of the bridge were determined theoretically from an analytical model of the vertical fluctuations in the wind, and were determined experimentally using the large-scale section model in the wind tunnel. These results are to be used by the design engineers HNTB in a fatigue analysis of the SDS supports.

The time dependent aerodynamic loading on an oscillating large scale section model was obtained experimentally in the wind tunnel. At the large scale of the section model (1:50), fine geometric details, that have been shown to be very important, were reproduced with accuracy. The time dependent aerodynamic loading on the bridge deck section was characterized by a series of flutter derivatives and static aerodynamic coefficients (Ref 1). The aerodynamic loads that contribute towards an aerodynamic instability of the entire bridge consisted primarily of the aerodynamic loads on the bridge deck. Again, these were readily obtained from the section model tests.

Required to determine the bridge stability are the aerodynamic load characteristics of the bridge (from section model tests), a description of the aerodynamic turbulence, and a description of the mechanical dynamic properties of the bridge.

The aerodynamic turbulence field is best described analytically (which can include low frequency components, not readily generated in a wind tunnel). The horizontal and vertical turbulence fields can be described by spectra (Ref 1), or can be described by a series of wind speed time histories (horizontal and vertical) at a number of nodes along the length of the bridge (Ref 2) that conform to those spectra.

The dynamic properties of the bridge mechanical model are best described analytically using a very detailed finite element model. Needed for the wind study are the dominant mode shapes and frequencies (provided by DMJM Harris/AECOM for the preliminary design phase of the SDS - Ref 6 and used in this study).

Motions of the bridge in strong winds were simulated numerically by the West Wind Laboratory using the aerodynamic load characteristics of the bridge deck (from the section model studies), the analytically generated wind speed time histories, and the mechanical dynamic properties from the finite element model. The numerical simulation procedure used is similar to that described in Reference 3, with the exception that time dependent aeroelastic flutter derivatives are used in place of the impulse response functions described in Reference 3. Wind speed time histories at 30 nodes on the bridge deck were included in the analysis. Ten of the most significant modes of vibration were included in the numerical simulations for the bridge analysis. Numerical simulations for a duration of 5.33 minutes (with a typical step size of 0.04 seconds) were generated. Bridge stability was evaluated by comparing the modal responses at the end of the simulation to the corresponding modal responses at the beginning of the simulations.

Flutter wind speeds, should they be found, are lower bound estimates for a number of reasons: First, all stability analyses are performed in smooth flow. Typically, turbulence will disrupt the flow around the prismatic deck section, creating a lack of coherence in the aerodynamic loading along the span, which in general forces any aerodynamic instability up to a higher wind speed. It is not the policy of the West Wind Laboratory to rely upon beneficial aerodynamic effects due to turbulence (consistent with the recommendations in Ref 4). Second, winds are assumed to be exactly perpendicular to the axis of the bridge. Destabilizing aerodynamic effects on the deck are generally strongest when they can occur exactly at the same time along the bridge axis, when winds are perpendicular to the deck. And third, the mean wind speed is assumed to be absolutely uniform along the length of the bridge. If these lower bound estimates are greater then the design criteria, the bridge will be stable for realistically varying and turbulent winds.

At the beginning of each simulation, all modes of vibration began with a modal displacement of unity. Each mode was released in the specified wind, and all were allowed to vibrate freely and simultaneously (allowing for any cross coupling should there be an aerodynamic tendency to do so). Dynamic flutter instabilities (single-degree-of-freedom and coupled multi-degree-of-freedom flutter instabilities) were then identified by the ratios of the modal standard deviations at the end of the simulations to the corresponding initial modal standard deviations. If a modal ratio was greater than unity, then that mode was diverging and the bridge was dynamically unstable.

Critical threshold wind speeds used typically are 10-minute averaged wind speeds (to allow a sufficient time for an instability to develop). Since an instability can lead to a catastrophic failure of the bridge, such instabilities should be avoided at all cost. Should an instability be identified, it should not occur for a wind less than a very extreme event. The wind speed criteria used for this study are presented in Appendix 1.

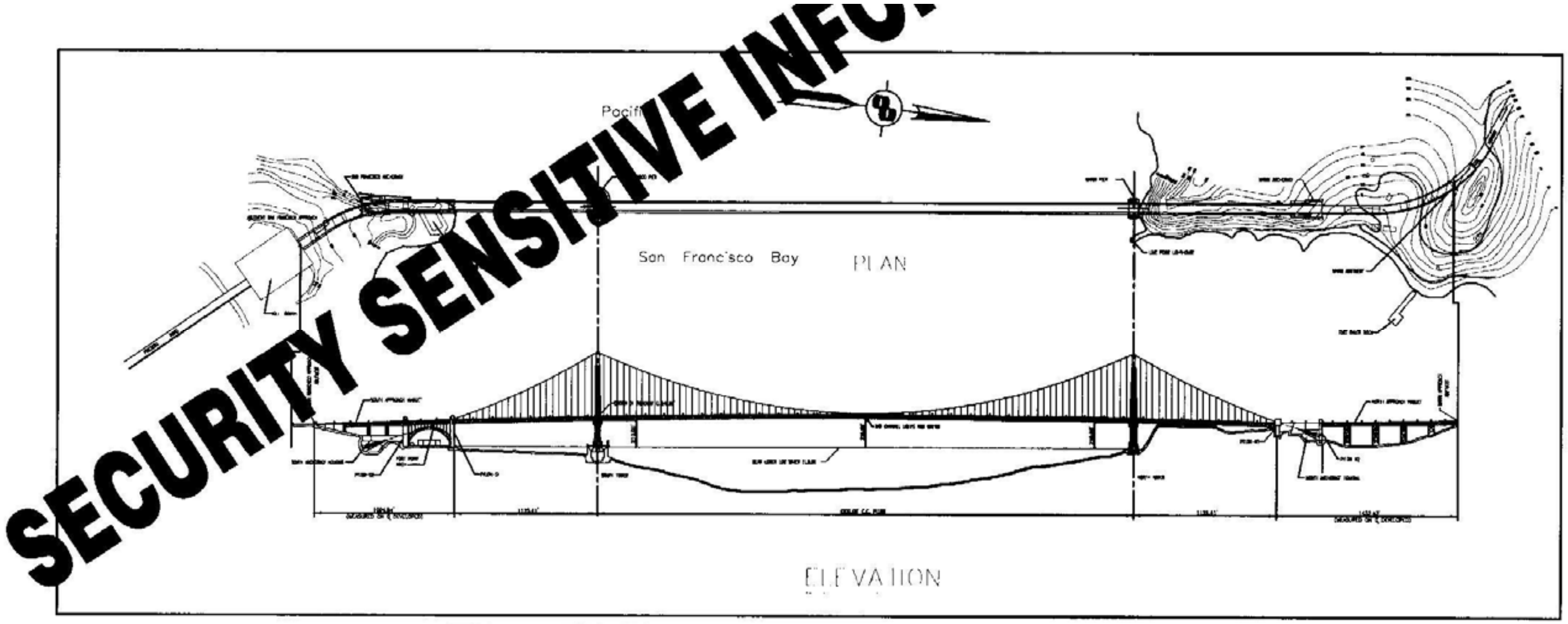

FIGURE A.1

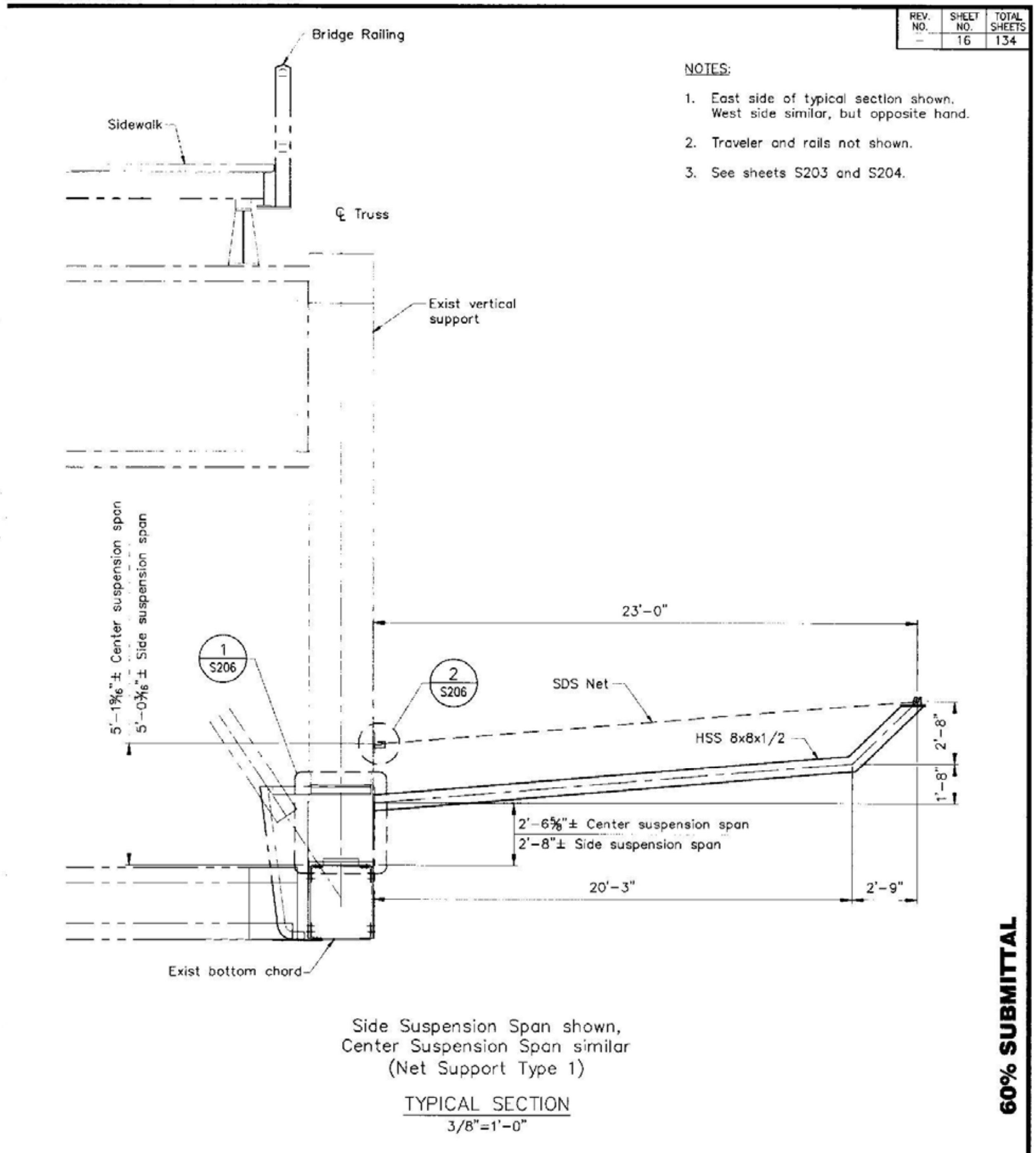
REV. NO. | SHEET NO. | TOTAL SHEETS
– | 16 | 134
NOTES:
1. East side of typical section shown. West side similar, but opposite hand.
2. Traveler and rails not shown.
3. See sheets S203 and S204.
Bridge Railing
Sidewalk
℄ Truss
Exist vertical support
5'-1⁹⁄₁₆"± Center suspension span
5'-0³⁄₁₆"± Side suspension span
23'-0"
1 S206
2 S206
SDS Net
HSS 8x8x1/2
2'-8"
1'-8"
2'-6⅝"± Center suspension span
2'-8"± Side suspension span
20'-3"
2'-9"
Exist bottom chord
Side Suspension Span shown,
Center Suspension Span similar
(Net Support Type 1)
TYPICAL SECTION
3/8"=1'-0"
60% SUBMITTAL

FIGURE A.2

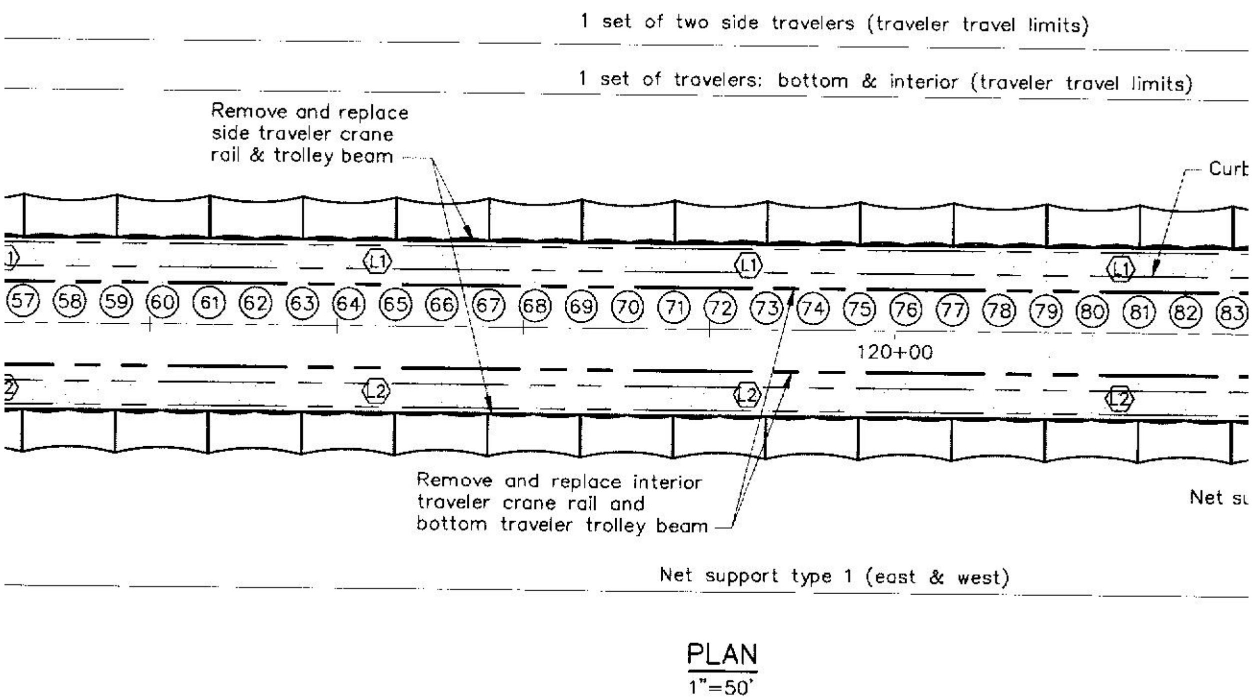
1 set of two side travelers (traveler travel limits)
1 set of travelers: bottom & interior (traveler travel limits)
Remove and replace side traveler crane rail & trolley beam
Curb
L1
57 58 59 60 61 62 63 64 65 66 67 68 69 70 71 72 73 74 75 76 77 78 79 80 81 82 83
120+00
L2
Remove and replace interior traveler crane rail and bottom traveler trolley beam
Net su
Net support type 1 (east & west)
PLAN
1"=50'

FIGURE A.3

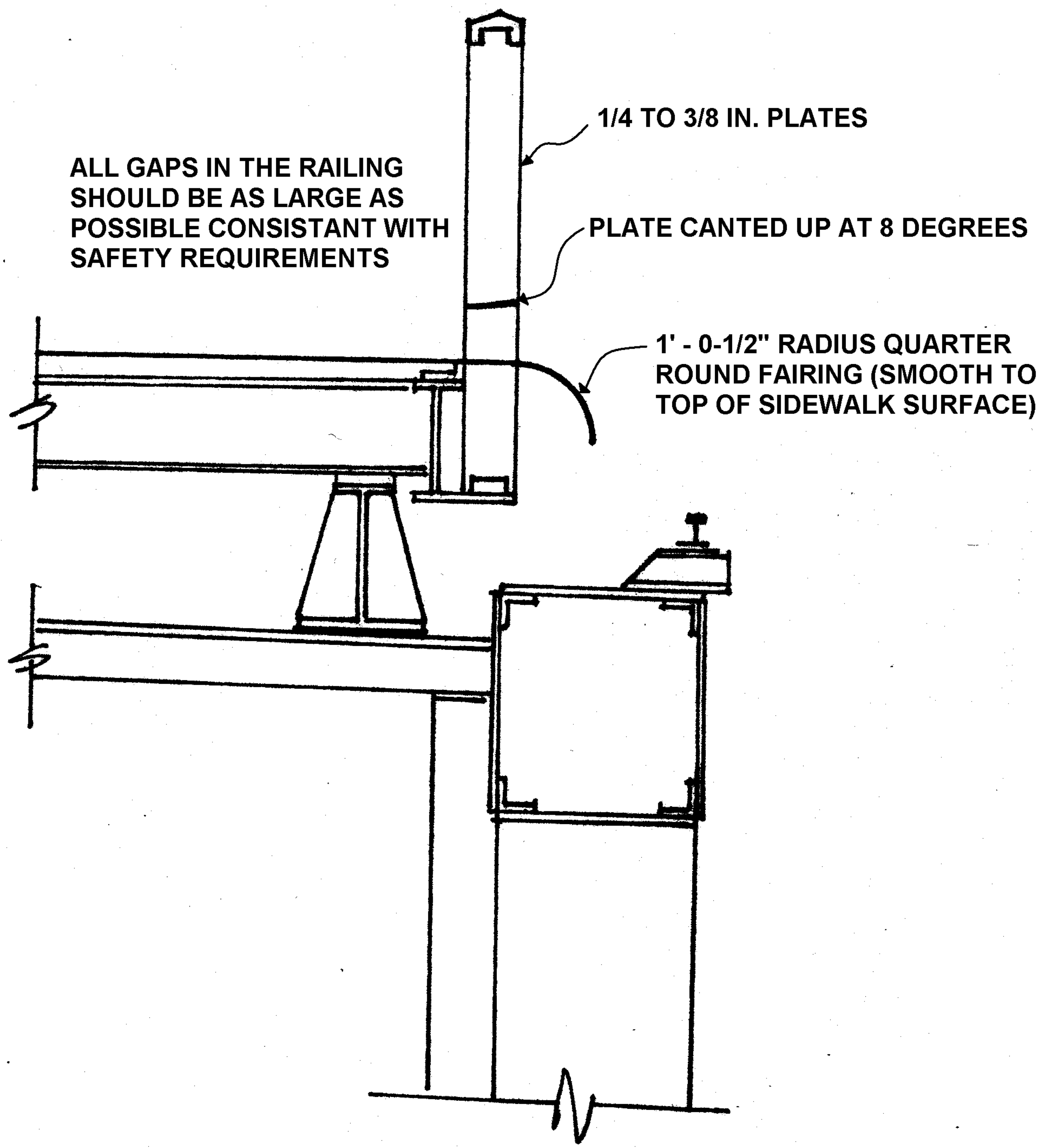
1/4 TO 3/8 IN. PLATES
ALL GAPS IN THE RAILING SHOULD BE AS LARGE AS POSSIBLE CONSISTANT WITH SAFETY REQUIREMENTS
PLATE CANTED UP AT 8 DEGREES
1' - 0-1/2" RADIUS QUARTER ROUND FAIRING (SMOOTH TO TOP OF SIDEWALK SURFACE)

FIGURE A.4

CHAPTER B
STABILITY ANALYSES
BRIDGE WITH SDS AND AERODYNAMIC ENHANCEMENTS

Stability analyses were performed for the existing bridge configuration which is defined specifically in Appendix 7. Aerodynamic stability analyses were performed for eight cases. Those cases are defined in Table B.1.

CASE	FAIRINGS	SDS	ANGLE OF INCIDENCE (DEGREES)
10	WINDWARD	NO	0
20	LEEWARD	NO	0
30	WINDWARD	YES	0
40	WINDWARD	YES	-3
50	WINDWARD	YES	+3
60	LEEWARD	YES	0
70	LEEWARD	YES	-3
80	LEEWARD	YES	+3

TABLE B.1 - CASES STUDIED

Cases 10 and 20 are the bases, without the SDS, to be used for comparison, and to be used to evaluate specifically the effect of the SDS on the aerodynamic stability of the GGB,

Flutter wind speeds, should they be found, are lower bound estimates for a number of reasons: The stability of the bridge is evaluated primarily from the smooth flow results. Typically, turbulence will disrupt the flow around the prismatic deck section, creating a lack of coherence in the aerodynamic loading along the span, which in general forces any aerodynamic instability up to a higher wind speed. It is not the policy of the West Wind Laboratory to rely upon beneficial aerodynamic effects due to turbulence (consistent with the recommendations in Ref 4). Second, winds are assumed to be exactly perpendicular to the axis of the bridge. Destabilizing aerodynamic effects on the deck are generally strongest when they can occur exactly at the same time along the bridge axis, when winds are perpendicular to the deck. And third, the mean wind speed is assumed to be absolutely uniform along the length of the bridge. If these lower bound estimates are greater than the design criteria, the bridge will be stable for realistically varying and turbulent winds.

At the beginning of each simulation, all modes of vibration began with a modal displacement of unity. Each mode was released in the specified wind, and all were allowed to vibrate freely and simultaneously (allowing for any cross coupling should there be an aerodynamic tendency to do so). Dynamic flutter instabilities (single-degree-of-freedom and coupled multi-degree-of-freedom flutter instabilities) were then identified by the ratios of the modal standard deviations at the end of the simulations to the corresponding initial modal standard deviations. If a modal ratio was greater than unity, then that mode was diverging and the bridge was dynamically unstable. The modal ratios are shown in Tables B.3 through B. 10 for Cases 10 through 80 respectively.

Another form of an aeroelastic instability is static divergence (at a specified wind speed the bridge deforms without bound, but without oscillations). Final modal deformations at various wind speed are presented in Tables B.11 through B.18 for Cases 10 through 80 respectively. While some Mode 1 (sway) responses are very large at the end of the numerical simulations, those motions are expected and do not represent a static divergence. No static divergence instabilities were identified for any mode of vibration for any of the eight cases studied.

Critical threshold wind speeds used typically are 10-minute averaged wind speeds (to allow a sufficient time for an instability to develop). Since an instability can lead to a catastrophic failure of the bridge, such instabilities should be avoided at all cost. Should an instability be identified, it should not occur for a wind less than a very extreme event. A wind speed with a return period of at least 10,000 years was used as critical flutter threshold wind speed for the final configuration.

In Appendix 1 the maximum 10-minute averaged wind speed, at the site, at the bridge deck elevation of 70.87 m (232.5 ft) , with a return period of 10,000 years, was determined to be 44.7 m/s (100 mph) for winds from the West, and 29.50 m/s (66 mph) for winds from the East, for horizontal winds. Wind speeds for non-horizontal winds are less likely to occur. It is standard practice to use reduced critical flutter wind speed thresholds for non-horizontal winds. For mean wind angles of incidence of plus or minus 3 degrees, critical flutter wind speeds equal to 0.75 of the corresponding 0 degree angle of incidence values typically were used. For mean wind angles of incidence of plus or minus 3 degrees, the corresponding critical flutter wind speed thresholds, UTH, are 33.53 m/s (75 mph) for winds from the West, and 22.13 m/s (49.50 mph) for winds from the East.

Stability analyses were performed for mean wind speeds up to 55 m/s (123.03 mph). No instabilities were identified up to this wind speed for Case 30 (fairing to windward - West wind - with the SDS). For all other cases, a torsional instability did occur (Mode 7) for wind speeds less than 55 m/s (123.03 mph). Critical flutter wind speeds, UCR, identified (from Tables B.3 through B.10) are summarized in Table B.2.

CASE	ANGLE	UCR(m/s)	UTH(m/s)	UCR(mph)	UTH(mph)
10	0	49.3	44.7	110.3	100
20	0	31.0	29.5	69.3	66
30	0	>55.0	44.7	>123	100
40	-3	42.0	33.5	94.0	75
50	+3	47.0	33.5	105.1	75
60	0	31.7	29.5	70.9	66
70	-3	27.5	22.1	61.5	49.5
80	+3	31.2	22.1	69.8	49.5

TABLE B.2 - CRITICAL FLUTTER WIND SPEEDS

Note that all cases studied meet the critical wind speed criteria. For winds from the West, the winds will have a mean angle of incidence of approximately -7 degrees, over the Marin Headlands, on the North side-span. The fundamental torsional mode of vibration (Mode 7), has no significant torsional component in Mode 7 (see Appendix 7), and therefore, there will be no contribution to the aerodynamic generalized moment for Mode 7 from winds on the North side-span (or similarly from the South side-span). For a steady horizontal wind from the West, there will be a slight static rotation of the bridge deck in a positive sense. For a positive angle of incidence, for winds from the West (Case 50), the critical flutter wind speed of 47 m/s (105.1 mph) exceeds the critical flutter wind speed threshold of 44.7 m/s (100 mph) for horizontal winds. Neither the non-horizontal wind flows over the Marin Headlands, or the static rotation of the bridge deck in horizontal winds, will not cause a critical case for winds from the West. It should also be noted that the SDS has a beneficial effect on the aerodynamic stability of the GGB.

GG10 4/26/13

RATIO OF FINAL MODAL STANDARD DEVIATION RESPONSES TO
INITIAL MODAL STANDARD DEVIATION RESPONSES

LENGTH OF RECORD (SEC) 320

WWL MODE	DMJM MODE	U(M/S) - TEN MINUTE AVERAGED WIND SPEED AT DECK 25.0	30.0	35.0	40.0	45.0	50.0	55.0
1	1	0.190	0.149	0.116	0.091	0.071	0.056	0.044
2	2	0.018	0.024	0.032	0.048	0.112	0.237	0.631
3	3	0.073	0.055	0.042	0.031	0.024	0.020	0.025
4	4	0.021	0.043	0.074	0.135	0.237	0.549	0.980
5	5	0.042	0.031	0.040	0.054	0.142	0.319	0.933
6	6	0.008	0.017	0.032	0.068	0.147	0.469	1.078
7	7	0.100	0.128	0.231	0.350	0.643	1.124	2.419
8	8	0.071	0.101	0.131	0.217	0.330	0.735	1.276
9	9	0.001	0.002	0.004	0.008	0.017	0.031	0.075
10	10	0.034	0.049	0.068	0.115	0.192	0.496	0.960

TABLE B.3

GG20 4/26/13

RATIO OF FINAL MODAL STANDARD DEVIATION RESPONSES TO
INITIAL MODAL STANDARD DEVIATION RESPONSES

LENGTH OF RECORD (SEC) 320

WWL	DMJM	U(M/S) - TEN MINUTE AVERAGED WIND SPEED AT DECK						
MODE	MODE	25.0	30.0	35.0	40.0	45.0	50.0	55.0
1	1	0.190	0.149	0.116	0.091	0.071	0.057	0.049
2	2	0.025	0.081	0.273	0.744	1.759	4.051	9.400
3	3	0.073	0.055	0.042	0.039	0.059	0.117	0.253
4	4	0.038	0.174	0.611	1.451	2.718	5.842	13.037
5	5	0.032	0.082	0.288	0.802	2.098	5.339	13.918
6	6	0.014	0.066	0.260	0.766	1.992	5.443	15.189
7	7	0.248	0.822	2.134	4.616	8.484	15.567	29.672
8	8	0.140	0.367	1.010	2.106	3.914	7.797	16.583
9	9	0.003	0.014	0.047	0.139	0.311	0.666	1.542
10	10	0.041	0.151	0.470	1.038	2.015	4.655	11.266

TABLE B.4

GG30 4/26/13

RATIO OF FINAL MODAL STANDARD DEVIATION RESPONSES TO
INITIAL MODAL STANDARD DEVIATION RESPONSES

LENGTH OF RECORD (SEC) 320

WWL	DMJM	U(M/S) - TEN MINUTE AVERAGED WIND SPEED AT DECK						
MODE	MODE	25.0	30.0	35.0	40.0	45.0	50.0	55.0
1	1	0.190	0.149	0.116	0.091	0.071	0.056	0.044
2	2	0.017	0.022	0.033	0.035	0.047	0.102	0.164
3	3	0.073	0.055	0.042	0.031	0.023	0.018	0.014
4	4	0.022	0.026	0.057	0.138	0.124	0.230	0.410
5	5	0.041	0.031	0.038	0.038	0.057	0.135	0.246
6	6	0.008	0.010	0.025	0.072	0.076	0.185	0.436
7	7	0.088	0.097	0.206	0.234	0.260	0.502	0.648
8	8	0.077	0.057	0.098	0.221	0.163	0.292	0.528
9	9	0.001	0.001	0.003	0.005	0.007	0.014	0.019
10	10	0.031	0.035	0.048	0.121	0.103	0.206	0.399

TABLE B.5

GG40 4/26/13

RATIO OF FINAL MODAL STANDARD DEVIATION RESPONSES TO
INITIAL MODAL STANDARD DEVIATION RESPONSES

LENGTH OF RECORD (SEC) 320

WWL	DMJM	U(M/S) - TEN MINUTE AVERAGED WIND SPEED AT DECK						
MODE	MODE	25.0	30.0	35.0	40.0	45.0	50.0	55.0
1	1	0.190	0.149	0.116	0.091	0.071	0.056	0.044
2	2	0.029	0.032	0.043	0.100	0.367	0.642	0.800
3	3	0.073	0.055	0.042	0.031	0.027	0.029	0.030
4	4	0.048	0.106	0.158	0.234	0.639	1.692	2.686
5	5	0.046	0.047	0.052	0.114	0.458	0.859	1.183
6	6	0.018	0.043	0.072	0.125	0.456	1.618	3.146
7	7	0.226	0.316	0.355	0.644	1.986	2.845	2.911
8	8	0.132	0.220	0.267	0.344	0.870	2.209	3.352
9	9	0.003	0.005	0.007	0.015	0.049	0.086	0.096
10	10	0.061	0.105	0.135	0.183	0.535	1.535	2.539

TABLE B.6

GG50 4/26/13

RATIO OF FINAL MODAL STANDARD DEVIATION RESPONSES TO
INITIAL MODAL STANDARD DEVIATION RESPONSES

LENGTH OF RECORD (SEC) 320

WWL	DMJM	U(M/S) - TEN MINUTE AVERAGED WIND SPEED AT DECK						
MODE	MODE	25.0	30.0	35.0	40.0	45.0	50.0	55.0
1	1	0.190	0.149	0.116	0.091	0.071	0.056	0.045
2	2	0.017	0.019	0.057	0.128	0.141	0.925	5.390
3	3	0.073	0.055	0.042	0.032	0.024	0.034	0.163
4	4	0.024	0.045	0.119	0.305	0.301	0.789	5.046
5	5	0.038	0.033	0.062	0.143	0.166	1.325	8.701
6	6	0.009	0.018	0.053	0.154	0.196	0.670	5.608
7	7	0.108	0.194	0.442	0.783	0.706	3.783	17.967
8	8	0.091	0.117	0.216	0.477	0.417	1.044	6.395
9	9	0.001	0.003	0.009	0.020	0.020	0.129	0.727
10	10	0.032	0.057	0.110	0.262	0.240	0.689	4.710

TABLE B.7

GG60   4/26/13

RATIO OF FINAL MODAL STANDARD DEVIATION RESPONSES TO
INITIAL MODAL STANDARD DEVIATION RESPONSES

LENGTH OF RECORD (SEC) 320

WWL MODE	DMJM MODE	U(M/S) - TEN MINUTE AVERAGED WIND SPEED AT DECK 25.0	30.0	35.0	40.0	45.0	50.0	55.0
1	1	0.190	0.149	0.116	0.091	0.073	0.072	0.098
2	2	0.026	0.066	0.360	1.561	4.627	11.991	28.610
3	3	0.073	0.055	0.044	0.060	0.144	0.339	0.800
4	4	0.051	0.142	0.705	2.618	9.678	24.258	50.998
5	5	0.033	0.068	0.396	1.788	6.043	17.926	50.854
6	6	0.019	0.055	0.312	1.589	8.301	26.161	69.700
7	7	0.280	0.665	2.735	8.851	19.939	41.273	78.430
8	8	0.177	0.295	1.128	3.757	13.062	30.009	63.945
9	9	0.003	0.011	0.056	0.234	0.650	1.626	3.593
10	10	0.061	0.134	0.575	2.163	8.518	22.382	52.140

TABLE B.8

GG70 4/29/13

RATIO OF FINAL MODAL STANDARD DEVIATION RESPONSES TO
INITIAL MODAL STANDARD DEVIATION RESPONSES

LENGTH OF RECORD (SEC) 320

WWL	DMJM	U(M/S) - TEN MINUTE AVERAGED WIND SPEED AT DECK						
MODE	MODE	25.0	30.0	35.0	40.0	45.0	50.0	55.0
1	1	0.190	0.149	0.116	0.092	0.074	0.071	0.104
2	2	0.043	0.173	0.575	1.679	4.595	12.091	28.701
3	3	0.073	0.056	0.047	0.066	0.143	0.350	0.841
4	4	0.095	0.397	1.613	4.310	10.661	26.434	53.733
5	5	0.046	0.175	0.617	2.005	6.019	18.235	52.609
6	6	0.034	0.152	0.763	2.603	8.772	28.913	76.855
7	7	0.552	1.805	4.360	9.782	19.656	40.649	78.266
8	8	0.274	0.795	2.516	6.125	13.688	32.076	66.078
9	9	0.006	0.027	0.087	0.233	0.549	1.481	3.290
10	10	0.125	0.380	1.332	3.631	9.323	24.817	55.605

TABLE B.9

GG80 4/29/13

RATIO OF FINAL MODAL STANDARD DEVIATION RESPONSES TO
INITIAL MODAL STANDARD DEVIATION RESPONSES

LENGTH OF RECORD (SEC) 320

WWL	DMJM	U(M/S) - TEN MINUTE AVERAGED WIND SPEED AT DECK						
MODE	MODE	25.0	30.0	35.0	40.0	45.0	50.0	55.0
1	1	0.190	0.149	0.116	0.091	0.071	0.058	0.051
2	2	0.027	0.074	0.279	0.635	1.438	3.520	8.795
3	3	0.073	0.055	0.043	0.037	0.050	0.097	0.228
4	4	0.063	0.192	0.577	1.358	3.148	7.029	16.179
5	5	0.041	0.075	0.293	0.742	1.926	5.323	15.308
6	6	0.024	0.075	0.262	0.827	2.530	7.264	20.236
7	7	0.380	0.781	2.091	3.513	6.175	11.794	23.723
8	8	0.221	0.474	0.996	2.070	4.183	8.578	18.852
9	9	0.004	0.013	0.046	0.094	0.208	0.496	1.295
10	10	0.076	0.194	0.484	1.133	2.710	6.379	15.698

TABLE B.10

GG10 4/26/13

CHECK FOR STATIC DIVERGENCE
FINAL AVERAGE MODAL RESPONSES

LENGTH OF RECORD (SEC) 320

WWL	DMJM	U(M/S) - TEN MINUTE AVERAGED WIND SPEED AT DECK						
MODE	MODE	25.0	30.0	35.0	40.0	45.0	50.0	55.0
1	1	-1.379	-2.005	-2.744	-3.599	-4.567	-5.650	-6.847
2	2	-0.002	-0.004	-0.007	-0.002	-0.000	-0.018	0.042
3	3	-0.003	-0.002	-0.001	-0.000	0.000	0.001	0.001
4	4	-0.047	-0.066	-0.086	-0.109	-0.131	-0.152	-0.190
5	5	-0.001	-0.001	0.001	0.003	-0.004	0.016	-0.049
6	6	-0.017	-0.024	-0.033	-0.043	-0.054	-0.067	-0.077
7	7	-0.003	-0.009	0.002	0.012	-0.051	0.077	-0.233
8	8	-0.036	-0.052	-0.066	-0.089	-0.116	-0.141	-0.157
9	9	0.000	0.000	0.000	0.001	-0.000	0.003	-0.004
10	10	0.024	0.035	0.050	0.065	0.080	0.101	0.125

TABLE B.11

GG20 4/26/13

CHECK FOR STATIC DIVERGENCE
FINAL AVERAGE MODAL RESPONSES

LENGTH OF RECORD (SEC) 320

WWL	DMJM	U(M/S) - TEN MINUTE AVERAGED WIND SPEED AT DECK						
MODE	MODE	25.0	30.0	35.0	40.0	45.0	50.0	55.0
1	1	-1.379	-2.005	-2.745	-3.599	-4.568	-5.648	-6.849
2	2	-0.002	0.001	-0.004	0.004	-0.164	0.418	-1.010
3	3	-0.003	-0.002	-0.001	0.000	-0.003	0.007	-0.015
4	4	-0.046	-0.067	-0.092	-0.128	-0.161	-0.073	-0.333
5	5	-0.000	-0.002	-0.008	-0.023	0.009	0.048	-0.211
6	6	-0.017	-0.025	-0.034	-0.045	-0.059	-0.038	-0.131
7	7	0.004	-0.033	-0.123	-0.264	0.025	0.304	-0.972
8	8	-0.037	-0.056	-0.061	-0.065	-0.058	-0.135	-0.172
9	9	0.000	-0.000	-0.001	-0.005	0.006	-0.001	0.004
10	10	0.024	0.033	0.049	0.066	0.089	0.132	0.068

TABLE B.12

GG30 4/26/13

CHECK FOR STATIC DIVERGENCE
FINAL AVERAGE MODAL RESPONSES

LENGTH OF RECORD (SEC) 320

WWL MODE	DMJM MODE	U(M/S) - TEN MINUTE AVERAGED WIND SPEED AT DECK 25.0	30.0	35.0	40.0	45.0	50.0	55.0
1	1	-1.379	-2.005	-2.744	-3.599	-4.567	-5.650	-6.846
2	2	-0.002	-0.004	-0.003	-0.000	-0.010	-0.005	-0.010
3	3	-0.003	-0.002	-0.001	-0.000	0.000	0.001	0.001
4	4	-0.047	-0.066	-0.085	-0.109	-0.130	-0.155	-0.180
5	5	-0.001	-0.000	0.000	0.001	0.001	0.007	-0.008
6	6	-0.017	-0.024	-0.033	-0.043	-0.054	-0.067	-0.078
7	7	-0.003	-0.005	0.000	-0.006	-0.014	0.025	-0.056
8	8	-0.036	-0.050	-0.069	-0.091	-0.114	-0.141	-0.165
9	9	0.000	0.000	0.000	0.001	0.001	0.002	-0.000
10	10	0.024	0.036	0.049	0.064	0.081	0.101	0.123

TABLE B.13

GG40 4/26/13

CHECK FOR STATIC DIVERGENCE
FINAL AVERAGE MODAL RESPONSES

LENGTH OF RECORD (SEC) 320

WWL	DMJM	U(M/S) - TEN MINUTE AVERAGED WIND SPEED AT DECK						
MODE	MODE	25.0	30.0	35.0	40.0	45.0	50.0	55.0
1	1	-1.379	-2.005	-2.744	-3.599	-4.567	-5.650	-6.847
2	2	-0.003	-0.004	-0.005	0.008	-0.036	-0.034	0.052
3	3	-0.003	-0.002	-0.001	-0.000	-0.000	0.000	0.001
4	4	-0.012	-0.015	-0.016	-0.016	-0.021	-0.001	-0.023
5	5	-0.002	-0.002	-0.000	0.001	-0.012	0.043	-0.064
6	6	-0.005	-0.007	-0.008	-0.011	-0.015	-0.018	-0.020
7	7	-0.011	-0.014	0.005	0.008	-0.096	0.230	-0.281
8	8	-0.037	-0.049	-0.065	-0.090	-0.117	-0.149	-0.144
9	9	0.000	-0.000	0.000	0.001	-0.001	0.006	-0.005
10	10	0.023	0.036	0.051	0.064	0.078	0.099	0.129

TABLE B.14

GG50 4/26/13

CHECK FOR STATIC DIVERGENCE
FINAL AVERAGE MODAL RESPONSES

LENGTH OF RECORD (SEC) 320

WWL	DMJM	U(M/S) - TEN MINUTE AVERAGED WIND SPEED AT DECK						
MODE	MODE	25.0	30.0	35.0	40.0	45.0	50.0	55.0
1	1	-1.379	-2.005	-2.744	-3.599	-4.567	-5.650	-6.847
2	2	-0.002	-0.004	-0.005	0.007	0.010	-0.109	0.720
3	3	-0.003	-0.002	-0.001	-0.000	0.000	-0.001	0.007
4	4	-0.082	-0.117	-0.155	-0.200	-0.245	-0.275	-0.472
5	5	-0.000	0.000	0.003	0.005	-0.001	0.057	-0.487
6	6	-0.029	-0.042	-0.056	-0.075	-0.094	-0.116	-0.149
7	7	-0.000	-0.012	0.016	0.020	-0.034	0.269	-1.907
8	8	-0.036	-0.051	-0.065	-0.092	-0.116	-0.141	-0.160
9	9	0.000	0.000	0.001	0.001	0.000	0.009	-0.042
10	10	0.024	0.035	0.051	0.064	0.081	0.103	0.095

TABLE B.15

GG60 4/26/13

CHECK FOR STATIC DIVERGENCE
FINAL AVERAGE MODAL RESPONSES

LENGTH OF RECORD (SEC) 320

WWL	DMJM	U(M/S) - TEN MINUTE AVERAGED WIND SPEED AT DECK						
MODE	MODE	25.0	30.0	35.0	40.0	45.0	50.0	55.0
1	1	-1.379	-2.005	-2.744	-3.598	-4.567	-5.653	-6.946
2	2	-0.001	-0.005	-0.017	0.162	-0.482	-1.079	1.057
3	3	-0.003	-0.002	-0.002	0.003	-0.006	-0.024	0.052
4	4	-0.047	-0.066	-0.079	-0.124	-0.024	-0.235	-0.910
5	5	-0.000	-0.001	0.015	-0.049	0.322	-0.446	1.494
6	6	-0.017	-0.025	-0.031	-0.049	-0.026	-0.019	-1.166
7	7	0.003	-0.033	0.155	-0.416	1.874	-1.529	3.059
8	8	-0.039	-0.051	-0.052	-0.136	0.002	0.338	-1.947
9	9	0.000	-0.000	0.003	-0.009	0.043	0.001	-0.028
10	10	0.023	0.035	0.058	0.041	0.167	0.292	-0.980

TABLE B.16

GG70 4/29/13

CHECK FOR STATIC DIVERGENCE
FINAL AVERAGE MODAL RESPONSES

LENGTH OF RECORD (SEC) 320

WWL	DMJM	U(M/S) - TEN MINUTE AVERAGED WIND SPEED AT DECK						
MODE	MODE	25.0	30.0	35.0	40.0	45.0	50.0	55.0
1	1	-1.379	-2.005	-2.744	-3.599	-4.566	-5.643	-6.937
2	2	-0.003	-0.014	0.021	0.008	0.689	-1.140	3.516
3	3	-0.003	-0.002	-0.001	-0.000	0.012	0.003	-0.014
4	4	-0.012	-0.015	-0.002	-0.056	-0.039	0.405	0.750
5	5	-0.002	-0.004	0.022	-0.096	-0.056	1.237	-3.309
6	6	-0.005	-0.006	-0.005	-0.022	-0.036	0.121	1.126
7	7	-0.030	-0.056	0.261	-0.806	-0.285	4.589	-8.095
8	8	-0.035	-0.036	-0.067	-0.136	-0.252	-0.279	2.887
9	9	-0.000	-0.000	0.004	-0.013	-0.015	0.077	-0.097
10	10	0.024	0.040	0.057	0.028	0.017	0.170	1.852

TABLE B.17

GG80 4/29/13

CHECK FOR STATIC DIVERGENCE
FINAL AVERAGE MODAL RESPONSES

LENGTH OF RECORD (SEC) 320

WWL MODE	DMJM MODE	U(M/S) - TEN MINUTE AVERAGED WIND SPEED AT DECK 25.0	30.0	35.0	40.0	45.0	50.0	55.0
1	1	-1.379	-2.005	-2.744	-3.598	-4.567	-5.650	-6.852
2	2	-0.000	-0.001	-0.025	0.062	-0.104	-0.518	0.969
3	3	-0.003	-0.002	-0.002	0.001	-0.001	-0.007	-0.004
4	4	-0.082	-0.119	-0.157	-0.196	-0.216	-0.251	-0.615
5	5	-0.000	-0.001	0.002	-0.012	0.105	0.016	-0.988
6	6	-0.029	-0.043	-0.056	-0.072	-0.090	-0.075	-0.276
7	7	0.003	-0.039	-0.000	-0.114	0.546	0.093	-2.504
8	8	-0.040	-0.058	-0.050	-0.101	-0.097	-0.000	0.014
9	9	0.000	-0.000	0.001	-0.002	0.013	0.017	-0.038
10	10	0.023	0.032	0.055	0.062	0.098	0.175	0.140

TABLE B.18

CHAPTER C
WIND LOAD INPUT FOR A FATIGUE ANALYSIS OF THE NET STRUTS

Turbulent winds on the windward and leeward sides of the bridge will cause the SDS net to bounce. That bouncing will produce a fluctuating moment in the net support struts, particularly at the attachment plate welds. The objective of this portion of the wind study was to determine the expected number of fluctuating moment cycles, at different moment levels, for a specific period of time (one year). Those performing the fatigue analysis can then determine the total number of cycles expected over the life of the SDS net, at different stress levels, and then using Minor's Rule (or equivalent), determine the likelihood of a fatigue failure occurring.

The distribution of all winds, not just extreme winds, at the GGB site, at the deck elevation, must be known. Windrose information (that provides those distributions, by direction, by month of the year) was obtained from the USDA (Ref 9) for winds at the San Francisco International Airport (SFO) and is shown in Figures C.1 through C.10. The data set is incomplete. Wind data for the months of September and November were missing. Windrose information from those months were linearly interpolated from the months of August and October for September, and October and December for November. The data was collected during the years of 1960 to 1990. For the first 20 years the anemometer was located 6 m above grade. For the last 10 years the anemometer was located at an elevation of 10 m. To correct the data to a common elevation of 10 m, using a weighted average, all wind speeds were adjusted upward by a factor of 1.06. The corrected windrose data, at SFO, is presented in Tables C.1 through C.12.

The windrose data was transferred in two steps from SFO to the GGB deck using data obtained from a topographic model study made of the wind environment at SFO and the GGB (Ref 8). Specifically, the winds at the gradient height were computed from winds at an elevation of 10 m at SFO using the factors in Table C.13 (Ref 8). The second step was to scale those gradient height wind speeds with the factors in Table C.14 (Ref 8) to obtain the corresponding wind speeds at the GGB deck elevation.

From the windrose data at the GGB deck elevation, by month, mean wind speeds were computed. Those mean wind speeds are presented in Table C.15. General wind speeds are assumed to have a Rayleigh Distribution (Ref 10). Rayleigh Distributions are single parameter distributions, with the mean wind speed as the single parameter. Therefore, wind speed distributions for all winds, coming from the 16 principal directions, were then known.

For a given mean wind speed, fluctuating moments in a SDS net support strut on the windward side of the bridge were computed analytically. Wind speed time histories at the bridge deck elevation were generated as described in Appendix 3 and Ref 2.Vertical wind loads on the SDS net were computed according to

$$F(t) = (1/2)(\rho)(w(t)^2)(Cdeff)(As)$$

where

F(t) total fluctuating wind induced vertical force on the support strut and the tributary net (spacing of 50 ft);

ρ density of air, 1.25 kg/m^3;

w(t) fluctuating vertical wind speed, m/s;

Cdeff effective drag coefficient for net and strut, 0.82; and

As solid area of members in tributary area, 10.81 m^2

It has been assumed that the admittance of the wind forces over the lateral net wire net dimension of 4 mm is unity. The proposed net has a solid ratio of 0.0879. A Cd = 0.7 for the net wires was assumed. A Cd = 1.6 for the square steel tube strut was assumed. Half of F(t) is supported at the end of the strut. The strut has a dimension of 7.01 m (23 ft). The fluctuating wind induced moment in the strut is therefore

$$M(t) = 3.505\ F(t) = 19.42\ w(t)^2\ Nm$$

It has also been assumed that, on the windward side of the bridge, the fluctuating wind induced moments are not directionally sensitive. Specifically, it is assumed that the fluctuating wind induced moments will be the same (for a given wind speed) for the 7 principal wind directions on the windward side of the bridge.

When winds blow through the bridge, the bridge filters and reduces the turbulence that is experienced on the windward side. The section model was installed in the wind tunnel with some general upwind turbulence generated with a grid (full-scale turbulence cannot be modeled in the wind tunnel at the scale of the section model, 1:50). The spectrum of the turbulence was measured to windward and to leeward at two positions along the deck. Those spectra are shown on Figures C.11 and C.12. While theoretically, one could create a leeward vertical wind speed time history using a frequency dependent modified windward vertical wind speed spectrum. Instead, the general filtering effect and reduction was noted that the leeward spectrum was no greater than about 0.30 times the windward spectrum. Since the spectrum is the square of the Fourier Transform of the upwind vertical wind speed time history, the leeward vertical time history is expected to be approximately 0.55 times the windward time history. This ratio was used to compute the total expected cycles of motion that the SDS support struts are expected to see in one year.

For the moment ranges given in Table C.16, the expected number of cycles in a 10-minute period for mean wind speeds of 2 m/s to 30 m/s are presented in Tables C.17 and C.18..

Using the probability distributions of the expected winds at the GGB deck, for the 16 principal wind directions, using 15 wind speed ranges from 2 m/s to 30 m/s, and using the fluctuating moment cycle counts obtained for specific wind speeds, the total fluctuating moment cycle counts expected in a one-year period were computed. For the SDS support struts on the West side of the GGB, cycle counts were computed including contributions from winds coming from the windward directions of SSW, SW, WSW, W, WNW, NW, and NNW, and contributions from winds from the leeward directions of NNE, NE, ENE, E, ESE, SE, and SSE. For the SDS support struts on the East side of the GGB, contributions to the total cycle counts were from the same winds, but the West winds were now on the leeward side, and the East winds were now on the windward side. For the moment ranges described in Table C.16, the total cycle counts expected in ONE YEAR for SDS support struts on the West and East sides of the GGB are shown in Table C.19.

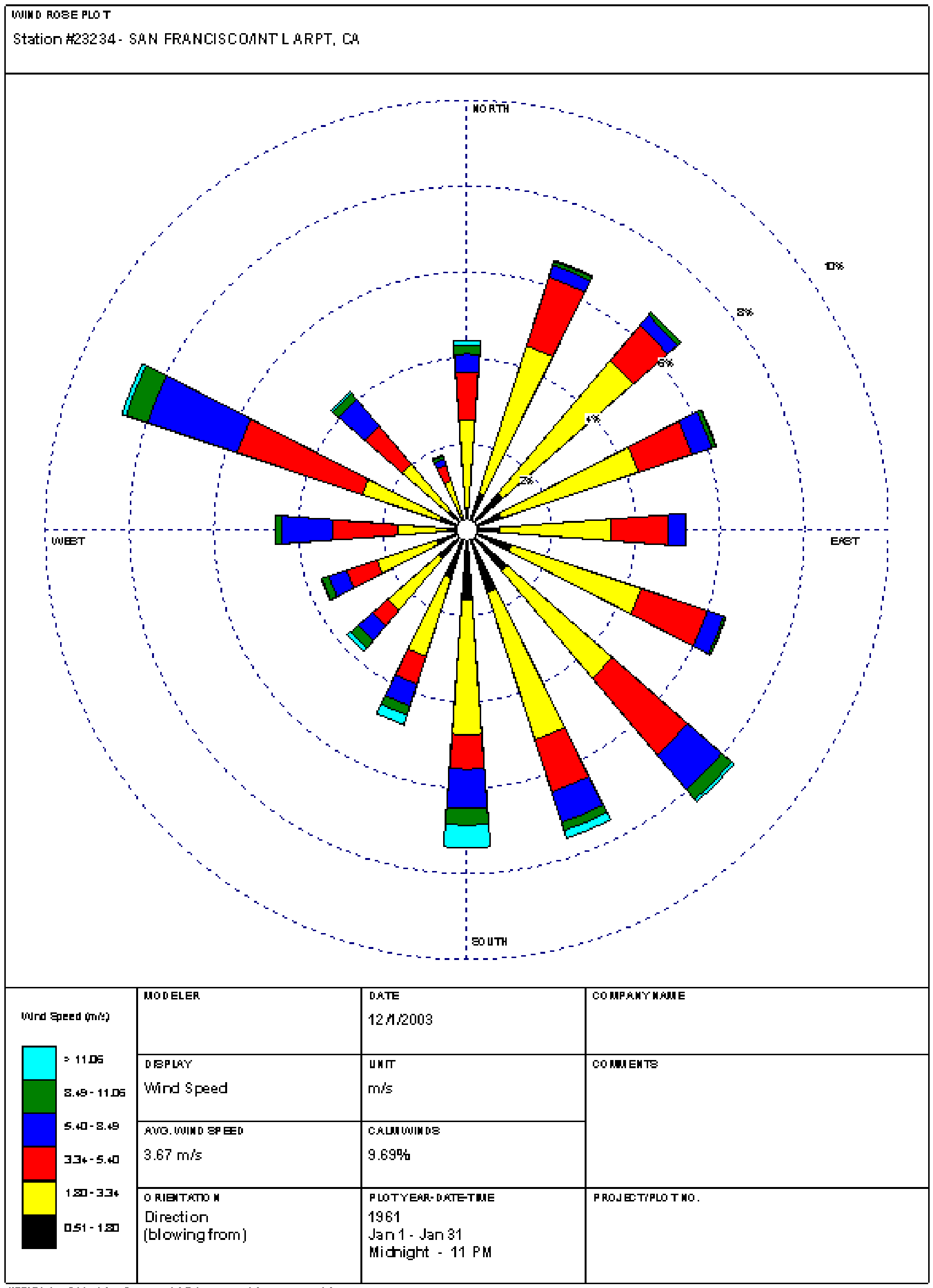

FIGURE C.1
JANUARY

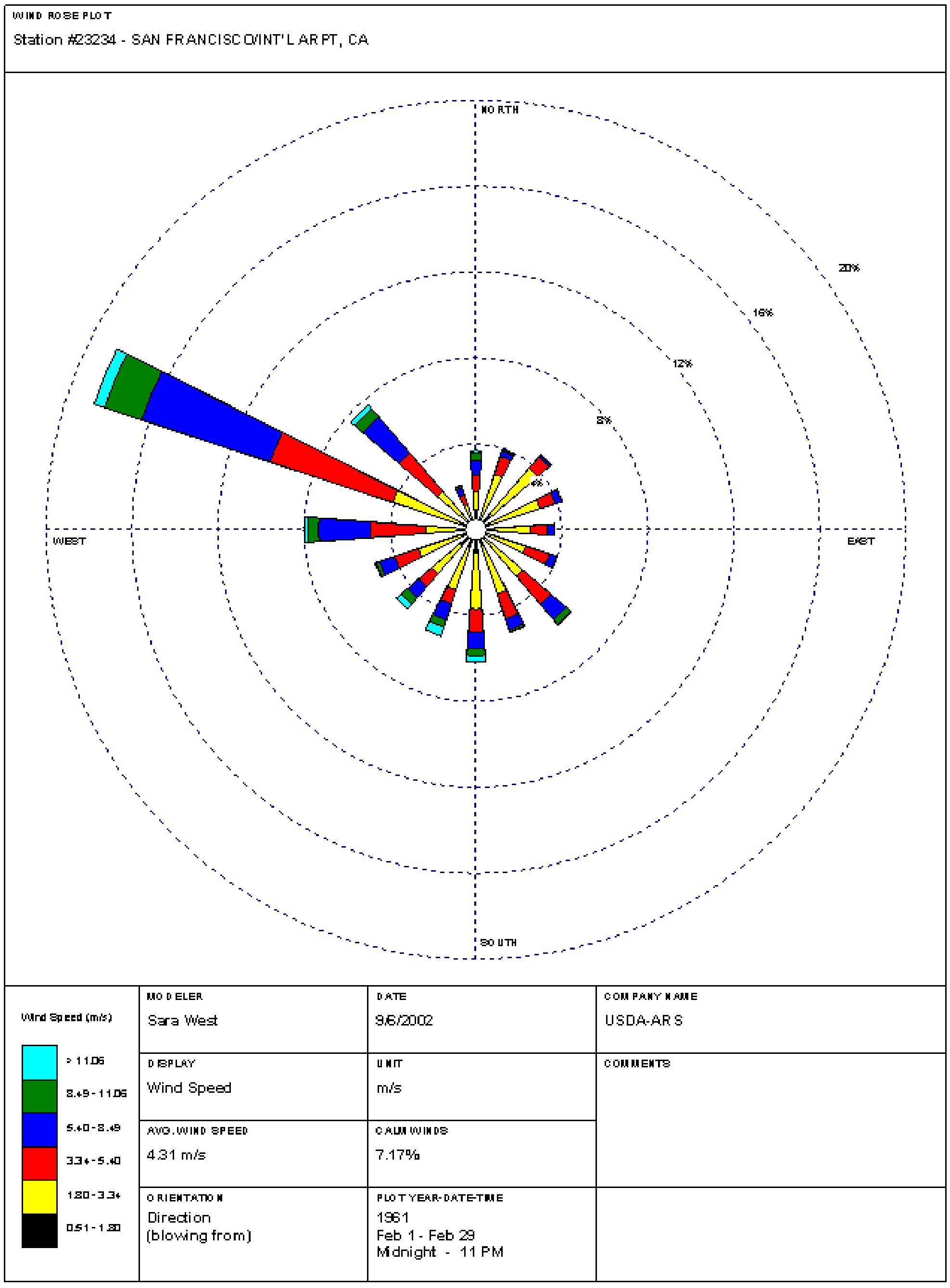

FIGURE C.2
FEBRUARY

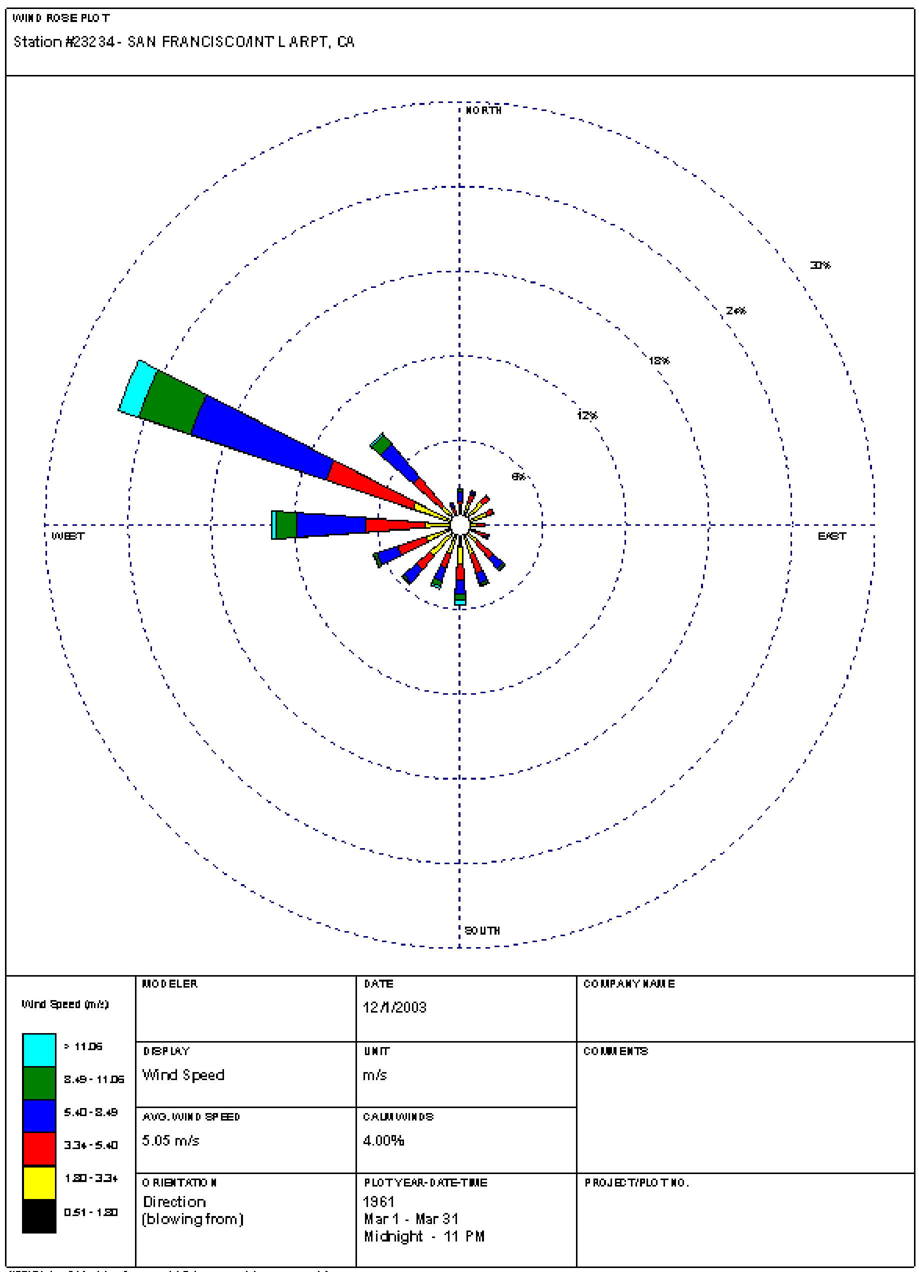

FIGURE C.3
MARCH

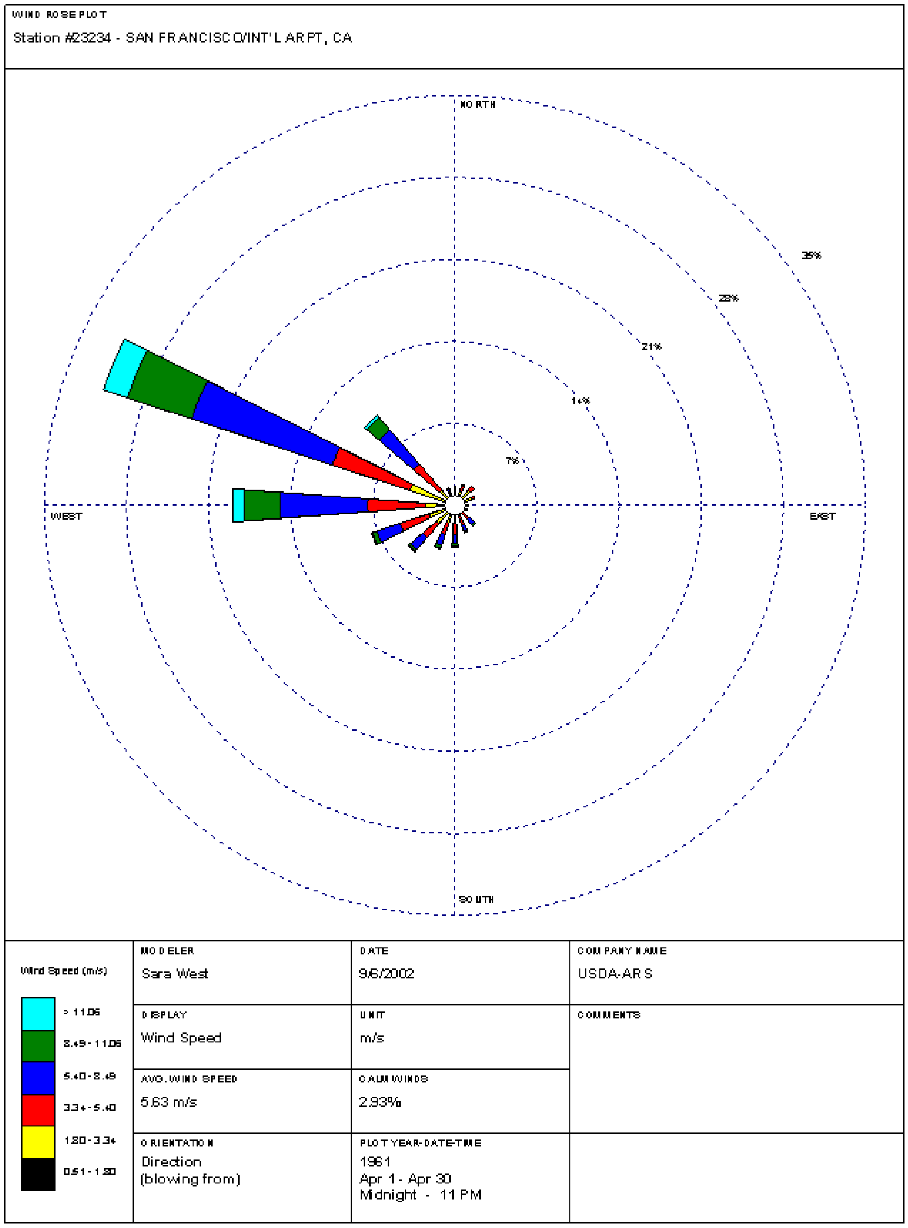

FIGURE C.4
APRIL

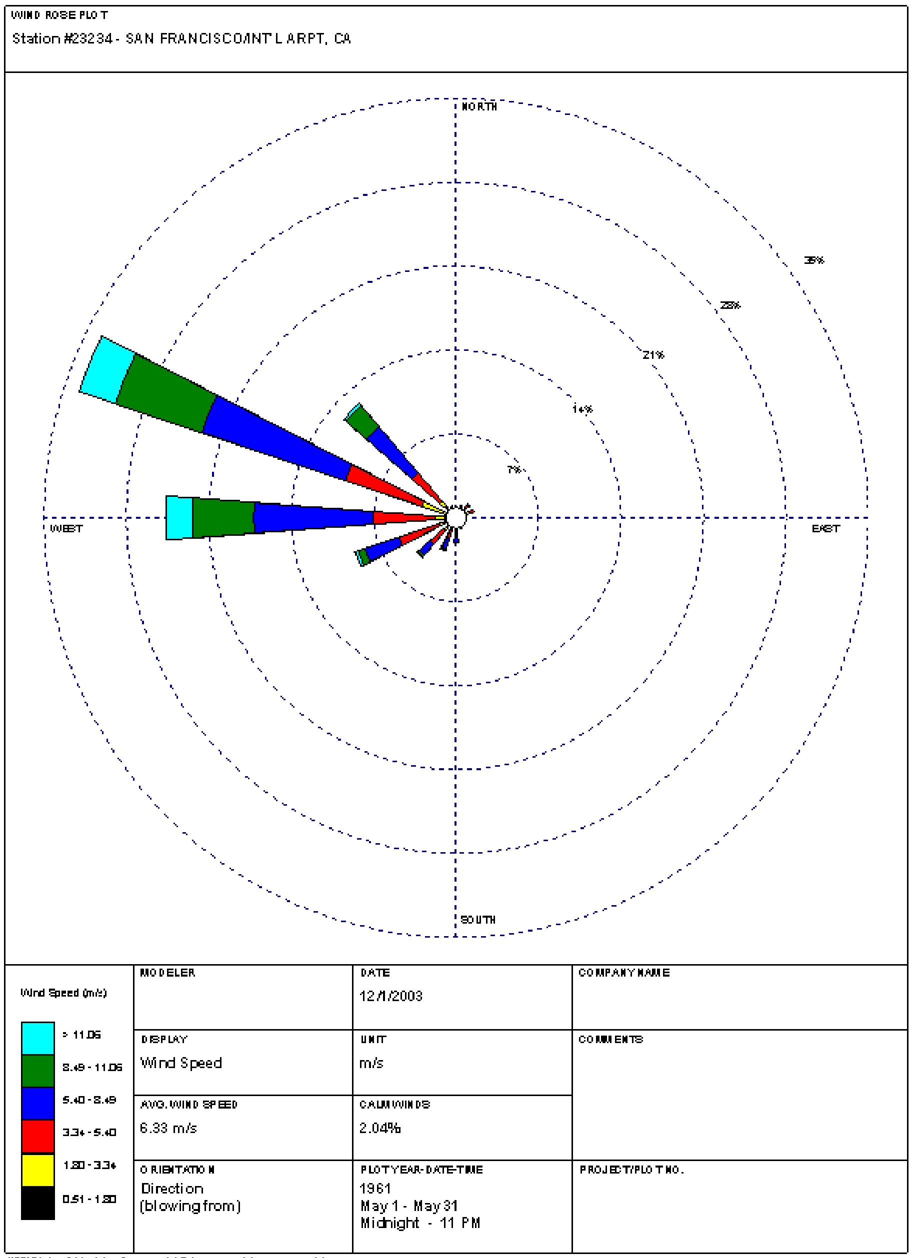

FIGURE C.5
MAY

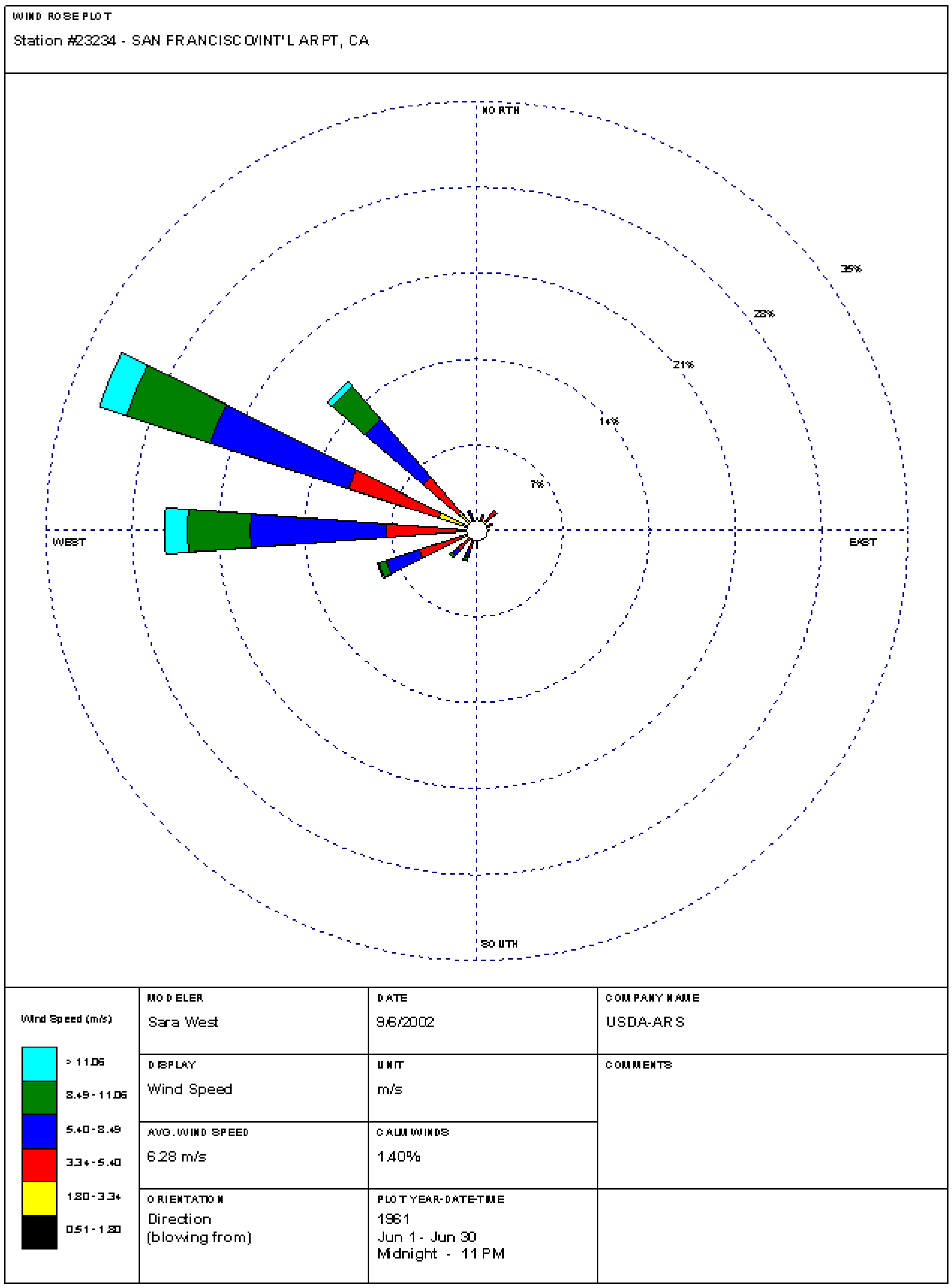

FIGURE C.6
JUNE

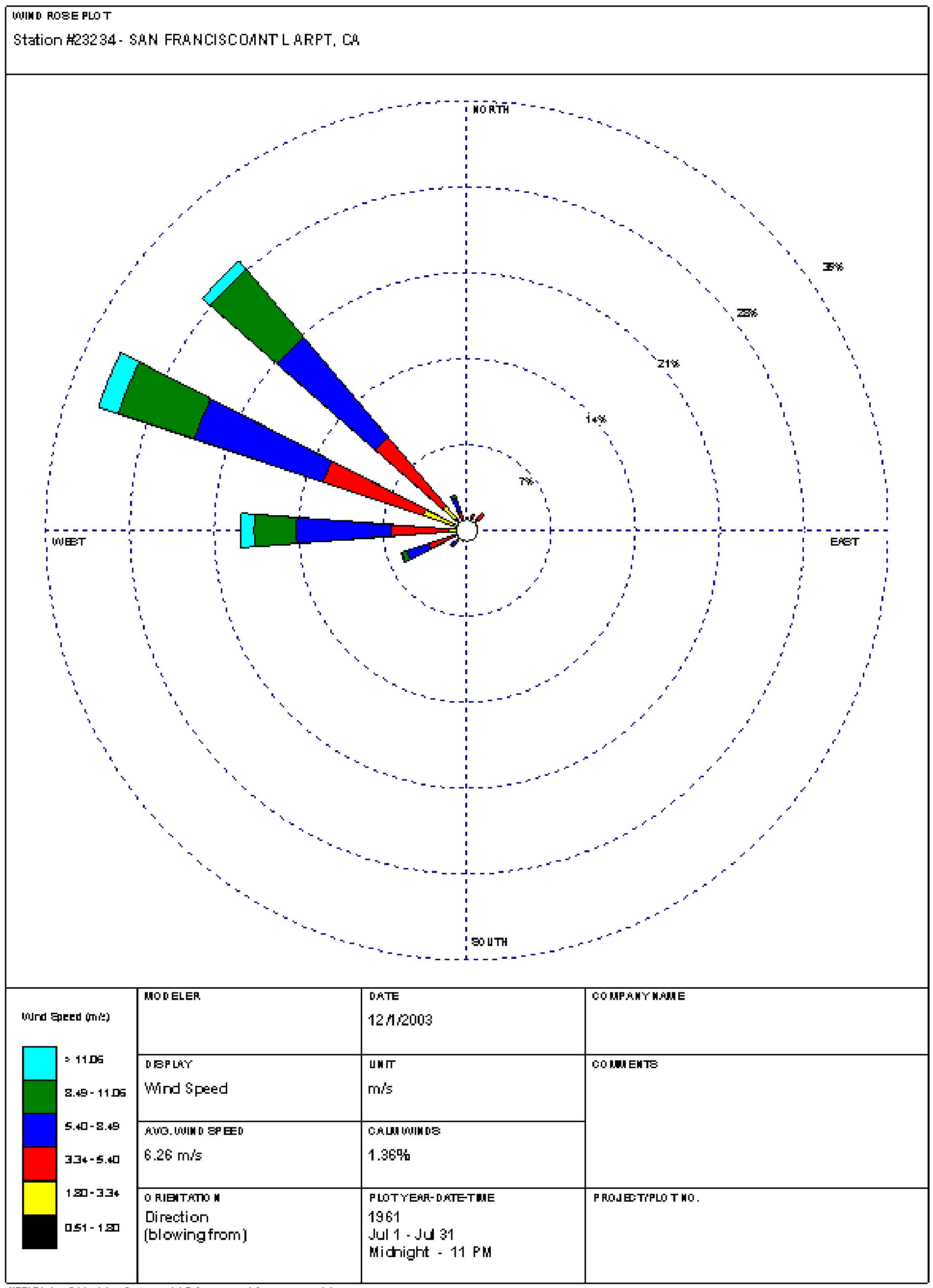

FIGURE C.7
JULY

WIND ROSE PLOT

Station #23234 - SAN FRANCISCO/INT'L ARPT, CA

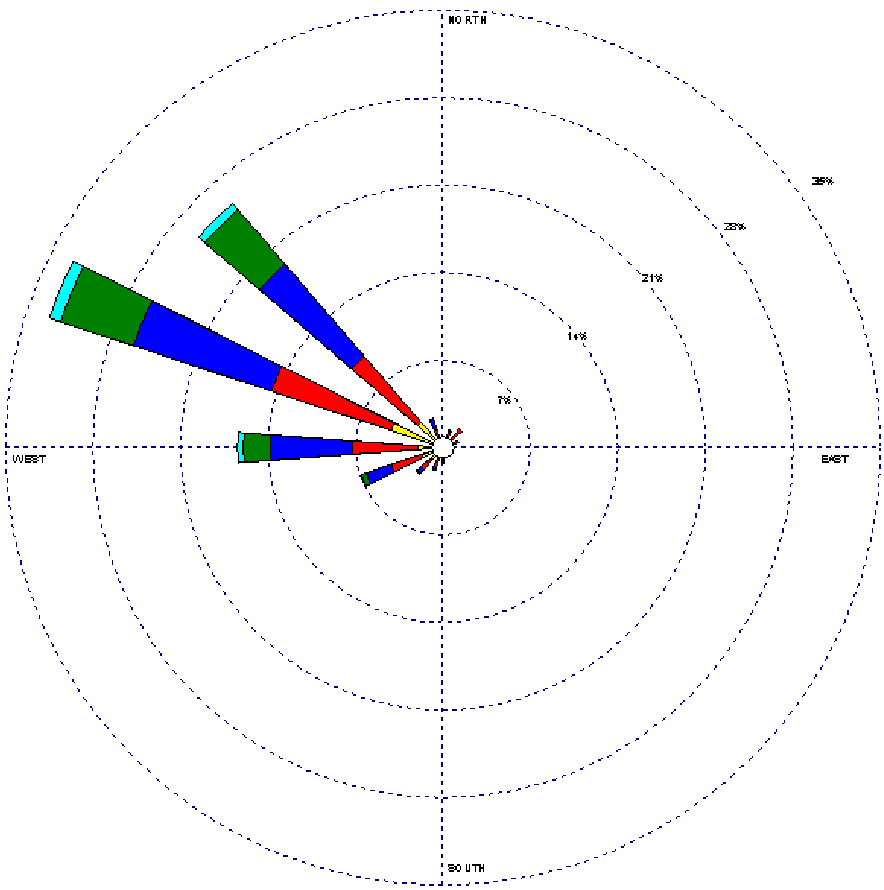

Wind Speed (m/s)		
> 11.06	MODELER: Sara West	DATE: 9/6/2002
8.49 - 11.06	DISPLAY: Wind Speed	UNIT: m/s
5.40 - 8.49	AVG. WIND SPEED: 5.77 m/s	CALM WINDS: 1.87%
3.34 - 5.40	ORIENTATION: Direction (blowing from)	PLOT YEAR-DATE-TIME: 1961 Aug 1 - Aug 31 Midnight - 11 PM
1.80 - 3.34		
0.51 - 1.80		

COMPANY NAME: USDA-ARS

COMMENTS:

WRPLOT View 3.5 by Lakes Environmental Software - www.lakes-environmental.com

FIGURE C.8
AUGUST

WEST WIND LABORATORY, INC

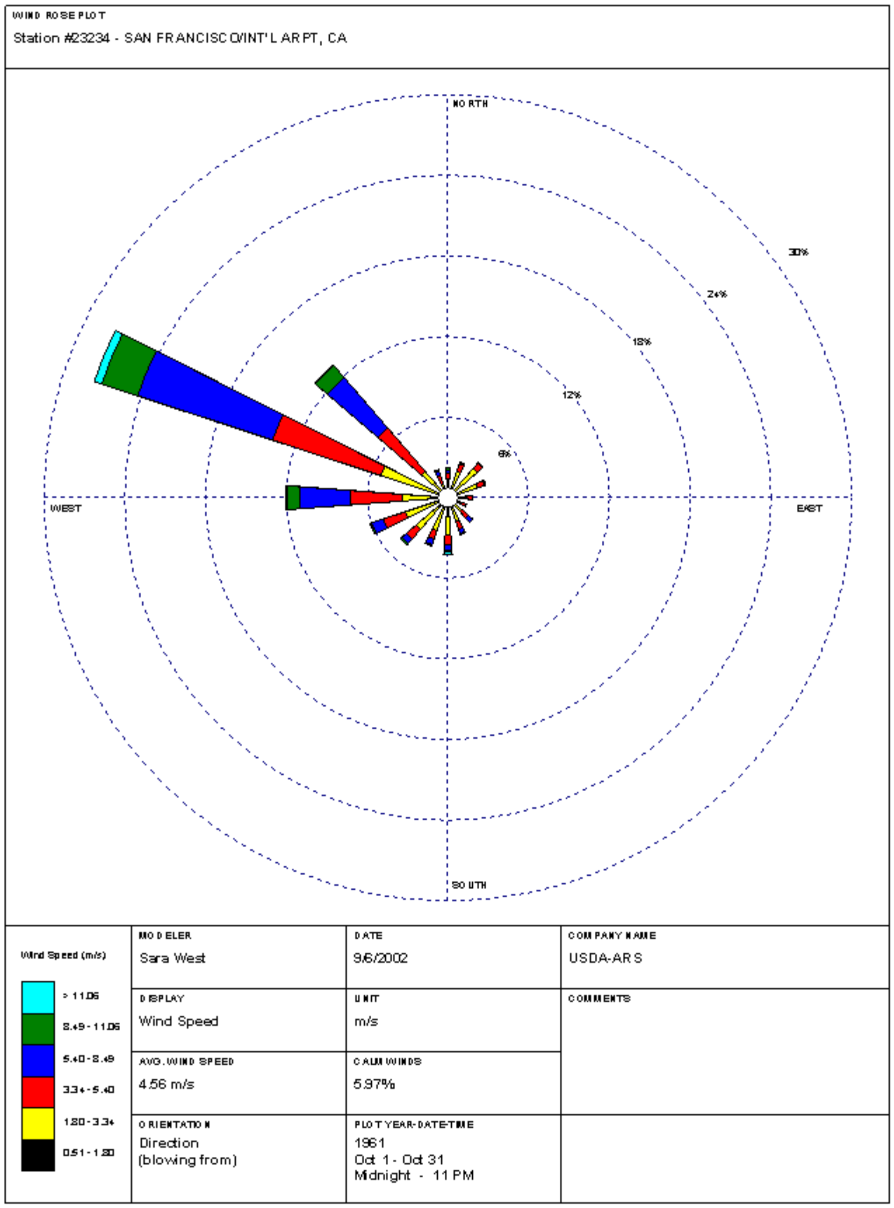

FIGURE C.9
OCTOBER

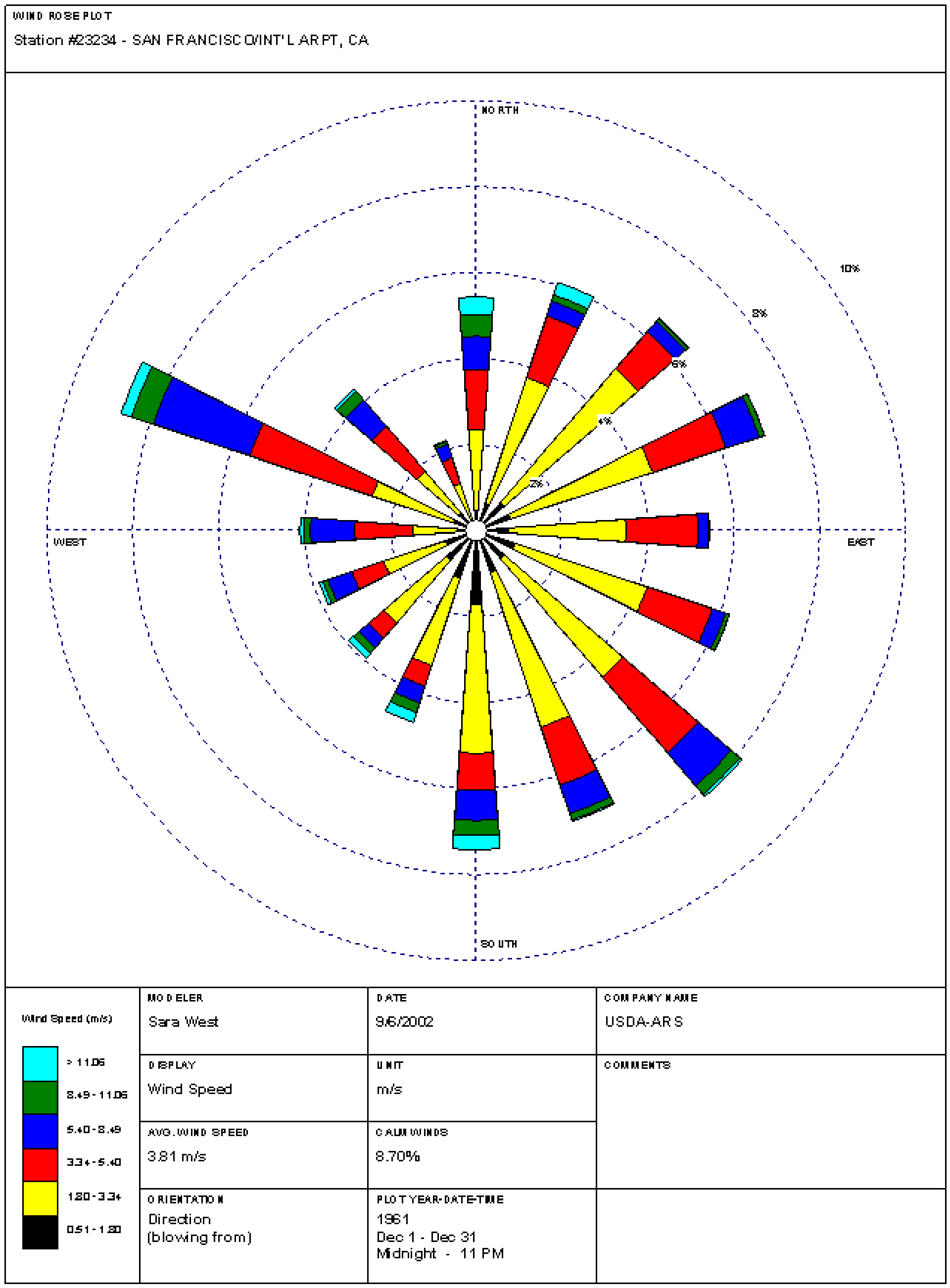

FIGURE C.10
DECEMBER

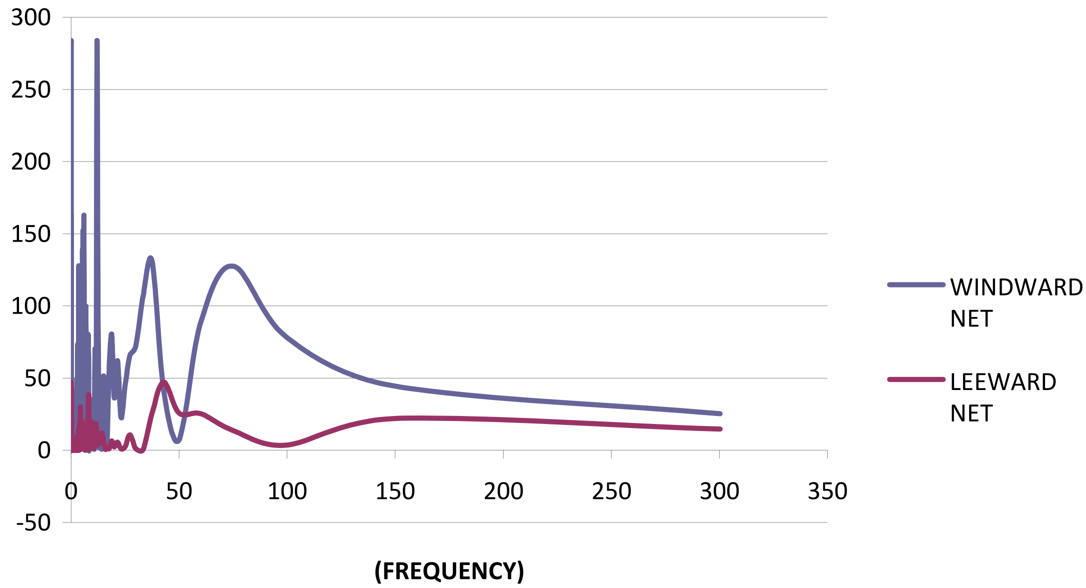

FIGURE C.11
VERTICAL WIND SPEED SPECTRA, POSITION 1

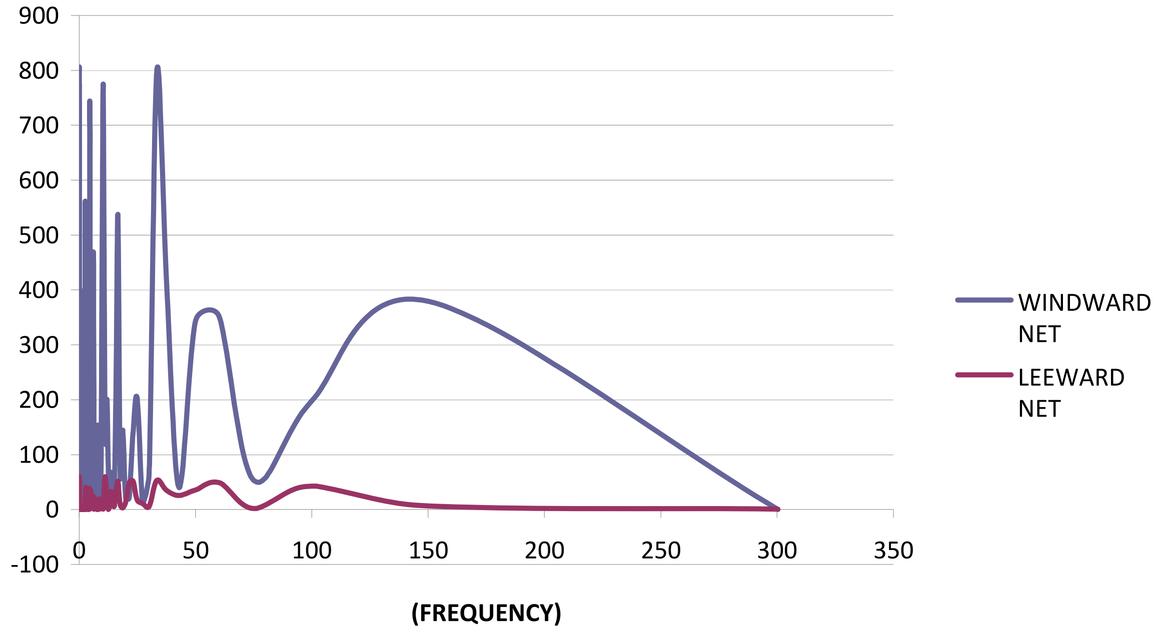

FIGURE C.12
VERTICAL WIND SPEED SPECTRA, POSITION 2

WIND DIRECT	WIND SPEED CATEGORY 1	2	3	4	5	6
1	0.29	2.17	1.16	0.36	0.22	0.14
2	0.73	3.77	1.74	0.29	0.14	0.00
3	0.94	4.28	1.16	0.29	0.14	0.00
4	0.58	3.63	1.38	0.51	0.14	0.00
5	0.58	2.78	1.38	0.44	0.00	0.00
6	0.87	3.41	1.74	0.44	0.07	0.00
7	1.01	3.48	2.54	1.09	0.29	0.07
8	1.30	3.84	1.30	0.80	0.29	0.22
9	1.45	3.34	0.87	1.09	0.44	0.51
10	1.01	2.03	0.73	0.58	0.28	0.28
11	0.58	1.67	0.51	0.44	0.29	0.07
12	0.58	1.52	0.80	0.44	0.14	0.00
13	0.17	1.23	1.60	1.23	0.14	0.00
14	0.44	2.03	3.26	2.32	0.58	0.14
15	0.22	1.48	1.23	0.87	0.14	0.03
16	0.00	0.94	0.36	0.14	0.07	0.00

SFO ANEMOMETER HEIGHT Z = 10 M

WIND DIRECT: 1=N, 2=NNE, 3=NE, 4=ENE, ETC

CATEGORY	WIND SPEED RANGE, M/S
1	0.54 - 1.91
2	1.91 - 3.55
3	3.55 - 5.73
4	5.73 - 9.02
5	9.02 - 11.74
6	> 11.74

WINDROSE INFORMATION, PERCENT OF ALL TIME
SAN FRANCISCO INTERNATIONAL AIRPORT

TABLE C.1 - JANUARY

WIND DIRECT	WIND SPEED CATEGORY 1	2	3	4	5	6
1	0.32	0.95	0.91	0.79	0.32	0.00
2	0.00	2.52	0.95	0.32	0.00	0.00
3	0.00	3.63	0.69	0.16	0.00	0.00
4	0.00	2.90	0.79	0.32	0.00	0.00
5	0.00	2.52	0.91	0.32	0.00	0.00
6	0.00	2.21	1.26	0.32	0.00	0.00
7	0.00	2.59	1.89	0.95	0.32	0.00
8	0.00	2.84	1.26	0.63	0.16	0.00
9	0.63	2.84	1.26	0.95	0.38	0.28
10	0.32	2.21	0.63	0.79	0.32	0.47
11	0.47	1.89	0.91	0.79	0.38	0.32
12	0.00	2.52	1.26	0.79	0.32	0.00
13	0.32	1.58	2.84	2.68	0.60	0.16
14	0.00	3.94	6.63	7.41	1.96	0.63
15	0.00	2.05	2.59	2.49	0.60	0.16
16	0.00	0.63	0.63	0.32	0.16	0.00

SFO ANEMOMETER HEIGHT Z = 10 M

WIND DIRECT: 1=N, 2=NNE, 3=NE, 4=ENE, ETC

CATEGORY	WIND SPEED RANGE, M/S
1	0.54 - 1.91
2	1.91 - 3.55
3	3.55 - 5.73
4	5.73 - 9.02
5	9.02 - 11.74
6	> 11.74

WINDROSE INFORMATION, PERCENT OF ALL TIME
SAN FRANCISCO INTERNATIONAL AIRPORT

TABLE C.2 - FEBRUARY

WIND DIRECT	WIND SPEED CATEGORY 1	2	3	4	5	6
1	0.00	0.00	1.05	0.86	0.19	0.00
2	0.00	1.10	0.72	0.29	0.00	0.00
3	0.00	1.67	0.62	0.14	0.00	0.00
4	0.00	1.43	0.48	0.10	0.00	0.00
5	0.00	0.38	0.62	0.00	0.00	0.00
6	0.00	0.00	1.43	0.24	0.00	0.00
7	0.00	0.96	1.58	0.96	0.24	0.00
8	0.00	1.43	1.67	1.29	0.24	0.00
9	0.86	1.34	1.19	1.05	0.57	0.38
10	0.00	1.62	1.19	1.10	0.48	0.19
11	0.00	2.39	1.43	1.43	0.24	0.00
12	0.00	2.06	2.39	1.82	0.29	0.00
13	0.00	2.06	4.92	5.74	1.67	0.48
14	0.00	3.35	7.65	11.95	4.64	1.77
15	0.00	1.19	3.20	3.58	0.96	0.19
16	0.00	0.00	0.72	0.24	0.00	0.00

SFO ANEMOMETER HEIGHT Z = 10 M

WIND DIRECT: 1=N, 2=NNE, 3=NE, 4=ENE, ETC

CATEGORY	WIND SPEED RANGE, M/S
1	0.54 - 1.91
2	1.91 - 3.55
3	3.55 - 5.73
4	5.73 - 9.02
5	9.02 - 11.74
6	> 11.74

WINDROSE INFORMATION, PERCENT OF ALL TIME
SAN FRANCISCO INTERNATIONAL AIRPORT

TABLE C.3 - MARCH

WIND DIRECT	WIND SPEED CATEGORY 1	2	3	4	5	6
1	0.60	0.00	0.00	0.00	0.00	0.00
2	0.00	0.00	0.60	0.00	0.00	0.00
3	0.00	0.90	0.60	0.00	0.00	0.00
4	0.00	0.60	0.00	0.00	0.00	0.00
5	0.00	0.00	0.00	0.00	0.00	0.00
6	0.00	0.00	0.00	0.00	0.00	0.00
7	0.00	0.00	0.60	1.20	0.00	0.00
8	0.00	0.00	1.20	1.20	0.00	0.00
9	0.60	0.00	1.20	1.14	0.30	0.00
10	0.00	1.20	1.20	1.20	0.60	0.00
11	0.00	1.49	1.79	1.49	0.30	0.00
12	0.00	1.79	2.99	2.39	0.60	0.00
13	0.00	1.79	5.98	8.97	3.59	1.20
14	0.00	3.59	8.37	14.94	6.87	2.39
15	0.00	0.60	3.59	4.78	1.79	0.30
16	0.60	0.00	0.00	0.00	0.00	0.00

SFO ANEMOMETER HEIGHT Z = 10 M

WIND DIRECT: 1=N, 2=NNE, 3=NE, 4=ENE, ETC

CATEGORY	WIND SPEED RANGE, M/S
1	0.54 - 1.91
2	1.91 - 3.55
3	3.55 - 5.73
4	5.73 - 9.02
5	9.02 - 11.74
6	> 11.74

WINDROSE INFORMATION, PERCENT OF ALL TIME
SAN FRANCISCO INTERNATIONAL AIRPORT

TABLE C.4 - APRIL

WIND DIRECT	WIND SPEED CATEGORY 1	2	3	4	5	6
1	0.00	0.00	0.00	0.00	0.00	0.00
2	0.00	0.00	0.28	0.00	0.00	0.00
3	0.00	0.00	0.56	0.11	0.00	0.00
4	0.00	0.00	0.83	0.00	0.00	0.00
5	0.00	0.00	0.00	0.00	0.00	0.00
6	0.00	0.00	0.00	0.00	0.00	0.00
7	0.00	0.00	0.00	0.00	0.00	0.00
8	0.00	0.00	0.00	0.00	0.00	0.00
9	0.00	0.00	1.00	0.39	0.00	0.00
10	0.00	0.00	0.89	0.72	0.17	0.00
11	0.00	0.45	1.78	1.50	0.33	0.00
12	0.00	0.56	4.23	3.62	0.67	0.33
13	0.00	1.00	6.12	11.97	6.12	2.67
14	0.00	2.23	7.96	15.03	8.91	3.90
15	0.00	0.95	3.67	5.96	2.73	0.28
16	0.00	0.00	0.00	0.00	0.00	0.00

SFO ANEMOMETER HEIGHT Z = 10 M

WIND DIRECT: 1=N, 2=NNE, 3=NE, 4=ENE, ETC

CATEGORY	WIND SPEED RANGE, M/S
1	0.54 - 1.91
2	1.91 - 3.55
3	3.55 - 5.73
4	5.73 - 9.02
5	9.02 - 11.74
6	> 11.74

WINDROSE INFORMATION, PERCENT OF ALL TIME
SAN FRANCISCO INTERNATIONAL AIRPORT

TABLE C.5 - MAY

WIND DIRECT	1	2	3	4	5	6
1	0.00	0.00	0.27	0.00	0.00	0.00
2	0.00	0.00	0.53	0.00	0.00	0.00
3	0.00	0.27	1.06	0.00	0.00	0.00
4	0.00	0.00	0.53	0.00	0.00	0.00
5	0.00	0.00	0.00	0.00	0.00	0.00
6	0.00	0.00	0.00	0.00	0.00	0.00
7	0.00	0.00	0.00	0.00	0.00	0.00
8	0.00	0.00	0.00	0.00	0.00	0.00
9	0.00	0.00	0.53	0.00	0.00	0.00
10	0.00	0.00	0.80	1.06	0.00	0.00
11	0.00	0.00	1.06	1.06	0.00	0.00
12	0.00	0.27	4.41	3.29	0.80	0.00
13	0.00	0.00	7.44	12.75	5.95	2.23
14	0.00	2.76	8.77	13.55	8.24	2.66
15	0.00	1.33	4.25	7.17	3.99	0.53
16	0.00	0.00	1.06	0.00	0.00	0.00

(Column heading: WIND SPEED CATEGORY)

SFO ANEMOMETER HEIGHT Z = 10 M

WIND DIRECT: 1=N, 2=NNE, 3=NE, 4=ENE, ETC

CATEGORY	WIND SPEED RANGE, M/S
1	0.54 - 1.91
2	1.91 - 3.55
3	3.55 - 5.73
4	5.73 - 9.02
5	9.02 - 11.74
6	> 11.74

WINDROSE INFORMATION, PERCENT OF ALL TIME
SAN FRANCISCO INTERNATIONAL AIRPORT

TABLE C.6 - JUNE

WIND DIRECT	WIND SPEED CATEGORY 1	2	3	4	5	6
1	0.00	0.00	0.00	0.00	0.00	0.00
2	0.00	0.00	0.30	0.00	0.00	0.00
3	0.00	0.00	0.72	0.00	0.00	0.00
4	0.00	0.00	0.00	0.00	0.00	0.00
5	0.00	0.00	0.00	0.00	0.00	0.00
6	0.00	0.00	0.00	0.00	0.00	0.00
7	0.00	0.00	0.00	0.00	0.00	0.00
8	0.00	0.00	0.00	0.00	0.00	0.00
9	0.00	0.00	0.00	0.00	0.00	0.00
10	0.00	0.00	0.00	0.00	0.00	0.00
11	0.00	0.00	0.00	0.60	0.00	0.00
12	0.00	0.00	2.98	2.39	0.60	0.00
13	0.00	0.60	2.39	9.55	4.18	1.49
14	0.00	3.28	10.45	13.43	8.06	2.09
15	0.00	1.49	8.95	13.13	8.66	0.90
16	0.00	0.00	0.60	1.49	0.30	0.00

SFO ANEMOMETER HEIGHT Z = 10 M

WIND DIRECT: 1=N, 2=NNE, 3=NE, 4=ENE, ETC

CATEGORY	WIND SPEED RANGE, M/S
1	0.54 - 1.91
2	1.91 - 3.55
3	3.55 - 5.73
4	5.73 - 9.02
5	9.02 - 11.74
6	> 11.74

WINDROSE INFORMATION, PERCENT OF ALL TIME
SAN FRANCISCO INTERNATIONAL AIRPORT

TABLE C.7 - JULY

WIND DIRECT	WIND SPEED CATEGORY 1	2	3	4	5	6
1	0.00	0.00	0.00	0.00	0.00	0.00
2	0.60	0.00	0.00	0.00	0.00	0.00
3	0.00	0.00	1.19	0.00	0.00	0.00
4	0.30	0.00	0.00	0.00	0.00	0.00
5	0.00	0.00	0.00	0.00	0.00	0.00
6	0.00	0.00	0.00	0.00	0.00	0.00
7	0.00	0.00	0.00	0.00	0.00	0.00
8	0.00	0.00	0.00	0.00	0.00	0.00
9	0.60	0.00	0.00	0.00	0.00	0.00
10	0.00	0.00	0.30	0.30	0.00	0.00
11	0.60	0.00	0.60	0.60	0.00	0.00
12	0.00	0.00	3.87	2.38	0.60	0.00
13	0.60	0.30	5.96	7.75	2.38	0.60
14	0.00	4.17	11.62	13.71	7.15	1.19
15	0.00	1.79	8.64	11.32	6.56	0.72
16	0.00	0.00	0.60	1.19	0.00	0.00

SFO ANEMOMETER HEIGHT Z = 10 M

WIND DIRECT: 1=N, 2=NNE, 3=NE, 4=ENE, ETC

CATEGORY	WIND SPEED RANGE, M/S
1	0.54 - 1.91
2	1.91 - 3.55
3	3.55 - 5.73
4	5.73 - 9.02
5	9.02 - 11.74
6	> 11.74

WINDROSE INFORMATION, PERCENT OF ALL TIME
SAN FRANCISCO INTERNATIONAL AIRPORT

TABLE C.8 - AUGUST

WIND DIRECT	1	2	3	4	5	6
	WIND SPEED CATEGORY					
1	0.00	0.00	0.53	0.23	0.00	0.00
2	0.30	0.74	0.23	0.07	0.00	0.00
3	0.00	1.28	0.90	0.07	0.00	0.00
4	0.15	0.93	0.30	0.07	0.00	0.00
5	0.00	0.00	0.60	0.00	0.00	0.00
6	0.00	0.00	0.42	0.00	0.00	0.00
7	0.00	0.28	0.28	0.12	0.00	0.00
8	0.00	0.58	0.35	0.23	0.00	0.00
9	0.30	1.16	0.42	0.23	0.23	0.00
10	0.00	1.05	0.45	0.38	0.07	0.00
11	0.30	1.35	0.85	0.60	0.07	0.00
12	0.00	1.56	2.93	1.65	0.37	0.00
13	0.30	1.78	5.29	6.07	1.72	0.34
14	0.00	4.75	10.71	13.10	5.26	0.94
15	0.00	1.94	6.81	8.54	3.96	0.36
16	0.00	0.00	0.83	0.73	0.00	0.00

SFO ANEMOMETER HEIGHT Z = 10 M

WIND DIRECT: 1=N, 2=NNE, 3=NE, 4=ENE, ETC

CATEGORY	WIND SPEED RANGE, M/S
1	0.54 - 1.91
2	1.91 - 3.55
3	3.55 - 5.73
4	5.73 - 9.02
5	9.02 - 11.74
6	> 11.74

WINDROSE INFORMATION, PERCENT OF ALL TIME
SAN FRANCISCO INTERNATIONAL AIRPORT

TABLE C.9 - SEPTEMBER

WIND DIRECT	WIND SPEED CATEGORY 1	2	3	4	5	6
1	0.00	0.00	1.07	0.46	0.00	0.00
2	0.00	1.48	0.46	0.14	0.00	0.00
3	0.00	2.55	0.60	0.14	0.00	0.00
4	0.00	1.85	0.60	0.14	0.00	0.00
5	0.00	0.00	1.20	0.00	0.00	0.00
6	0.00	0.00	0.83	0.00	0.00	0.00
7	0.00	0.56	0.56	0.23	0.00	0.00
8	0.00	1.16	0.69	0.46	0.00	0.00
9	0.00	2.32	0.83	0.46	0.46	0.00
10	0.00	2.08	0.60	0.46	0.14	0.00
11	0.00	2.69	1.11	0.60	0.14	0.00
12	0.00	3.10	1.99	0.93	0.14	0.00
13	0.00	3.24	4.63	4.40	1.07	0.09
14	0.00	5.33	9.82	12.51	3.38	0.69
15	0.00	2.08	5.00	5.79	1.39	0.00
16	0.00	0.00	1.07	0.28	0.00	0.00

SFO ANEMOMETER HEIGHT Z = 10 M

WIND DIRECT: 1=N, 2=NNE, 3=NE, 4=ENE, ETC

CATEGORY	WIND SPEED RANGE, M/S
1	0.54 - 1.91
2	1.91 - 3.55
3	3.55 - 5.73
4	5.73 - 9.02
5	9.02 - 11.74
6	> 11.74

WINDROSE INFORMATION, PERCENT OF ALL TIME
SAN FRANCISCO INTERNATIONAL AIRPORT

TABLE C.10 - OCTOBER

WIND DIRECT	1	2	3	4	5	6
	WIND SPEED CATEGORY					
1	0.10	1.03	1.29	0.63	0.27	0.22
2	0.23	2.42	1.06	0.25	0.08	0.16
3	0.34	3.48	0.91	0.22	0.05	0.00
4	0.31	2.79	1.29	0.52	0.08	0.00
5	0.28	1.51	1.49	0.14	0.02	0.00
6	0.39	1.77	1.26	0.20	0.05	0.00
7	0.35	2.27	1.55	0.66	0.14	0.03
8	0.45	2.64	1.11	0.61	0.08	0.02
9	0.83	3.01	0.87	0.61	0.39	0.18
10	0.52	2.16	0.58	0.45	0.19	0.12
11	0.35	2.29	0.76	0.44	0.16	0.08
12	0.27	2.30	1.38	0.75	0.14	0.05
13	0.09	2.11	2.97	2.66	0.58	0.10
14	0.16	3.63	6.35	7.28	1.92	0.47
15	0.14	1.69	3.12	3.18	0.80	0.03
16	0.00	0.50	0.84	0.31	0.06	0.00

SFO ANEMOMETER HEIGHT Z = 10 M

WIND DIRECT: 1=N, 2=NNE, 3=NE, 4=ENE, ETC

CATEGORY	WIND SPEED RANGE, M/S
1	0.54 - 1.91
2	1.91 - 3.55
3	3.55 - 5.73
4	5.73 - 9.02
5	9.02 - 11.74
6	> 11.74

WINDROSE INFORMATION, PERCENT OF ALL TIME
SAN FRANCISCO INTERNATIONAL AIRPORT

TABLE C.11 - NOVEMBER

WIND DIRECT	WIND SPEED CATEGORY 1	2	3	4	5	6
1	0.19	1.96	1.49	0.77	0.52	0.42
2	0.45	3.27	1.61	0.36	0.15	0.30
3	0.65	4.31	1.19	0.30	0.09	0.00
4	0.59	3.64	1.90	0.86	0.15	0.00
5	0.54	2.87	1.76	0.27	0.03	0.00
6	0.74	3.38	1.64	0.37	0.10	0.00
7	0.67	3.82	2.45	1.04	0.27	0.06
8	0.85	3.97	1.49	0.74	0.15	0.03
9	1.58	3.63	0.89	0.74	0.33	0.34
10	1.00	2.23	0.57	0.43	0.24	0.22
11	0.67	1.93	0.45	0.30	0.18	0.15
12	0.52	1.56	0.82	0.59	0.15	0.09
13	0.18	1.09	1.46	1.09	0.15	0.10
14	0.30	2.08	3.20	2.53	0.59	0.27
15	0.27	1.34	1.41	0.82	0.27	0.06
16	0.00	0.95	0.64	0.34	0.12	0.00

SFO ANEMOMETER HEIGHT Z = 10 M

WIND DIRECT: 1=N, 2=NNE, 3=NE, 4=ENE, ETC

CATEGORY	WIND SPEED RANGE, M/S
1	0.54 - 1.91
2	1.91 - 3.55
3	3.55 - 5.73
4	5.73 - 9.02
5	9.02 - 11.74
6	> 11.74

WINDROSE INFORMATION, PERCENT OF ALL TIME
SAN FRANCISCO INTERNATIONAL AIRPORT

TABLE C.12 - DECEMBER

WIND DIRECT	RATIO
1	2.326
2	1.961
3	2.020
4	2.020
5	2.020
6	2.020
7	2.020
8	2.150
9	2.300
10	2.500
11	2.500
12	2.326
13	2.273
14	2.062
15	2.041
16	2.083

WIND DIRECT: 1=N, 2=NNE, 3=NE, 4=ENE, etc

TABLE C.13
RATIO OF GRADIENT WIND SPEED TO WIND SPEED AT SFO AT Z = 10 M

WIND DIRECT	RATIO
1	0.500
2	0.570
3	0.610
4	0.620
5	0.640
6	0.600
7	0.510
8	0.500
9	0.520
10	0.530
11	0.550
12	0.595
13	0.595
14	0.450
15	0.420
16	0.460

WIND DIRECT: 1=N, 2=NNE, 3=NE, 4=ENE, etc

TABLE C.14
RATIO OF WIND SPEED AT GGB DECK TO GRADIENT WIND SPEED

WIND DIRECT	MEAN WIND SPEED, M/S
1	.11
2	.10
3	.13
4	.12
5	.08
6	.09
7	.13
8	.13
9	.20
10	.20
11	.23
12	.46
13	1.42
14	1.80
15	.84
16	.07

WIND DIRECT: 1=N, 2=NNE, 3=NE, 4=ENE, etc

TABLE C.15
MEAN WIND SPEEDS AT GGB DECK, M/S

BIN	MOMENT RANGE, Nm
1	0.0625 - 0.125
2	0 - 0.125
3	0.125 - 0.25
4	0.25 - 0.5
5	0.5 - 1
6	1 - 2
7	2 - 4
8	4 - 8
9	8 - 16
10	16 - 32
11	32 - 64
12	64 - 128
13	128 - 256
14	256 - 512
15	512 - 1024
16	> 1024

TABLE C.16
SDS SUPPORT STRUT MOMENT BINS

	MOMENT BIN														
U(M/S)	1	2	3	4	5	6	7	8	9	10	11	12	13	14	15
2	645	147	43	22	0	0	0	0	0	0	0	0	0	0	0
4	269	105	166	182	104	42	10	0	0	0	0	0	0	0	0
6	164	70	77	157	175	163	60	24	0	0	0	0	0	0	0
8	112	45	77	77	140	182	171	68	23	3	0	0	0	0	0
10	76	30	55	83	105	138	184	152	87	12	0	0	0	0	0
12	50	29	55	83	84	121	177	174	97	60	10	0	0	0	0
14	45	7	42	56	88	138	137	170	118	99	32	0	0	0	0
16	43	15	40	58	57	97	138	151	145	138	74	7	0	0	0
18	20	23	41	42	82	86	104	166	133	120	79	36	0	0	0
20	13	15	35	50	59	78	98	150	161	152	105	42	8	0	0
22	10	12	36	23	31	71	92	106	170	169	167	65	10	0	0
24	10	6	19	36	29	64	84	112	155	195	177	92	19	0	0
26	6	14	10	24	45	67	78	93	120	170	177	129	28	4	0
28	7	8	14	28	30	52	72	86	110	142	210	124	62	3	0
30	2	8	14	30	33	52	68	95	145	147	197	124	70	15	2

TABLE C.17
MOMENT CYCLE COUNTS, WINDWARD SIDE, T = 10 MINUTES

U(M/S)	1	2	3	4	5	6	7	8	9	10	11	12	13	14	15
	MOMENT BIN														
2	771	62	24	0	0	0	0	0	0	0	0	0	0	0	0
4	350	179	159	136	42	12	0	0	0	0	0	0	0	0	0
6	216	83	146	176	162	77	26	4	0	0	0	0	0	0	0
8	150	73	80	118	193	170	79	28	6	0	0	0	0	0	0
10	96	59	75	103	130	177	176	92	16	0	0	0	0	0	0
12	75	47	84	85	121	157	185	108	62	16	0	0	0	0	0
14	51	36	46	89	138	133	164	122	110	41	0	0	0	0	0
16	56	32	61	60	78	144	139	157	145	82	7	0	0	0	0
18	37	36	44	79	87	95	159	130	137	84	37	6	0	0	0
20	25	35	47	56	72	100	142	163	154	111	42	18	0	0	0
22	18	33	27	26	72	90	88	172	183	170	69	14	0	0	0
24	15	18	35	29	59	83	113	140	197	179	98	35	0	0	0
26	18	10	21	39	73	71	87	119	166	177	129	46	8	0	0
28	13	11	30	28	46	71	80	112	135	205	134	76	7	0	0
30	7	14	27	37	46	62	95	138	150	180	140	80	22	2	0

TABLE C.18
MOMENT CYCLE COUNTS, LEEWARD SIDE, T = 10 MINUTES

MOMENT BIN	WEST SIDE	EAST SIDE
1	5.088E+08	5.073E+08
2	7.553E+07	8.048E+07
3	2.825E+07	2.870E+07
4	1.311E+07	1.242E+07
5	3.371E+06	1.471E+06
6	1.472E+06	4.575E+05
7	3.766E+05	3.141E+04
8	2.896E+04	4.378E+03
9	1.976E+02	5.147E+01
10	2.577E+01	2.492E-05
11	1.557E-05	7.908E-16
12	7.908E-16	3.518E-22
13	3.048E-29	0.000E+00
14	0.000E+00	0.000E+00
15	0.000E+00	0.000E+00
16	0.000E+00	0.000E+00

TABLE C.19
TOTAL SDS SUPPORT STRUT MOMENT CYCLE COUNTS FOR A ONE YEAR PERIOD

APPENDIX 1
WIND ENVIRONMENT AT THE SITE

A detailed analysis of historical winds was not made for this study, but the results of a previous study, made specifically for the Golden Gate Bridge, Highway and Transportation District were used (Ref 8).

For a bridge that is a vital transportation link in a major disaster, it is appropriate that the design wind speed be a wind speed with a return period of at least 100 years. An omnidirectional, one hour averaged wind speed, at the bridge deck elevation, with a return period of 100 years, was found to be 76 mph (Ref 8).

An aeroelastic flutter instability can be catastrophic (as it was for the Tacoma Narrows Bridge), and is to be avoided at all cost. Consequently, it is appropriate to specify that an aeroelastic flutter instability should not occur for a wind speed with a return period less than 10,000 to 100,000 years. From the referenced historical wind speed analysis (Ref 8), such an appropriate critical flutter wind speed criterion was determined to be 100 mph. This is a 10-minute averaged wind speed at the bridge deck elevation (70.87 m).

Strong winds are most likely to come from the south and the west. See Figure 1.1, taken from Ref 8. Also note that, at the site, the percentage of time that strong winds (with a return period of 100 years or more) come from the east is three orders of magnitude lower than the percentage of time that strong winds come from the west. Probabilities are proportional to the percentages, and return periods are proportional to the inverse of the probabilities. Therefore, the return period for equal wind speeds from the east will have a return period approximately 1000 times longer than the return period for a comparable wind speed from the west. Obviously winds from the west are critical.

An omnidirectional 100 year wind (essentially equal to a 100 year wind from the south or the west) of 34 m/s (76 mph) was determined. It is reasonable to assume, therefore, from Figure 1.1 in Ref 8 that this wind speed, 34 m/s (76 mph, would have a return period of 100000 years for winds from the east. Assuming that the distribution of annual extremes at the site, for winds from the east, are similar to those from the west, it can be computed that for winds from the east, an hour averaged wind speed of 20.6 m/s (46 mph) would have a return period of 100 years, and a 10-minute averaged wind speed of 29.5 m/s (66 mph) would have return period of 10000 years. These are approximate values, but are suitable for the analyses for these non-critical directions.

Note that winds from the south may also be likely. However, winds that are essentially perpendicular to the axis of the bridge (the axis of the bridge is north-south) are critical from a stability and buffeting point of view.

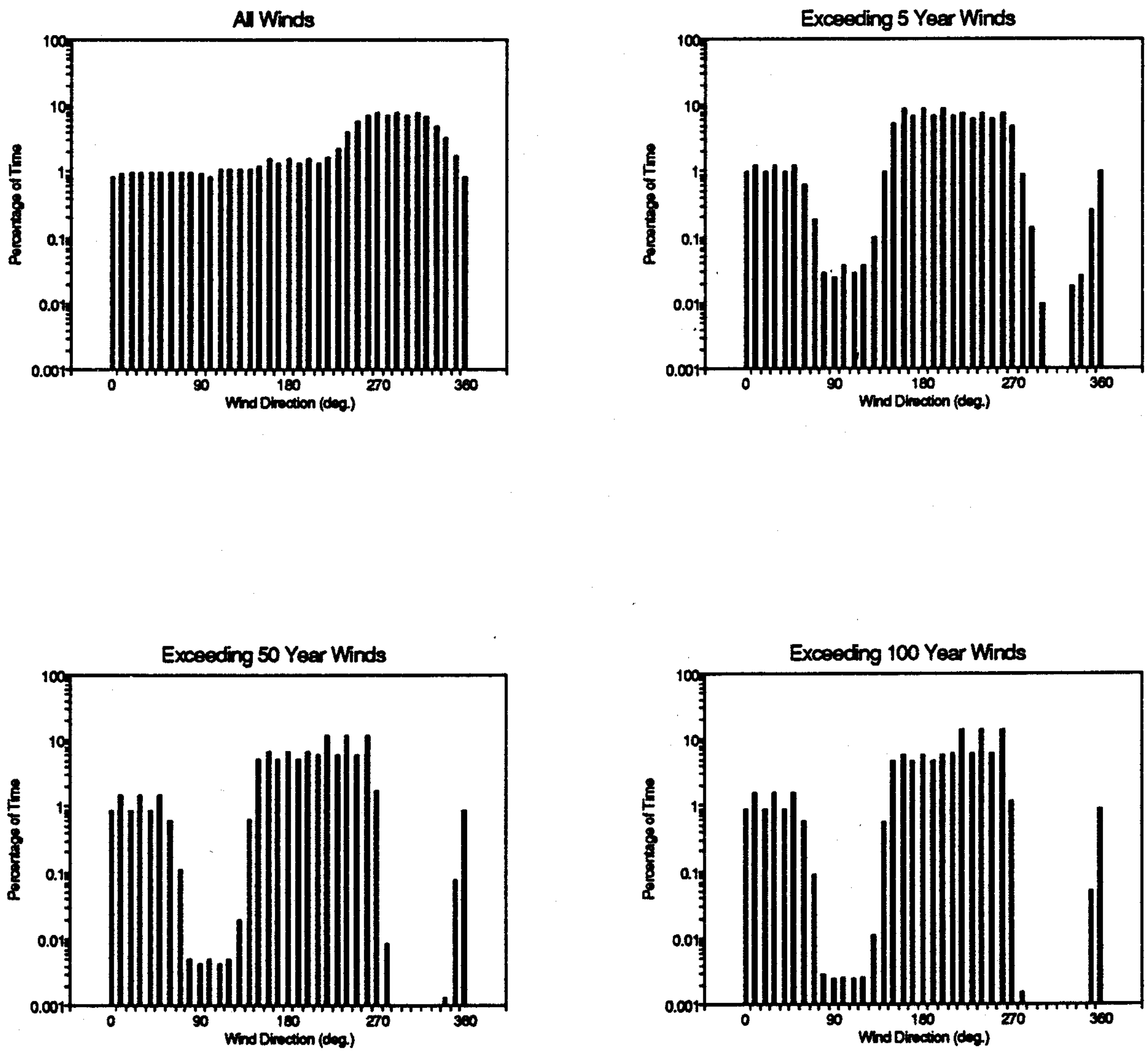
All Winds
Exceeding 5 Year Winds
Exceeding 50 Year Winds
Exceeding 100 Year Winds
Percentage of Time
100
10
1
0.1
0.01
0.001
0
90
180
270
360
Wind Direction (deg.)

FIGURE 1.1

APPENDIX 2
FACILITY

All wind tunnel tests were performed in the 1 x 1.65 m wind tunnel designed specifically for section model testing, owned and operated by the West Wind Laboratory. A schematic drawing of this wind tunnel and a photograph of it, are shown on Figure 2.1.

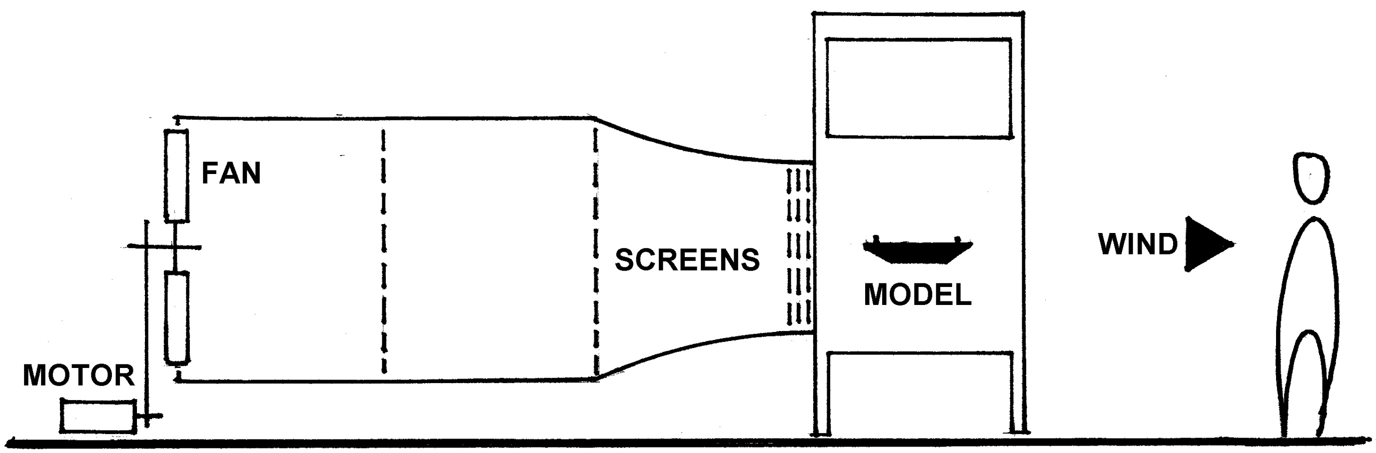

FIGURE 2.1
1 X 1.65 m WIND TUNNEL

APPENDIX 3
PROCEDURE TO PREDICT FULL BRIDGE MOTIONS IN STRONG TURBULENT WINDS

The procedure described here differs from that presented in Ref 3 only in the description of the aerodynamic loads on the bridge deck. Otherwise, they are the same. Specifically, the bridge deck is divided into finite sized elements. On each, the aerodynamic load is computed including motion dependent terms and buffeting terms. Generalized actions are computed for each mode. The response of each mode is computed for the next time step using these generalized actions, the total physical bridge motions are then computed, new aerodynamic loads are computed on each element using these elemental physical motions, and the process is once again repeated for the next step in time. The three dimensional flow field was generated analytically as described in Ref 2.

Chen, Matsumoto, and Kareem describe in Ref 3 the motion dependent aerodynamic loads, in the time domain, for arbitrary motions, in terms of impulse functions. While not as elegant mathematically, the motion dependent aerodynamic loads can also be described directly in terms of the aeroelastic flutter derivatives. This description is computationally more efficient and it eliminates numerical uncertainties associated with one additional series of transformations (to obtain impulse functions from flutter derivatives).

Central to this description is the assumption that the motion dependent aerodynamic loads can be described as the superposition of modal, motion dependent, aerodynamic loads. This has been demonstrated to be valid for years. See Appendix 4.

Motion dependent aerodynamic lift, L_{ij}, and moment, M_{ij}, on the ith deck element, due to the jth mode of vibration can be given by Simiu and Scanlan (Ref 1)

$$L_{ij} = 1/2\rho U^2 B(KH_{1ij}^*((dhij / dt) / U) + KH_{2ij}^*(B(d\alpha ij / dt) / U) + K^2 H_{3ij}^* \alpha_{ij} + K^2 H_{4ij}^*(h_{ij}/B)) \quad (3.1)$$

$$M_{ij} = 1/2\rho U^2 B^2(KA_{1ij}^*(dhij / dt) / U) + KA_{2ij}^*(B(d\alpha ij / dt) / U) + K^2 A_{ij}^* \alpha_{ij} + K^2 A_{4ij}^*(h_{ij}/B)) \quad (3.2)$$

where ρ = air density, $K = \omega B/U$ and $\omega = 2\pi n$, and A_{1ij}^*, A_{2ij}^*, A_{3ij}^*, A_{4ij}^*, H_{1ij}^*, H_{2ij}^*, H_{3ij}^*, and H_{4ij}^* aeroelastic flutter derivatives. See Figure 3.1 for positive coordinate directions, and positive action directions. The aeroelastic flutter derivatives can be interpreted as frequency dependent aerodynamic stiffness and damping terms, valid for steady, decaying, or diverging harmonic motions. The flutter derivatives typically are obtained as those damping and stiffness terms that must have existed to produce the observed, superimposed torsional and vertical motions of a section model, each with its own frequency of vibration.

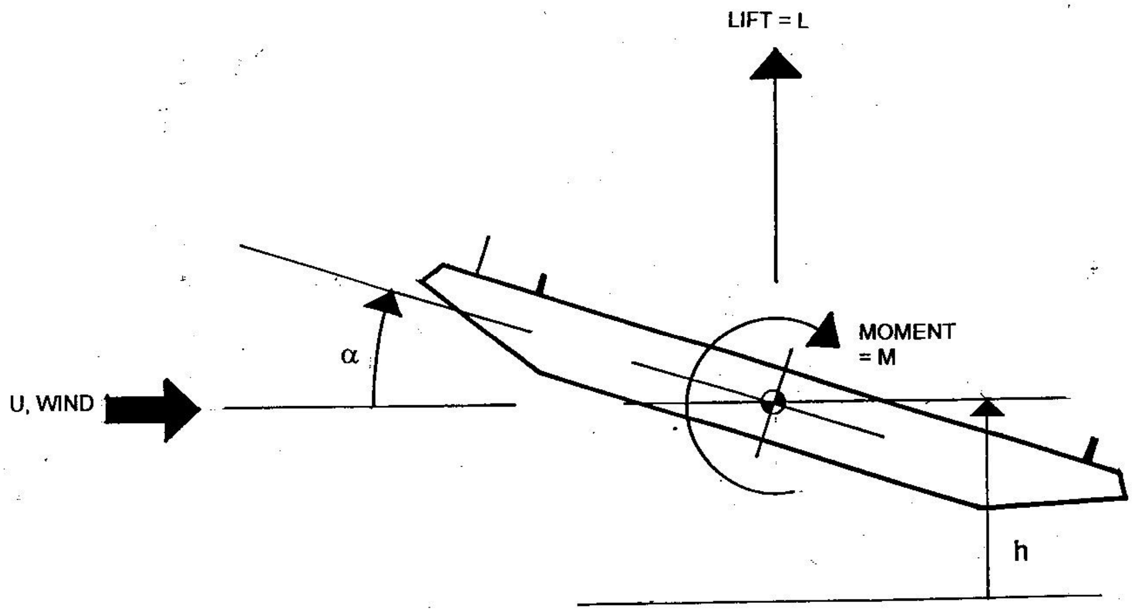

At the onset of each simulation, in smooth or turbulent flow, each mode is given a unit modal displacement. They are all released simultaneously. Although the bridge motion may look arbitrary and erratic, each mode of vibration typically is a slowly varying harmonic motion at a single frequency for which the flutter derivatives are valid. At the onset, each mode of vibration typically will vibrate near its aerodynamically stiffened (or softened) natural frequency. As the motion progresses, various modes will couple aerodynamically and gradually change their frequency to some other, but single, frequency of vibration.

The use of impulse functions, in convolution integrals, to describe the motion dependent aerodynamic loads on a bridge deck, is essentially equivalent to the use of continuously variable (with respect to frequency) flutter derivatives in (3.1) and (3.2). Because the products of K or K^2 and the flutter derivatives vary so slowly with frequency, the flutter derivatives can be varied at finite steps in time (as required), instead of being varied continuously, without loss of precision (certainly with respect to the experimental errors associated with the experimentally obtained flutter derivatives and associated impulse functions). In this procedure, at 20 second intervals (in a 10-minute simulation) all products of K or K^2 and the corresponding flutter derivatives are re-evaluated, for each element, for each mode of vibration, based upon the average frequency of vibration for the preceding 20-second time segment, for the mode in question and based upon the average wind speed for that 20-second time segment. The average 20-second wind speeds, and fluctuating wind speeds about that average, are used to compute the aerodynamic loads.

In the numerical simulations, the following longitudinal turbulence spectrum was assumed:

$$\frac{nS_u(z,n)}{u_*^2} = \frac{200f}{(1+50f)^{\frac{5}{3}}}$$

where

$S_u(z,n)$ longitudinal turbulence spectrum defined such that the variance of the velocity fluctuations equals $\int_0^\infty S_u(z,n)dn$;

z elevation above grade;

n frequency (Hz);

u_* friction velocity;

and

$$f = \frac{nz}{U(z)}$$

where

$U(z)$ mean wind speed at elevation, z;

The spectrum of vertical fluctuations used is

$$\frac{nS_w(z,n)}{u_*^2} = \frac{3.36f}{1+10f^{\frac{5}{3}}}$$

To define the coherence of longitudinal fluctuations in the spanwise direction, an exponential decay coefficient of C_y = 5 was assumed.

In this simulation procedure, a simplified, quasi-steady form of the buffeting forces (Ref 1) is also used. This is a conservative assumption, but it is not assumed to be too conservative. For normal values of U/nB at design wind speeds, the products (KH_{1ij}*) and (K^2H_{3ij}*) are very nearly frequency independent and are approximated well with quasi-steady lift in this flat, frequency independent range.

The step size in all simulations is 0.04 seconds. Bridge motions are simulated for a duration of 5.33 minutes (8,000 total steps in the simulation).

APPENDIX 4
IDENTIFICATION PROCEDURE FOR FLUTTER DERIVATIVES FROM SECTION MODEL TESTS

A linear description of the motion of this section model, for small motions, is

$$m(d^2h / dt^2) + c_h(dh / dt) + k_h h = Ll \quad (4.1)$$

$$I(d^2\alpha / dt^2) + c_\alpha(d\alpha / dt) + k_\alpha \alpha = Ml \quad (4.2)$$

where

m	mass of section model;
I	rotational inertia of section model;
c_h	damping coefficient for vertical motion
c_α	damping coefficient for torsional motion
k_h	vertical stiffness;
k_α	torsional stiffness; and
l	model length.

L and M, and positive coordinate and action directions are presented in Appendix 3.

It is assumed here that the bridge deck is symmetrical about its centerline, so there are no mechanical coupling terms. The linear description of the motion is valid because motions are constrained to be very small. Any motion that becomes large is of academic interest only, and is to be avoided at all costs by the bridge designer. If a large motion is expected over the life span of the bridge, the bridge deck geometry, structure, or energy dissipation capability is changed until that motion is again expected to be small. The linear description of small bridge structure motions is well established.

In this form, all of the aeroelastic flutter coefficients are dimensionless. For the description of the identification procedure here, consider the simplified description

$$(d^2h / dt^2) + 2\omega_h\zeta_h(dh / dt) + \omega_h^2 h = H_1(dh / dt) + H_2(d\alpha / dt) + H_3\alpha + H_4 h \quad (4.3)$$

$$(d^2\alpha / dt^2) + 2\omega_\alpha\zeta_\alpha(d\alpha / dt) + \omega_\alpha^2\alpha = A_1(dh / dt) + A_2(d\alpha / dt) + A_3\alpha + A_h h \quad (4.4)$$

where

$$\omega_h^2 = k_h \quad m$$

$$\omega_\alpha^2 = k_\alpha \quad I$$

$$\zeta_h = c_h \quad 2\omega_h m$$

$$\zeta_\alpha = c_\alpha \quad 2\omega_\alpha I$$

and H1 and A1 are related to their respective H1* and A1* in an obvious manner. Again the H1 and A1 are not constants, but are functions of the wind speed U, or the reduced velocity U/nB, or a form of its inverse (the reduced frequency) K = ωB/U.

Let Equations 4.3 and 4.4 be rearranged one more time for convenience, to the following form:

$$(d^2h / dt^2) + (2\omega_h\zeta_h - H_1)(dh / dt) + (\omega_h^2 - H_4)h = H_2(d\alpha / dt) + H_3\alpha \quad (4.5)$$

$$(d^2\alpha / dt^2) + (2\omega_\alpha\zeta_\alpha - A_2)(d\alpha / dt) + (\omega_\alpha^2 - A_3)\alpha = A_1(dh / dt) + A_4h \quad (4.6)$$

Consider first, the single Equation 4.5. This is simply the equation of motion of a single-degree-of-freedom oscillator with dynamic response characteristics ω and ζ where

$$\omega^2 = \omega_h^2 - H_4 \quad (4.7)$$

and

$$2\zeta\omega = 2\zeta_h\omega_h - H_1 \quad (4.8)$$

subject to the forcing function $F(t) = H_2(d\alpha / dt) + H_3\alpha$

The frequency ω typically will be close to the circular frequency for vertical motion, ω_h. The general solution to this equation (4.5) for an interval of time from t_1 to t_2, can be described as a linear combination of four solutions:

$$h(t) = Y_1y_1(t) + Y_2y_2(t) + Y_3y_3(t) + Y_4y_4(t) \quad (4.9)$$

where

$y_1(t)$ the response of the oscillator to a unit displacement at t_1;

$y_2(t)$ the response of the oscillator to a unit velocity at t_1;

$y_3(t)$ the response of the oscillator to the "forcing function", $(d\alpha / dt)$, with zero initial conditions at t_1; and

$y_4(t)$ the response of the oscillator to the "forcing function", $\alpha(t)$, with zero initial conditions at t_1; and

The coefficients Y_1, Y_2, Y_3, and Y_4 are assumed, in this linear representation of the motion, to be constants for a given ω, ζ, and reduced velocity U/nB for the particular test.

The four solutions are transient solutions. The solutions $y_1(t)$ and $y_2(t)$ are obviously exponentially varying (not necessarily decaying) harmonic functions with circular frequency, ω, and viscous damping coefficient, ζ (which is not necessarily positive). Since the torsional motions of the section model, α(t) and α(t), are also likely to be exponentially varying harmonic motions, the responses $y_3(t)$ and $y_4(t)$ are likely to be as well. These responses, $y_3(t)$ and $y_4(t)$, however will have a frequency equal to the circular frequency of the measured torsional motion, which in turn, typically is very close to the still-air torsional frequency, ω_α.

The objective for Equation 4.5 is again to identify, from recorded section model motions h(t) and α(t), and from the wind-off dynamic response characteristics ω_h, ω_α, ζ_h, and ζ_α, the four flutter coefficients H_1, H_2, H_3, and H_4. If ω_h and ζ_h are known (the observed dynamic response characteristics for the vertical motion with wind speed U), then H_1 and H_4 can be determined from Equations 4.7 and 4.8. If the observed response is decomposed in the form of Equation 4.9, then it follows that $H_2 = Y_3$ and $H_3 = Y_4$. A combined exhaustive search procedure (educated trial and error approach) and a linear-least-squares fitting procedure in the time domain is used to identify ω, ζ, Y_3, and Y_4.

In order for the response to be decomposed into the four transient responses as defined by Equation 4.9, the section model test set-up must be designed specifically to make that decomposition possible. All four transient responses, $y_1(t)$, $y_2(t)$, $y_3(t)$, and $y_4(t)$ are exponentially varying harmonic functions. If the vertical motion frequency and the torsional motion frequency are similar, there is no way that the response can be decomposed *uniquely* as shown in Equation 4.9. Whether or not the frequencies are separated, in reality, for the full-scale bridge, they must be separated in the section model test if this procedure is to be used. Since the objective from the section model test is to determine the flutter coefficients (not simulate the actual bridge behavior), the two section model frequencies can be separated as much as possible, by any amount that is convenient, in order to maximize the accuracy of the data to be collected. Once the flutter coefficients have been identified, they then can be used in an analytical model of the full bridge, including all modes of vibration, as outlined in Ref 1 to predict the critical flutter velocities, should they exist.

The precise identification procedure (for coefficients H_1, H_2, H_3, and H_4 from Equation 4.5) follows directly:

Define one more response

$$X(t) = Y_1 y_1(t) + Y_2 y_2(t) + Y_3 y_3(t) + Y_4 y_4(t) \qquad (4.10)$$

where the Y's and the y(t)'s are defined as before, for $t_1<t<t_2$. If the Y's, ω, and ζ will be found such that the squared error E

$$E = \int_{t_1}^{t_2} (X(t) - h(t))^2 dt \qquad (4.11)$$

is least.

First, for a given wind speed U, the model is perturbed such that significant, but still small, vertical and torsional motions are produced. A sample of the transient motions (either decaying motions or diverging motions) is recorded, i.e., h(t) and α(t) for $t_1<t_2$. It is assumed that the wind-off dynamic response characteristics have previously been recorded.

Second, values of ω and ζ are assumed. For this set of values, a linear-least-squares fitting procedure is used to determine the optimal values of Y_1, Y_2, Y_3, and Y_4, and the squared error E is computed using Equation 4.11. A modified version of a steepest descent procedure is used, with respect to the variables ω and ζ (and at each step the best-fit values of Y_1, Y_2, Y_3, and Y_4 are recalculated). In this manner an optimal set of ω, ζ, Y_1, Y_2, Y_3, and Y_4, are found from which the H_1, H_2, H_3, H_4, and in turn, the H_1^*, H_2^*, H_3^*, and H_4^* are found. It is assumed that these best-fit values of the flutter coefficients are in fact the best estimates of those true values for the section model.

The exact procedure is repeated using Equation 4.6 to determine the torsional flutter coefficients A_1^*, A_2^*, A_3^* and A_4^*.

There is no way to prove that this procedure will converge to the proper values of the flutter coefficients, but years of use seems to indicate that it will. Again, there is the possibility that a set of flutter coefficients is found that is locally optimal, but not globally optimal. The likelihood of that occurring is greatly reduced if small steps are made in incrementing the wind speed from one speed to another, and if the previous best-fit values of ω and ζ are used as initial estimates for the next wind speed (starting with wind-off values for the first step).

This identification procedure relies heavily upon the assumption that the mechanical vibrations of the model, and the unsteady aerodynamic loads are linear functions of the model motion. Shown on Figure 4.1, 4.2, and 4.3 are sets of two curves of A_2* and H_1* that were obtained for two different bridge sections. One A_2* curve in a set was obtained from observed torsional motions with the vertical motion suppressed. The second A_2* curve in the set was obtained using the procedure described in this paper from torsional motions that were superimposed upon vertical motions. Similarly, one H_1* curve in a set was obtained from observed vertical motions with torsional motion suppressed. The second H_1* curve in the set was obtained using the procedure described in this paper from vertical motions that were superimposed upon torsional motions. The good agreement between the two curves in each set verifies that validity of the assumption of linearity in the aerodynamic loads.

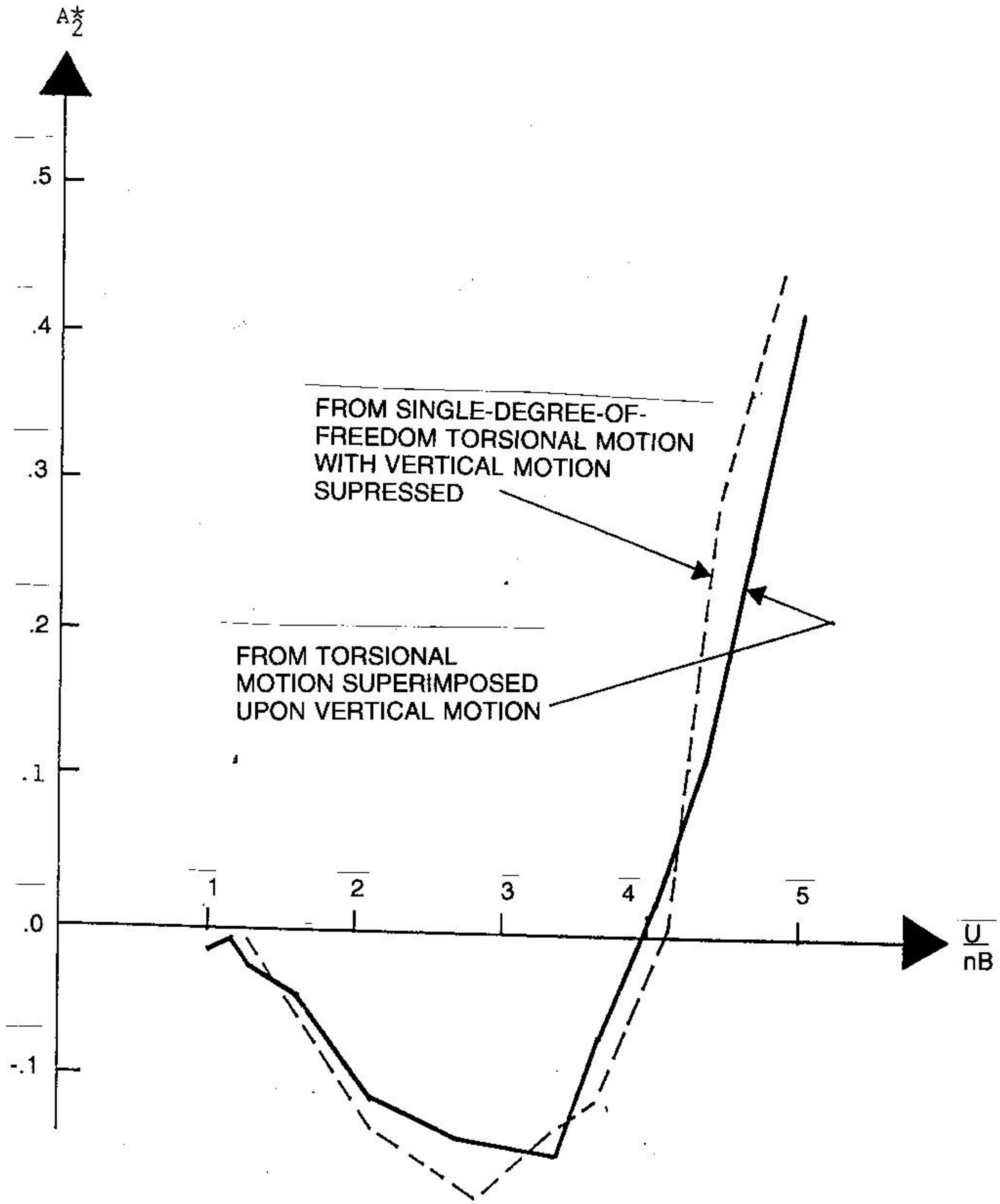
A*2
.5
.4
.3
.2
.1
.0
-.1
1
2
3
4
5
U/nB
FROM SINGLE-DEGREE-OF-FREEDOM TORSIONAL MOTION WITH VERTICAL MOTION SUPRESSED
FROM TORSIONAL MOTION SUPERIMPOSED UPON VERTICAL MOTION

FIGURE 4.01

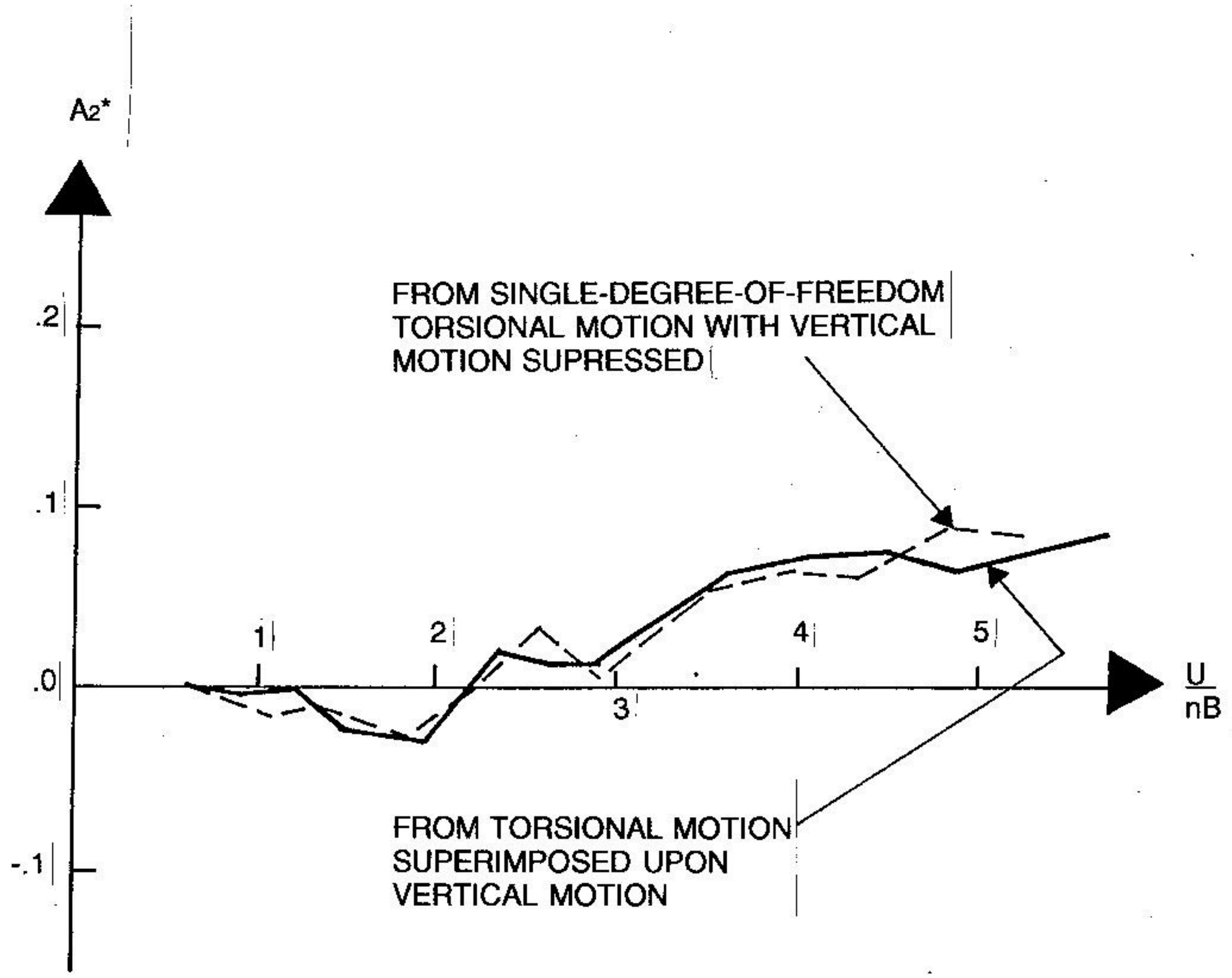
A2*
.2
.1
.0
-.1
1
2
3
4
5
U
nB
FROM SINGLE-DEGREE-OF-FREEDOM
TORSIONAL MOTION WITH VERTICAL
MOTION SUPRESSED
FROM TORSIONAL MOTION
SUPERIMPOSED UPON
VERTICAL MOTION

FIGURE 4.02

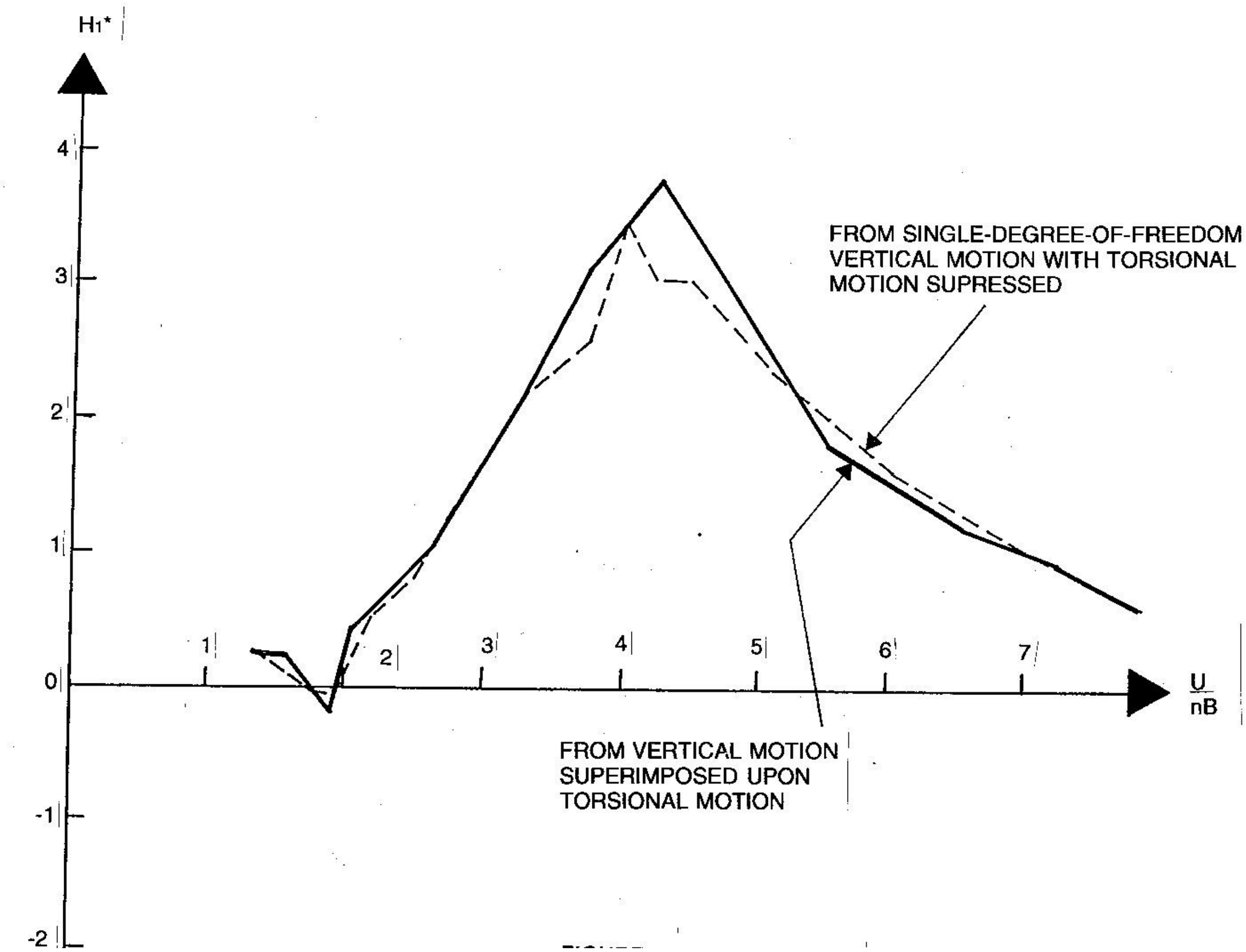
H1*
4
3
2
1
0
-1
-2
1
2
3
4
5
6
7
U
nB
FROM SINGLE-DEGREE-OF-FREEDOM VERTICAL MOTION WITH TORSIONAL MOTION SUPRESSED
FROM VERTICAL MOTION SUPERIMPOSED UPON TORSIONAL MOTION

FIGURE 4.03

APPENDIX 5
MODEL

Required for this study was a single 1:50th scale model of a portion of the bridge deck (81.28 m (266.67 ft) long). The model was constructed for a previous wind study (Ref 5), and has been modified to include railings between the roadway and sidewalk, to include moveable traffic barriers, and to include various aerodynamic enhancement configurations. The model is constructed of laser-cut plastic.

For this study the model was modified to include the single-fairing aerodynamic enhancements on the Western edge of the bridge (Ref 7), and the proposed suicide deterrent net system (SDS) on both sides. The model with those modifications are shown on Figures 5.1 through 5.3.

Wind tunnel tests on models in the wind tunnel (even at a relatively large scale of 1:50) can never be modeled satisfying Reynolds Number similitude. If the model has sharp edges, separation points in the flows around the model will occur at those sharp edges on the model and on the full-scale bridge. Therefore, those flows will be similar as will the pressures distributions. Errors in the wind flows and pressure distributions associated with the inevitable Reynolds Number mismatch can occur around smooth curved surfaces, and through small openings. Typical modeling techniques have been used to minimize errors in the results due to that Reynolds Number mismatch. At low Reynolds Numbers, the boundary layer flow over a curved surface will be laminar. At full scale, over that smooth surface, the boundary layer will be turbulent. The flow will separate from the smooth curved surface at different points on that surface for the two different boundary layers (laminar and turbulent). Therefore, the smooth surface (of the fairing) was artificially roughened (with fine sand) to force the development of a turbulent boundary layer, even at the low values of Reynolds Number.

Flows through railings and nets can also be Reynolds Number dependent. As the opening size in the railing or net gets smaller and smaller, what was otherwise turbulent flow becomes laminar flow, and the resistance to that flow (through the openings) gets artificially high. The full-scale net has wires that are approximately 4 mm (3/16 in) in diameter, with spacings of about 100 mm (4 in). If the net were modeled to be geometrically correct, the wires would be 0.08 mm (0.003 in) in diameter with a typical spacing of about 2 mm (0.08 in). The flow through the net would be at a very low Reynolds Number with a disproportionally high resistance to flow. Ideally, to minimize Reynolds Number effects, the Reynolds Number of the flow through the modeled net should be as close as possible to the Reynolds Number of the flow through the full-scale net. When the mesh size of the full-scale net is small, the full-scale net should be used as well on the model. The mesh size of the full-scale SDS net is too large to be used on the model as well, so a large-scale model of it (approximately 1:3 scale) was used. Member sizes were large (round members with a diameter of 1.56 mm (1/16 in)) with a spacing of 39 by 35 mm (1.42 by 1.38 in). The modeled and full-scale members were both round, and the ratio of projected solid area to gross area was the same for the modeled and full-scale net. Therefore, the resistance to the flow through the net will be similar (with minimal Reynolds Number effect), and the modeled net will still have a small enough mesh size so the smoothed, distribution of flow through the net will be similar to the smoothed, distribution of the flow through the full-scale net.

The railing on the Western edge of the bridge deck was modeled similarly. Specifically, the opening size between the railing pickets were not modeled to be geometrically similar to the full-scale opening size, but were modeled as being larger. The members in the model and on the full-scale bridge are sharp edged, and again, the ratio of the projected solid area to the projected gross area are the same. Therefore, the aerodynamic flow through the modeled railing and full-scale railing will be similar, and Reynolds Number effects will be minimized.

FIGURE 5.1

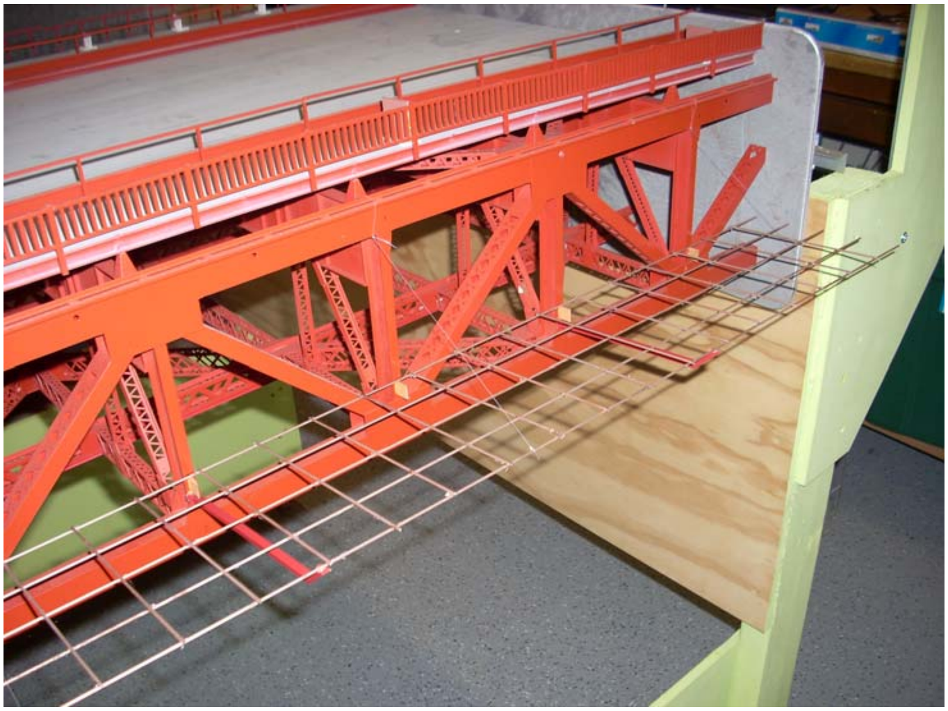

FIGURE 5.2

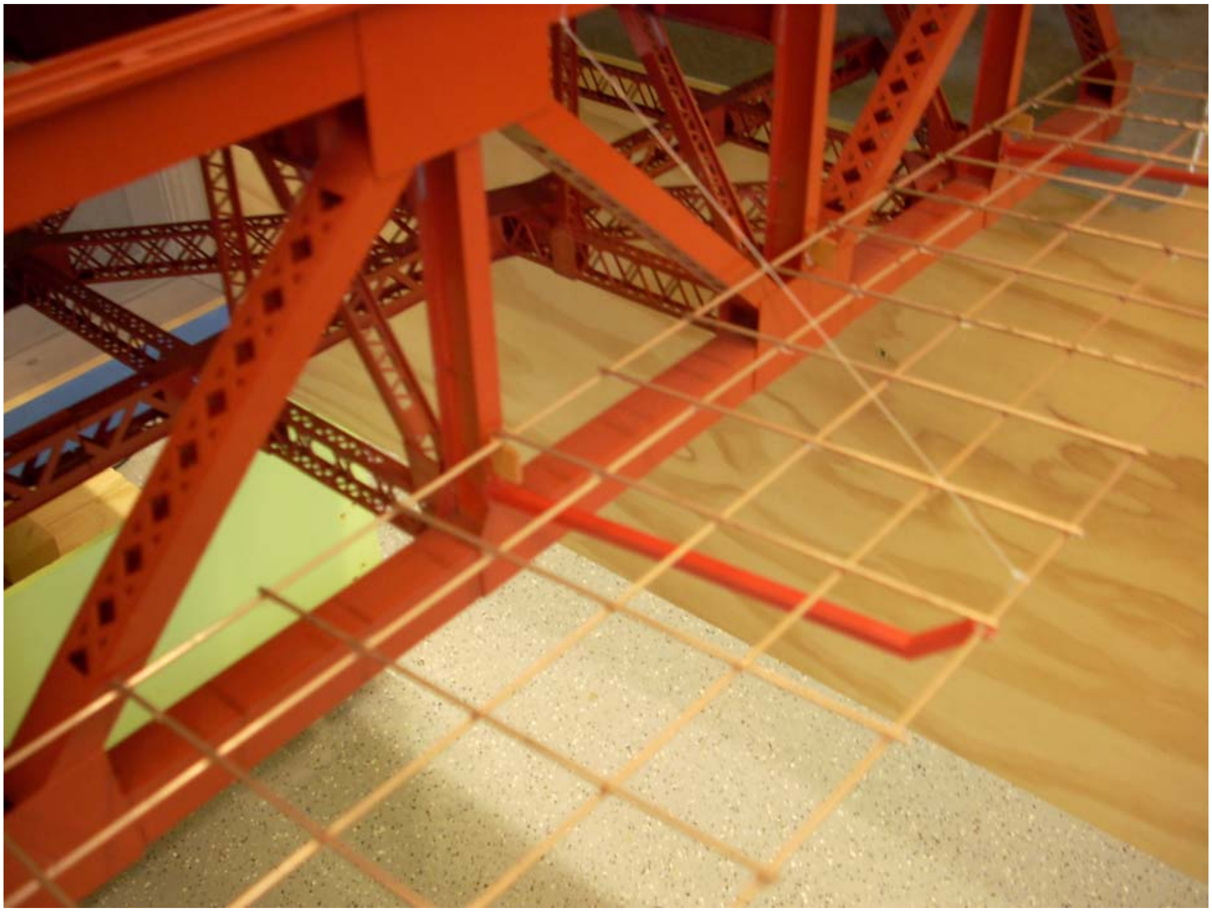

FIGURE 5.3

APPENDIX 6
AERODYNAMIC INPUT PARAMETERS

Required for the simulation procedure are static and dynamic aerodynamic characteristics of the bridge deck. These characteristics were obtained from large scale models of a section of the bridge deck in the wind tunnel, as described elsewhere in this report.

Static aerodynamic coefficients are used to describe the steady state lift, drag, and moment on the deck section, and were obtained by

$$D = (1/2\rho U^2)(B)(I)(C_D)$$

$$L = (1/2\rho U^2)(B)(I)(C_L)$$

$$M = (1/2\rho U^2)(B)(I)(C_M)$$

where

D	drag on section model, N;
L	lift on section model, N;
M	moment about section model axis, N*m;
ρ	density of air, 1.25 kg/m^3;
U	mean wind speed, m/s;
B	model reference length, 0.54864 m (model bridge deck width);
I	model length, 1.6256 m; and
C_D, C_L, C_M	dimensionless aerodynamic coefficients.

Positive coordinate directions are shown in Figure 6.1. Buffeting analyses were not performed on the bridge in this study, only stability analyses. Only the drag coefficient, C_D, will be of significance in the stability analyses. Static coefficients for the bridge deck, from the Reference 7 study, were used for this study. Those static coefficients are shown in Table 6.1. SCL and SCM are the slopes of the lift and moment coefficients respectively.

CD	CL	CM	SCL	SCM
0.34	0.21	0.005	2.864	0.008

TABLE 6.1
STATIC COEFFICIENTS USED IN ANALYSES

Motion dependent aerodynamic loading on the bridge deck is described in terms of flutter derivatives as described in Ref 1, and as presented in Equations 3.1 and 3.2. Positive coordinate directions for the motion dependent terms are shown on Figure 3.1. The aeroelastic flutter derivatives obtained, and used in these stability analyses, are presented in Tables 6.3 through 6.10 for the eight cases studied, defined again in Table 6.2.

CASE	FAIRINGS	SDS	ANGLE OF INCIDENCE (DEGREES)
10	WINDWARD	NO	0
20	LEEWARD	NO	0
30	WINDWARD	YES	0
40	WINDWARD	YES	-3
50	WINDWARD	YES	+3
60	LEEWARD	YES	0
70	LEEWARD	YES	-3
80	LEEWARD	YES	+3

TABLE 6.2 - CASES STUDIED

GG10 4/26/13

U/nB	A1	A4	H1	H4
0.6225	-0.0755	-0.0565	-0.0349	-0.0407
0.9244	-0.1253	-0.0182	-0.1854	-0.1577
1.3083	-0.1497	-0.0460	-0.3386	-0.1664
1.6403	-0.2054	-0.0649	-0.4503	-0.2393
2.1179	-0.2888	-0.0517	-0.6176	-0.4219
2.5238	-0.3394	-0.0701	-0.8750	-0.6026
2.7532	-0.3842	-0.0632	-1.2049	-0.6779
3.0922	-0.4372	-0.0549	-1.6200	-0.7473
3.7453	-0.4882	-0.0176	-2.0081	-0.3722
4.2885	-0.5147	-0.1262	-2.5488	-0.4805
4.7680	-0.4847	-0.0158	-2.4216	-0.1021
5.3833	-0.5085	0.0439	-2.7557	0.1759
6.1615	-0.4976	0.1299	-2.8858	0.0064
6.7398	-0.5540	0.1930	-3.1497	0.2812
7.1311	-0.5684	0.1544	-3.2801	0.0122
7.5600	-0.5532	0.1495	-3.2754	-0.0091
8.2062	-0.5784	0.1298	-3.7465	-0.0922
8.8517	-0.6300	0.2346	-4.3338	0.1193
9.4866	-0.5439	0.1624	-3.6808	-0.3520
9.8852	-0.5962	0.1955	-4.1096	-0.0733
10.4901	-0.7889	0.3655	-5.0246	-0.0348
11.2019	-0.7080	0.3809	-4.3690	-0.1467
12.4243	-0.7199	0.4566	-4.4605	0.1027
13.3366	-0.8382	0.2470	-3.8335	-0.6662

U/nB	A2	A3	H2	H3
0.4677	-0.0064	0.3101	0.1025	0.3315
0.6972	-0.0142	0.3765	0.1216	0.3990
0.9890	-0.0264	0.3902	0.1685	0.4372
1.2436	-0.0392	0.4079	0.2340	0.5348
1.6067	-0.0515	0.4156	0.3047	0.5960
1.9200	-0.0587	0.4197	0.3842	0.6603
2.1107	-0.0727	0.4538	0.3351	0.7337
2.3756	-0.0852	0.5040	0.3324	0.9167
2.8800	-0.0881	0.5727	0.3965	1.3071
3.3053	-0.0908	0.6358	0.3552	1.5545
3.6730	-0.0822	0.6889	0.7002	1.9203
4.1644	-0.0653	0.7663	0.7921	2.4041
4.7941	-0.0600	0.8808	1.1412	2.6999
5.2666	-0.0235	0.8837	1.2707	3.2655
5.5906	-0.0225	0.9496	1.3767	3.4392
5.9431	-0.0294	1.0518	1.5223	3.7817
6.4992	-0.0049	1.1665	1.7154	4.4656
7.0085	0.0281	1.2668	1.9024	4.5622
7.5626	0.0443	1.3250	2.2161	5.0675
7.9008	0.0476	1.3792	2.1834	5.4587
8.4810	0.0738	1.5195	2.3717	6.7483
9.1148	0.1067	1.7082	2.9950	7.1321
10.1415	0.1368	2.0315	3.8984	8.2531
11.1523	0.1900	2.3680	4.0785	9.9214

TABLE 6.3

GG20 4/26/13

U/nB	A1	A4	H1	H4
0.5692	-0.0652	-0.2363	-0.0237	-0.0286
0.9675	-0.0838	-0.1913	-0.1085	-0.1356
1.1965	-0.1263	-0.2105	-0.2583	-0.1668
1.6725	-0.2545	-0.2539	-0.2999	-0.1772
2.1854	-0.3414	-0.2364	-0.4873	-0.5482
2.5580	-0.4265	-0.1839	-0.8034	-0.8521
2.7999	-0.4916	-0.1756	-1.1206	-1.0627
3.2552	-0.5121	-0.1504	-1.6991	-1.1107
3.7551	-0.4922	-0.1411	-2.3748	-0.8098
4.4821	-0.4750	-0.0157	-2.9440	-0.5009
4.8995	-0.4781	0.0816	-3.0623	-0.3953
5.4196	-0.5271	0.0506	-3.1519	-0.4928
6.0408	-0.4811	0.1006	-3.5146	-0.1343
6.6026	-0.5027	0.1582	-3.8634	0.0506
7.2467	-0.4218	0.2507	-4.0773	0.3455
7.8807	-0.5032	0.3007	-4.8688	0.1706
8.2857	-0.5291	0.2527	-4.2711	-0.1906
8.9282	-0.4950	0.2851	-4.4947	-0.0698
9.4502	-0.5648	0.3342	-5.2199	-0.4859
10.1338	-0.5586	0.3870	-4.8197	0.3541

U/nB	A2	A3	H2	H3
0.4313	-0.0020	0.1736	0.0765	0.0774
0.7336	-0.0029	0.2473	0.1318	0.1565
0.9075	-0.0102	0.2668	0.1662	0.1592
1.2650	-0.0221	0.2562	0.2694	0.3143
1.6764	-0.0713	0.2425	0.3554	0.3268
1.9710	-0.0821	0.2656	0.3766	0.3551
2.1665	-0.0919	0.3197	0.3600	0.4042
2.5313	-0.1017	0.3920	0.2130	0.5581
2.9319	-0.0897	0.4845	0.0745	0.9881
3.5019	-0.0498	0.6345	0.0924	1.4946
3.8416	-0.0276	0.6960	0.2953	1.8600
4.2506	0.0122	0.7397	0.3565	2.1722
4.7428	0.0170	0.7658	0.6054	2.6789
5.2038	0.0860	0.8647	0.6946	3.2365
5.7049	0.1361	0.9425	1.0044	3.9446
6.2408	0.1979	1.0182	0.9673	4.3654
6.6269	0.2309	1.0554	1.3645	4.8517
7.1491	0.2693	1.0675	1.6944	5.5509
7.6278	0.3023	1.0642	1.4984	6.1410
8.1596	0.3389	1.0606	2.1245	6.9037

TABLE 6.4

GG30 4/26/13

U/nB	A1	A4	H1	H4
0.6225	-0.0755	-0.0565	-0.0349	-0.0407
0.9244	-0.1253	-0.0182	-0.1854	-0.1577
1.3083	-0.1497	-0.0460	-0.3386	-0.1664
1.6403	-0.2054	-0.0649	-0.4503	-0.2393
2.1179	-0.2888	-0.0517	-0.6176	-0.4219
2.5238	-0.3394	-0.0701	-0.8750	-0.6026
2.7532	-0.3842	-0.0632	-1.2049	-0.6779
3.0922	-0.4372	-0.0549	-1.6200	-0.7473
3.7453	-0.4882	-0.0176	-2.0081	-0.3722
4.2885	-0.5147	-0.1262	-2.5488	-0.4805
4.7680	-0.4847	-0.0158	-2.4216	-0.1021
5.3833	-0.5085	0.0439	-2.7557	0.1759
6.1615	-0.4976	0.1299	-2.8858	0.0064
6.7398	-0.5540	0.1930	-3.1497	0.2812
7.1311	-0.5684	0.1544	-3.2801	0.0122
7.5600	-0.5532	0.1495	-3.2754	-0.0091
8.2062	-0.5784	0.1298	-3.7465	-0.0922
8.8517	-0.6300	0.2346	-4.3338	0.1193
9.4866	-0.5439	0.1624	-3.6808	-0.3520
9.8852	-0.5962	0.1955	-4.1096	-0.0733
10.4901	-0.7889	0.3655	-5.0246	-0.0348
11.2019	-0.7080	0.3809	-4.3690	-0.1467
12.4243	-0.7199	0.4566	-4.4605	0.1027
13.3366	-0.8382	0.2470	-3.8335	-0.6662

U/nB	A2	A3	H2	H3
0.4677	-0.0394	0.4079	0.1025	0.3315
0.6972	-0.0160	0.3402	0.1216	0.3990
0.9890	-0.0140	0.2883	0.1685	0.4372
1.2436	-0.0308	0.3310	0.2340	0.5348
1.6067	-0.0648	0.3919	0.3047	0.5960
1.9200	-0.0630	0.4136	0.3842	0.6603
2.1107	-0.0562	0.4174	0.3351	0.7337
2.3756	-0.0635	0.4407	0.3324	0.9167
2.8800	-0.0822	0.5293	0.3965	1.3071
3.3053	-0.0865	0.5698	0.3552	1.5545
3.6730	-0.0825	0.6642	0.7002	1.9203
4.1644	-0.0605	0.6656	0.7921	2.4041
4.7941	-0.0488	0.8534	1.1412	2.6999
5.2666	-0.0859	0.9627	1.2707	3.2655
5.5906	-0.0853	1.0200	1.3767	3.4392
5.9431	-0.0572	1.1601	1.5223	3.7817
6.4992	-0.0409	1.3506	1.7154	4.4656
7.0085	0.0184	1.4426	1.9024	4.5622
7.5626	0.0424	1.4163	2.2161	5.0675
7.9008	0.0095	1.4771	2.1834	5.4587
8.4810	-0.0184	1.7182	2.3717	6.7483
9.1148	0.0096	1.7945	2.9950	7.1321
10.1415	0.0567	2.0332	3.8984	8.2531
11.1523	0.0347	2.4169	4.0785	9.9214

TABLE 6.5

GG40 4/26/13

U/nB	A1	A4	H1	H4
0.4863	-0.0207	0.0009	-0.0069	-0.0696
0.8951	-0.0853	0.0104	-0.0789	-0.1082
1.1749	-0.1174	0.0270	-0.2099	-0.2416
1.6762	-0.2101	0.0201	-0.3445	-0.3302
2.1340	-0.2634	0.0273	-0.4915	-0.4811
2.5422	-0.3439	0.0667	-0.7932	-0.6376
2.8264	-0.3885	0.0508	-1.0886	-0.8061
3.3610	-0.4112	0.0537	-1.5058	-0.7227
3.8076	-0.4761	0.0675	-2.0295	-0.5328
4.4976	-0.5004	0.0858	-2.3721	-0.1350
4.8381	-0.4449	0.1460	-2.5553	-0.1701
5.3490	-0.5288	0.2026	-2.5438	-0.0692
6.0553	-0.5480	0.1492	-2.7252	-0.1455
6.7156	-0.5525	0.2641	-3.0159	0.0319
7.2239	-0.5997	0.2721	-2.9927	0.1218
7.6439	-0.5252	0.2958	-2.8818	0.1010
8.1999	-0.7263	0.2632	-3.2527	0.0157
8.8643	-0.6507	0.3819	-3.6644	0.1220
9.3481	-0.5919	0.4898	-3.8085	0.1408
10.0401	-0.7204	0.4939	-4.2689	0.2155
10.7318	-0.8080	0.5741	-4.8380	-0.0039
11.5118	-0.6446	0.5004	-4.1931	0.1339
12.2169	-0.9266	0.5278	-5.3736	-0.9529
13.5381	-0.9123	0.5972	-5.0555	-0.5152

U/nB	A2	A3	H2	H3
0.3687	-0.0026	0.2988	0.0242	0.4851
0.6795	-0.0079	0.3362	0.1083	0.5560
0.8910	-0.0205	0.3302	0.1712	0.5800
1.2746	-0.0403	0.3765	0.2617	0.6596
1.6274	-0.0570	0.3514	0.3428	0.7342
1.9453	-0.0668	0.3919	0.3472	0.8011
2.1707	-0.0677	0.4190	0.3525	0.8981
2.5834	-0.0678	0.5311	0.3464	1.1100
2.9347	-0.0870	0.5293	0.3760	1.4547
3.4596	-0.0643	0.6913	0.3887	1.9735
3.7524	-0.0505	0.7132	0.5963	2.2533
4.1597	-0.0304	0.8255	0.9085	2.6643
4.7316	0.0180	0.9436	1.0429	2.8902
5.2501	0.0592	1.0529	1.4588	3.2892
5.6651	0.0414	1.0199	1.5910	3.8178
6.0024	0.0608	1.1444	1.7566	3.9569
6.4952	0.0747	1.2149	2.0007	4.4855
7.0702	0.0677	1.2707	2.0485	5.0515
7.4702	0.0834	1.3865	2.3002	5.4353
8.0758	0.1227	1.5176	2.6741	6.2080
8.6857	0.2012	1.7291	2.8468	6.5797
9.3733	0.2328	1.8647	3.4822	7.6303
10.2549	0.2270	2.0982	3.0396	8.9558
11.4535	0.1966	2.5569	4.2804	10.2965

TABLE 6.6

GG50 4/26/13

U/nB	A1	A4	H1	H4
0.6978	-0.0765	-0.1383	-0.0923	0.0288
0.8494	-0.0858	-0.1222	-0.1547	-0.0582
1.1314	-0.1011	-0.1245	-0.2570	-0.1564
1.4604	-0.1582	-0.1539	-0.4385	-0.1394
2.0832	-0.2910	-0.1732	-0.6055	-0.3888
2.4480	-0.3436	-0.1512	-0.8377	-0.5650
2.7408	-0.4068	-0.1577	-1.1292	-0.7030
3.1559	-0.4534	-0.1555	-1.6800	-0.7647
3.9186	-0.5370	-0.1536	-2.5168	-0.6361
4.3446	-0.4400	-0.0425	-2.4561	-0.4493
4.7651	-0.4512	-0.0245	-2.6461	-0.2002
5.3736	-0.5239	-0.0036	-2.8722	-0.0270
6.0623	-0.5428	-0.0038	-2.8077	-0.2641
6.6822	-0.5061	0.1020	-3.2773	0.0702
7.1150	-0.5440	0.0336	-3.4329	-0.3548
7.6294	-0.5947	0.0429	-3.5046	-0.4102
8.3292	-0.5086	0.1168	-3.7954	-0.0640
8.7783	-0.5822	0.2606	-3.9689	0.7119
9.2668	-0.6095	0.3704	-4.6313	-0.0279
9.8223	-0.6464	0.4066	-4.8814	0.1633
10.5899	-0.6755	0.3293	-4.7494	0.1015
11.3938	-0.7337	0.4858	-4.4232	-0.1183
12.4997	-0.7006	0.3781	-6.0869	-0.9161
13.1028	-0.9870	0.0811	-7.4089	-2.3866

U/nB	A2	A3	H2	H3
0.5298	-0.0080	0.2557	0.0619	0.2474
0.6450	-0.0038	0.2968	0.1017	0.3374
0.8588	-0.0145	0.2940	0.1542	0.3238
1.1084	-0.0287	0.2772	0.1815	0.3826
1.5824	-0.0531	0.3039	0.3369	0.5487
1.8732	-0.0717	0.3434	0.3773	0.5768
2.1046	-0.0859	0.3844	0.3420	0.6651
2.4289	-0.1009	0.3928	0.3707	0.7714
3.0196	-0.0709	0.5422	0.1959	1.2038
3.3685	-0.0622	0.5287	0.3308	1.6457
3.6964	-0.0598	0.6222	0.4226	1.8890
4.1734	-0.0529	0.7277	0.7513	2.2739
4.7369	-0.0280	0.8002	0.9526	2.6476
5.2242	-0.0483	0.8356	1.1773	3.0825
5.5785	0.0052	0.9673	1.2212	3.1862
6.0195	0.0151	1.1034	1.4526	3.8304
6.6149	0.0569	1.2299	1.6603	4.5775
6.9312	0.0788	1.2916	1.7376	5.1160
7.3720	0.1150	1.3876	1.8665	5.1305
7.8837	0.1257	1.4549	2.2446	6.2979
8.5251	0.0582	1.4120	2.5723	7.0894
9.3627	0.1274	1.7707	3.1543	8.0194
10.4363	0.2813	2.0603	2.9924	10.2995
11.2122	0.3313	2.3684	1.9696	11.1380

TABLE 6.7

GG60 4/26/13

U/nB	A1	A4	H1	H4
0.5692	-0.0652	-0.2363	-0.0237	-0.0286
0.9675	-0.0838	-0.1913	-0.1085	-0.1356
1.1965	-0.1263	-0.2105	-0.2583	-0.1668
1.6725	-0.2545	-0.2539	-0.2999	-0.1772
2.1854	-0.3414	-0.2364	-0.4873	-0.5482
2.5580	-0.4265	-0.1839	-0.8034	-0.8521
2.7999	-0.4916	-0.1756	-1.1206	-1.0627
3.2552	-0.5121	-0.1504	-1.6991	-1.1107
3.7551	-0.4922	-0.1411	-2.3748	-0.8098
4.4821	-0.4750	-0.0157	-2.9440	-0.5009
4.8995	-0.4781	0.0816	-3.0623	-0.3953
5.4196	-0.5271	0.0506	-3.1519	-0.4928
6.0408	-0.4811	0.1006	-3.5146	-0.1343
6.6026	-0.5027	0.1582	-3.8634	0.0506
7.2467	-0.4218	0.2507	-4.0773	0.3455
7.8807	-0.5032	0.3007	-4.8688	0.1706
8.2857	-0.5291	0.2527	-4.2711	-0.1906
8.9282	-0.4950	0.2851	-4.4947	-0.0698
9.4502	-0.5648	0.3342	-5.2199	-0.4859
10.1338	-0.5586	0.3870	-4.8197	0.3541

U/nB	A2	A3	H2	H3
0.4313	0.0024	0.3297	0.0765	0.0774
0.7336	0.0040	0.3655	0.1318	0.1565
0.9075	-0.0080	0.3408	0.1662	0.1592
1.2650	-0.0437	0.2722	0.2694	0.3143
1.6764	-0.0952	0.2916	0.3554	0.3268
1.9710	-0.1129	0.3342	0.3766	0.3551
2.1665	-0.1143	0.3151	0.3600	0.4042
2.5313	-0.1058	0.4698	0.2130	0.5581
2.9319	-0.0681	0.6307	0.0745	0.9881
3.5019	-0.0220	0.6979	0.0924	1.4946
3.8416	-0.0144	0.7043	0.2953	1.8600
4.2506	0.0020	0.7512	0.3565	2.1722
4.7428	0.0576	0.8332	0.6054	2.6789
5.2038	0.0653	0.8434	0.6946	3.2365
5.7049	0.1096	1.0666	1.0044	3.9446
6.2408	0.1826	1.1339	0.9673	4.3654
6.6269	0.2499	1.2602	1.3645	4.8517
7.1491	0.2979	1.3518	1.6944	5.5509
7.6278	0.3491	1.5035	1.4984	6.1410
8.1596	0.4167	1.6325	2.1245	6.9037

TABLE 6.8

GG70 4/29/13

U/nB	A1	A4	H1	H4
0.4878	-0.0131	0.0009	-0.0848	0.0468
0.8602	-0.0735	0.0069	-0.1855	-0.0627
1.1547	-0.0831	0.0008	-0.3550	-0.0487
1.6718	-0.2187	-0.0156	-0.4123	-0.1106
2.0779	-0.3076	0.0119	-0.5279	-0.3767
2.5422	-0.4232	0.0701	-0.9295	-0.7262
2.9260	-0.4307	0.0492	-1.3993	-0.7919
3.3677	-0.5286	0.0992	-1.8871	-0.8563
3.8126	-0.5260	0.0967	-2.3502	-0.5106
4.4604	-0.5008	0.1606	-2.7026	-0.4767
4.9127	-0.5031	0.1945	-2.8347	-0.3451
5.4319	-0.4652	0.2187	-2.7798	-0.2302
6.1887	-0.5574	0.3756	-3.6238	0.1059
6.8971	-0.5159	0.3685	-3.6152	0.2342
7.2380	-0.5002	0.3621	-3.7331	0.3360
7.5899	-0.5301	0.3299	-3.6927	-0.2847
8.3575	-0.5026	0.3761	-4.5824	0.0556
8.7031	-0.5818	0.3763	-4.1100	0.1550
9.3477	-0.6213	0.4735	-4.2894	-0.0992

U/nB	A2	A3	H2	H3
0.3653	0.0074	0.3557	0.0072	0.1719
0.6457	-0.0077	0.3314	0.0761	0.2564
0.8687	0.0030	0.3817	0.0939	0.2591
1.2588	-0.0095	0.3927	0.2117	0.4171
1.5732	-0.0457	0.4415	0.3143	0.4449
1.9358	-0.0696	0.4767	0.3514	0.4972
2.2401	-0.0495	0.5719	0.2431	0.5868
2.5888	-0.0474	0.6476	0.1292	0.7273
2.9400	-0.0434	0.6907	0.1077	1.0519
3.4613	-0.0320	0.7593	0.1389	1.6275
3.8184	0.0011	0.8250	0.2518	1.9393
4.2283	0.0441	0.9252	0.4791	2.2786
4.8307	0.1140	1.0133	0.7156	2.8594
5.3927	0.1783	1.0910	0.9622	3.3357
5.6656	0.2064	1.1312	0.9685	3.6270
5.9954	0.2501	1.1584	1.0994	3.8737
6.6305	0.3095	1.3390	1.2566	4.9677
6.9081	0.3213	1.4082	1.4873	5.0206
7.4899	0.3707	1.5176	1.5800	5.6586

TABLE 6.9

GG80 4/29/13

U/nB	A1	A4	H1	H4
0.5902	-0.0154	-0.2427	-0.0810	0.0140
0.8210	-0.0694	-0.2547	-0.1257	-0.0289
1.1060	-0.0806	-0.2570	-0.2823	-0.1395
1.4875	-0.1656	-0.2933	-0.3570	-0.0669
2.0195	-0.3140	-0.2644	-0.4380	-0.5888
2.3871	-0.3757	-0.2246	-0.8126	-0.8772
2.6783	-0.4056	-0.2542	-1.1694	-1.0553
3.1249	-0.4849	-0.2413	-1.8889	-1.3052
3.7038	-0.4930	-0.2367	-2.6655	-0.8640
4.1887	-0.4099	-0.1092	-2.4469	-0.6071
4.6416	-0.3709	-0.0341	-3.1418	-0.2592
5.2097	-0.3743	0.0128	-3.2581	-0.1832
5.9562	-0.3535	0.0151	-3.3627	0.0467
6.4616	-0.3426	0.1179	-3.4213	0.1110
7.0829	-0.4104	0.1142	-4.0096	0.1216
7.5916	-0.3390	0.0968	-4.1114	0.0838
8.2362	-0.4104	0.0673	-4.4963	0.3108
8.6109	-0.2893	0.1353	-4.6418	0.2634
9.1967	-0.4957	0.1986	-5.2006	0.2021

U/nB	A2	A3	H2	H3
0.4400	0.0035	0.3537	-0.0217	-0.0675
0.6119	-0.0001	0.3586	0.0146	-0.0475
0.8253	-0.0053	0.3642	0.0319	0.0051
1.1057	-0.0174	0.3979	0.1193	0.0557
1.5078	-0.0628	0.3563	0.2668	0.1624
1.7938	-0.0925	0.3757	0.3117	0.1479
2.0212	-0.0964	0.4305	0.2928	0.1898
2.3701	-0.0779	0.4643	0.1609	0.2260
2.8112	-0.0447	0.5225	-0.0448	0.6136
3.2057	-0.0243	0.5518	-0.0082	1.1549
3.5176	-0.0047	0.6326	0.0478	1.6856
3.9565	0.0371	0.7271	0.2242	2.0116
4.5281	0.0660	0.8028	0.5131	2.5469
4.9484	0.0943	0.8542	0.7114	2.7714
5.4332	0.1581	0.8845	0.7760	3.2242
5.8199	0.1506	0.9725	0.9977	3.7772
6.3862	0.2007	1.0925	1.1900	4.6372
6.6631	0.2395	1.1428	1.3694	4.9581
7.1456	0.2596	1.2537	1.7481	5.5794

TABLE 6.10

APPENDIX 7
BRIDGE INPUT PARAMETERS
FINAL BRIDGE CONFIGURATION

Required for the analysis of the bridge performance in strong winds are the parameters that describe the dynamic response of the mechanical bridge system. These were obtained from DMJM Harris / AECOM for the final bridge configuration for a previous study (Ref 6).

For the numerical simulations performed in this study, wind load time histories were generated. at 30 locations along the bridge deck. Mode shape information at these 30 locations were extracted from the finite element model provided by DMJM Harris / AECOM and is presented here. For use in the numerical simulation procedure, the positive coordinate directions (non-standard) shown in Figure 7.1 were used. Furthermore, the mode shapes were renormalized such that for dominant sway modes, the maximum transverse deflection was set to 1.0; for dominant vertical modes, the maximum vertical deflection at the bridge centerline was set to 1.0; and for dominant torsional modes, the maximum vertical deflection at the bridge deck edge was set to 1.0.

The mechanical damping of for all modes of vibration for the bridge was assumed to be 0.006. This value was determined experimentally using a system identification procedure and motion data on the full-scale bridge (Ref 5).

The most significant 10 modes of vibration that are most likely to be excited by winds (i.e., those modes of vibration that had the highest percentage of total modal kinetic energy associated with deck sway, vertical motion, and torsional motion about a longitudinal axis) were included simultaneously in the numerical simulations. The parameters that describe these 10 modes of vibration, reformatted to the positive coordinate directions shown on Figure 7.1 and renormalized as described previously, are presented in the tables following Figure 7.1 (Tables 7.1 through 7.12).

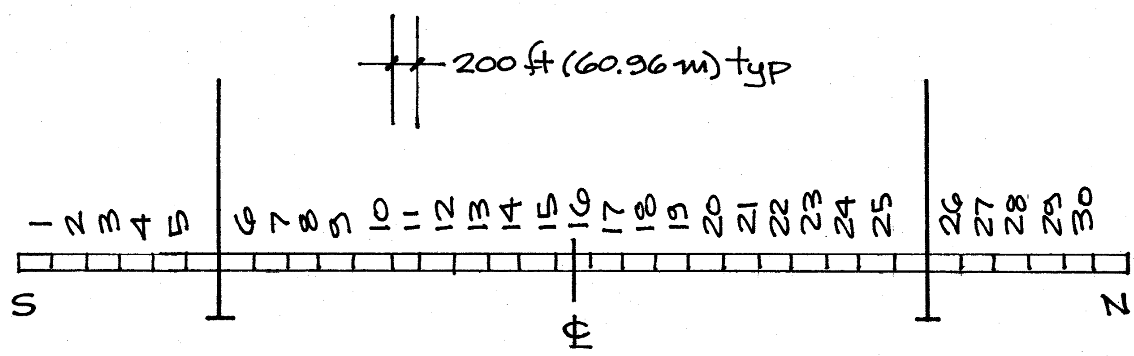

WEST WIND LABORATORY NODE NUMBERS

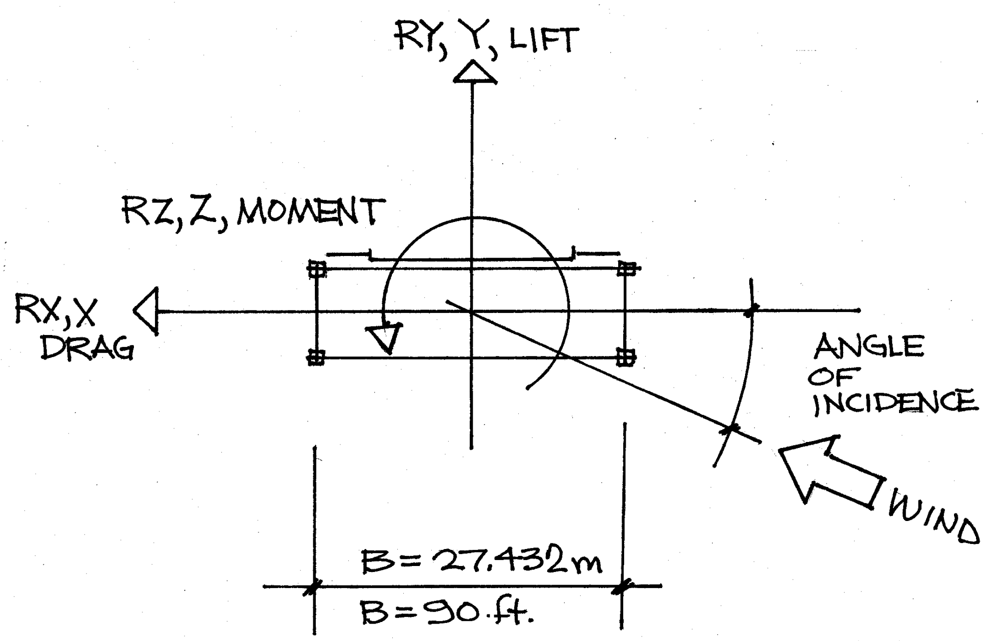

POSITIVE COORDINATE DIRECTIONS

FIGURE 7.1
POSITIVE COORDINATE DIRECTIONS FOR STATIC AERODYNAMIC COEFFICIENTS

WWL NODE	AECOM NODE
1	100580
2	101380
3	102180
4	102980
5	103780
6	105330
7	106130
8	106930
9	107730
10	108530
11	109330
12	110130
13	110930
14	111730
15	112530
16	212530
17	211730
18	210930
19	210130
20	209330
21	208530
22	207730
23	206930
24	206130
25	205330
26	203780
27	202980
28	202180
29	201380
30	200580

FIGURE 7.1 (Cont)
POSITIVE COORDINATE DIRECTIONS FOR STATIC AERODYNAMIC COEFFICIENTS

GOLDEN GATE BRIDGE 4/26/13

B(M)= 27.432
NUMBER OF MODES= 10
NUMBER OF NODES= 30

NODE	DL(M)	M(KG/M)	MMI(KG*M^2/M)
1	60.96	29123	4.168E+06
2	60.96	29123	4.168E+06
3	60.96	29123	4.168E+06
4	60.96	29123	4.168E+06
5	60.96	29123	4.168E+06
6	60.96	29123	4.168E+06
7	60.96	29123	4.168E+06
8	60.96	29123	4.168E+06
9	60.96	29123	4.168E+06
10	60.96	29123	4.168E+06
11	60.96	29123	4.168E+06
12	60.96	29123	4.168E+06
13	60.96	29123	4.168E+06
14	60.96	29123	4.168E+06
15	60.96	29123	4.168E+06
16	60.96	29123	4.168E+06
17	60.96	29123	4.168E+06
18	60.96	29123	4.168E+06
19	60.96	29123	4.168E+06
20	60.96	29123	4.168E+06
21	60.96	29123	4.168E+06
22	60.96	29123	4.168E+06
23	60.96	29123	4.168E+06
24	60.96	29123	4.168E+06
25	60.96	29123	4.168E+06
26	60.96	29123	4.168E+06
27	60.96	29123	4.168E+06
28	60.96	29123	4.168E+06
29	60.96	29123	4.168E+06
30	60.96	29123	4.168E+06

TABLE 7.1

GOLDEN GATE BRIDGE 4/26/13

WWL MODE	DMJM MODE	WR(RPS)	DR	MT	MRAT
1	1	0.306	0.006	1.000	0.849
2	2	0.542	0.006	2.000	0.501
3	3	0.702	0.006	1.000	1.000
4	4	0.808	0.006	2.000	0.795
5	5	0.836	0.006	2.000	0.271
6	6	1.029	0.006	2.000	0.773
7	7	1.153	0.006	3.000	0.730
8	8	1.230	0.006	1.000	0.813
9	9	1.244	0.006	2.000	0.728
10	10	1.278	0.006	1.000	0.930

MT=1 FOR SWAY, 2 FOR VERTICAL, 3 FOR TORSION
MRAT IS THE RATIO OF GENERALIZED MASS ASSOCIATED WITH DECK MOTION
TO THE TOTAL GENERALIZED MASS

TABLE 7.2

GOLDEN GATE BRIDGE 4/26/13

WWL MODE 1
DMJM MODE 1

NODE	RX	RY	RZ
1	-0.0004	0.0000	0.0000
2	-0.0009	0.0000	0.0000
3	-0.0013	0.0000	0.0000
4	-0.0015	0.0000	0.0000
5	-0.0016	0.0000	0.0000
6	-0.1461	0.0000	0.0000
7	-0.3033	0.0000	0.0000
8	-0.4506	0.0000	-0.0001
9	-0.5844	0.0000	-0.0001
10	-0.7023	0.0000	-0.0002
11	-0.8022	0.0000	-0.0002
12	-0.8827	0.0000	-0.0002
13	-0.9424	0.0000	-0.0001
14	-0.9813	0.0000	-0.0001
15	-1.0000	0.0000	0.0000
16	-1.0000	0.0000	0.0000
17	-0.9814	0.0000	-0.0001
18	-0.9426	0.0000	-0.0002
19	-0.8830	0.0000	-0.0002
20	-0.8025	0.0000	-0.0002
21	-0.7025	0.0000	-0.0002
22	-0.5843	0.0000	-0.0001
23	-0.4503	0.0000	-0.0001
24	-0.3031	0.0000	0.0000
25	-0.1459	0.0000	0.0000
26	-0.0015	0.0000	0.0000
27	-0.0014	0.0000	0.0000
28	-0.0012	0.0000	0.0000
29	-0.0008	0.0000	0.0000
30	-0.0003	0.0000	0.0000

TABLE 7.3

GOLDEN GATE BRIDGE 4/26/13

WWL MODE 2
DMJM MODE 2

NODE	RX	RY	RZ
1	0.0001	0.0254	0.0000
2	0.0001	0.0535	0.0000
3	0.0000	0.0642	0.0000
4	0.0000	0.0573	0.0000
5	0.0000	0.0334	0.0000
6	0.0000	0.2809	0.0000
7	-0.0001	0.5575	0.0000
8	-0.0001	0.7770	0.0000
9	0.0000	0.9262	0.0000
10	-0.0001	0.9951	0.0000
11	0.0000	0.9772	0.0000
12	-0.0001	0.8732	0.0000
13	0.0000	0.6896	0.0000
14	0.0000	0.4406	0.0000
15	0.0000	0.1487	0.0000
16	0.0000	-0.1579	0.0000
17	0.0001	-0.4495	0.0000
18	0.0001	-0.6978	0.0000
19	0.0002	-0.8806	0.0000
20	0.0003	-0.9834	0.0000
21	0.0003	-1.0000	0.0000
22	0.0002	-0.9299	0.0000
23	0.0001	-0.7794	0.0000
24	0.0001	-0.5588	0.0000
25	0.0000	-0.2813	0.0000
26	0.0000	-0.0329	0.0000
27	0.0000	-0.0564	0.0000
28	0.0000	-0.0633	0.0000
29	0.0000	-0.0526	0.0000
30	0.0000	-0.0250	0.0000

TABLE 7.4

GOLDEN GATE BRIDGE 4/26/13

WWL MODE 3
DMJM MODE 3

NODE	RX	RY	RZ
1	-0.0011	0.0000	0.0001
2	-0.0023	0.0000	0.0001
3	-0.0031	0.0000	0.0001
4	-0.0034	0.0000	0.0001
5	-0.0032	0.0000	0.0000
6	-0.2843	0.0000	0.0007
7	-0.5664	0.0001	0.0007
8	-0.7893	-0.0001	0.0007
9	-0.9352	0.0000	0.0005
10	-0.9951	0.0000	0.0004
11	-0.9660	-0.0001	0.0003
12	-0.8528	-0.0001	0.0001
13	-0.6658	-0.0001	0.0000
14	-0.4231	-0.0002	-0.0001
15	-0.1467	-0.0003	-0.0003
16	0.1418	-0.0001	-0.0004
17	0.4208	-0.0001	-0.0004
18	0.6662	0.0000	-0.0003
19	0.8557	0.0000	-0.0002
20	0.9704	0.0001	-0.0001
21	1.0000	0.0001	-0.0002
22	0.9393	0.0001	-0.0004
23	0.7921	0.0001	-0.0005
24	0.5681	0.0001	-0.0007
25	0.2849	0.0001	-0.0006
26	0.0029	0.0000	0.0000
27	0.0030	0.0000	-0.0001
28	0.0028	0.0000	-0.0001
29	0.0021	0.0000	-0.0001
30	0.0010	0.0000	0.0000

TABLE 7.5

GOLDEN GATE BRIDGE 4/26/13

WWL MODE 4
DMJM MODE 4

NODE	RX	RY	RZ
1	0.0003	0.1316	0.0000
2	0.0003	0.2810	0.0000
3	0.0003	0.3397	0.0000
4	0.0002	0.3019	0.0000
5	0.0001	0.1743	0.0000
6	0.0000	0.1171	0.0000
7	0.0000	0.1911	0.0000
8	0.0000	0.1798	0.0000
9	0.0001	0.0826	0.0000
10	0.0001	-0.0863	0.0000
11	0.0001	-0.3035	0.0000
12	0.0001	-0.5373	0.0000
13	0.0000	-0.7526	0.0000
14	-0.0001	-0.9157	0.0000
15	-0.0001	-1.0000	0.0000
16	0.0004	-0.9920	0.0000
17	0.0003	-0.8922	0.0000
18	0.0001	-0.7158	0.0000
19	0.0000	-0.4906	0.0000
20	-0.0001	-0.2516	0.0000
21	-0.0003	-0.0343	0.0000
22	-0.0003	0.1297	0.0000
23	-0.0001	0.2178	0.0000
24	-0.0001	0.2171	0.0000
25	0.0000	0.1297	0.0000
26	0.0001	0.1678	0.0000
27	0.0001	0.2905	0.0000
28	0.0001	0.3268	0.0000
29	0.0002	0.2703	0.0000
30	0.0001	0.1265	0.0000

TABLE 7.6

GOLDEN GATE BRIDGE 4/26/13

WWL MODE 5
DMJM MODE 5

NODE	RX	RY	RZ
1	0.0003	0.1121	0.0000
2	0.0003	0.2396	0.0000
3	0.0002	0.2899	0.0000
4	0.0002	0.2575	0.0000
5	0.0001	0.1484	0.0000
6	0.0000	-0.2509	0.0000
7	0.0001	-0.5174	0.0000
8	0.0002	-0.7477	0.0000
9	0.0001	-0.9115	0.0000
10	0.0001	-0.9845	0.0000
11	0.0000	-0.9537	0.0000
12	0.0001	-0.8220	0.0000
13	0.0000	-0.6054	0.0000
14	-0.0001	-0.3310	0.0000
15	-0.0002	-0.0287	0.0000
16	-0.0003	0.2734	0.0000
17	-0.0006	0.5499	0.0000
18	-0.0007	0.7769	0.0000
19	-0.0009	0.9327	0.0000
20	-0.0009	1.0000	0.0000
21	-0.0009	0.9733	0.0000
22	-0.0007	0.8585	0.0000
23	-0.0003	0.6747	0.0000
24	-0.0002	0.4493	0.0000
25	-0.0001	0.2117	0.0000
26	-0.0001	-0.1914	0.0000
27	-0.0001	-0.3320	0.0000
28	-0.0002	-0.3736	0.0000
29	-0.0002	-0.3088	0.0000
30	-0.0001	-0.1443	0.0000

TABLE 7.7

GOLDEN GATE BRIDGE 4/26/13

WWL MODE 6
DMJM MODE 6

NODE	RX	RY	RZ
1	0.0007	0.2673	0.0000
2	0.0008	0.5797	0.0000
3	0.0007	0.7064	0.0000
4	0.0005	0.6265	0.0000
5	0.0002	0.3581	0.0000
6	0.0000	-0.3399	0.0000
7	0.0001	-0.6736	0.0000
8	0.0001	-0.9080	0.0000
9	-0.0001	-0.9962	0.0000
10	-0.0001	-0.9206	0.0000
11	-0.0001	-0.6961	0.0000
12	-0.0001	-0.3728	0.0000
13	0.0000	-0.0233	0.0000
14	0.0001	0.2700	0.0000
15	0.0002	0.4362	0.0000
16	-0.0007	0.4358	0.0000
17	-0.0005	0.2687	0.0000
18	-0.0001	-0.0255	0.0000
19	0.0002	-0.3758	0.0000
20	0.0005	-0.6997	0.0000
21	0.0006	-0.9245	0.0000
22	0.0006	-1.0000	0.0000
23	0.0002	-0.9111	0.0000
24	0.0002	-0.6757	0.0000
25	0.0001	-0.3408	0.0000
26	0.0001	0.3625	0.0000
27	0.0002	0.6340	0.0000
28	0.0003	0.7149	0.0000
29	0.0003	0.5866	0.0000
30	0.0002	0.2705	0.0000

TABLE 7.8

GOLDEN GATE BRIDGE 4/26/13

WWL MODE 7
DMJM MODE 7

NODE	RX	RY	RZ
1	0.0027	0.0000	-0.0003
2	0.0049	0.0000	-0.0006
3	0.0059	0.0000	-0.0007
4	0.0058	0.0000	-0.0006
5	0.0045	0.0000	-0.0004
6	-0.1171	0.0001	0.0221
7	-0.1827	0.0000	0.0412
8	-0.2264	0.0004	0.0568
9	-0.2438	0.0001	0.0677
10	-0.2375	-0.0002	0.0729
11	-0.2111	-0.0002	0.0718
12	-0.1692	-0.0002	0.0645
13	-0.1160	-0.0001	0.0517
14	-0.0571	0.0005	0.0346
15	0.0030	0.0015	0.0145
16	0.0507	0.0007	-0.0072
17	0.0865	0.0003	-0.0286
18	0.1138	0.0001	-0.0474
19	0.1335	0.0001	-0.0618
20	0.1467	0.0001	-0.0704
21	0.1549	0.0001	-0.0725
22	0.1570	0.0001	-0.0678
23	0.1486	0.0002	-0.0572
24	0.1243	0.0000	-0.0417
25	0.0875	0.0000	-0.0223
26	-0.0008	-0.0001	-0.0003
27	-0.0008	-0.0002	-0.0004
28	-0.0006	-0.0003	-0.0005
29	-0.0002	-0.0002	-0.0004
30	0.0003	-0.0001	-0.0002

TABLE 7.9

GOLDEN GATE BRIDGE 4/26/13

WWL MODE 8
DMJM MODE 8

NODE	RX	RY	RZ
1	0.0608	0.0000	-0.0103
2	0.0982	0.0001	-0.0194
3	0.1124	0.0004	-0.0228
4	0.1052	0.0005	-0.0205
5	0.0756	0.0006	-0.0128
6	-0.3503	0.0001	-0.0012
7	-0.6804	0.0002	-0.0002
8	-0.8943	0.0001	0.0049
9	-0.9601	-0.0004	0.0140
10	-0.8780	-0.0009	0.0260
11	-0.6736	-0.0012	0.0399
12	-0.3958	-0.0012	0.0540
13	-0.1041	-0.0008	0.0669
14	0.1376	-0.0006	0.0769
15	0.2742	-0.0003	0.0832
16	0.2786	0.0001	0.0850
17	0.1453	0.0005	0.0819
18	-0.1002	0.0007	0.0741
19	-0.4021	0.0008	0.0625
20	-0.6935	0.0006	0.0487
21	-0.9111	0.0003	0.0344
22	-1.0000	-0.0002	0.0214
23	-0.9320	-0.0005	0.0111
24	-0.7094	-0.0005	0.0043
25	-0.3672	-0.0003	0.0012
26	0.0770	0.0002	-0.0131
27	0.1074	-0.0002	-0.0210
28	0.1149	-0.0004	-0.0233
29	0.1005	-0.0005	-0.0198
30	0.0622	-0.0003	-0.0105

TABLE 7.10

GOLDEN GATE BRIDGE 4/26/13

WWL MODE 9
DMJM MODE 9

NODE	RX	RY	RZ
1	0.0011	0.3666	0.0000
2	0.0014	0.8117	0.0000
3	0.0013	1.0000	0.0000
4	0.0010	0.8854	0.0000
5	0.0005	0.5005	0.0000
6	0.0001	0.0469	0.0000
7	0.0003	0.0835	0.0000
8	0.0003	0.0915	0.0000
9	0.0004	0.0704	0.0000
10	0.0004	0.0289	0.0000
11	0.0003	-0.0190	0.0000
12	0.0001	-0.0572	0.0000
13	0.0000	-0.0724	0.0000
14	-0.0001	-0.0591	0.0000
15	-0.0002	-0.0227	0.0000
16	-0.0002	0.0226	0.0000
17	-0.0002	0.0590	0.0000
18	0.0000	0.0721	0.0000
19	0.0001	0.0568	0.0000
20	0.0003	0.0185	0.0000
21	0.0004	-0.0295	0.0000
22	0.0005	-0.0710	0.0000
23	0.0004	-0.0919	0.0000
24	0.0003	-0.0838	0.0000
25	0.0001	-0.0470	0.0000
26	-0.0002	-0.4968	0.0000
27	-0.0004	-0.8790	0.0000
28	-0.0005	-0.9928	0.0000
29	-0.0005	-0.8061	0.0000
30	-0.0003	-0.3642	0.0000

TABLE 7.11

GOLDEN GATE BRIDGE 4/26/13

WWL MODE 10
DMJM MODE 10

NODE	RX	RY	RZ
1	0.0585	-0.0004	-0.0095
2	0.0960	-0.0008	-0.0179
3	0.1106	-0.0008	-0.0210
4	0.1035	-0.0006	-0.0189
5	0.0740	-0.0001	-0.0118
6	0.4239	0.0008	-0.0019
7	0.7931	0.0012	0.0010
8	0.9919	0.0016	0.0079
9	0.9917	0.0009	0.0178
10	0.8015	-0.0001	0.0297
11	0.4594	-0.0009	0.0421
12	0.0320	-0.0015	0.0537
13	-0.3981	-0.0017	0.0635
14	-0.7451	-0.0012	0.0706
15	-0.9370	-0.0003	0.0741
16	-0.9374	0.0007	0.0738
17	-0.7448	0.0016	0.0696
18	-0.3954	0.0020	0.0621
19	0.0383	0.0016	0.0521
20	0.4688	0.0008	0.0403
21	0.8116	-0.0003	0.0279
22	1.0000	-0.0013	0.0160
23	0.9976	-0.0019	0.0062
24	0.7972	-0.0016	-0.0003
25	0.4264	-0.0009	-0.0026
26	0.0738	0.0007	-0.0121
27	0.1037	0.0008	-0.0193
28	0.1110	0.0007	-0.0215
29	0.0967	0.0004	-0.0183
30	0.0591	0.0001	-0.0097

TABLE 7.12

APPENDIX 8
REFERENCES

1. Simiu, E., and Scanlan, R. H. *Wind Effects on Structures,* Third Edition, John Wiley & Sons, New York, 1996.

2. Yinghong Cao, Haifan Xiang, and Ying Zhou, "Simulation of Stochastic Wind Velocity Field on Long-Span Bridges", *Journal of Engineering Mechanics*, Vol. 126, No. 1, ASCE, January, 2000

3. Xinzhong Chen, Masaru Matsumoto, and Ahsan Kareem, "Time Domain Flutter and Buffeting Response Analysis of Bridges", *Journal of Engineering Mechanics*, Vol. 126, No. 1, ASCE, January, 2000

4. British Highways Agency, Design Manual for Roads and Bridges, BD 37/01, Loads for Highway Bridges and BD 49/01 Rules for Aeroedynamic Effects on Bridges.

.5. "Section Model Wind Tunnel Studies, Golden Gate Bridge Seismic and Wind Retrofit, San Franciso, California", West Wind Laboratory, Inc., June 1995.

.6. "Wind Study, Golden Gate Bridge, Horizontal Net Suicide Deterrent System, San Francisco, California", West Wind Laboratory, Inc., Januaray 2009, Revised January 2011.

7. Wind Study, Golden Gate Bridge, Simplified Aerodynamic Enhancements", West Wind Laboratory, Inc., August 23, 2012, Revised August 27, 2012, Revised October 10, 2012.

8. "A Study of Wind Data and Topographic Effects for Golden Gate Bridge", Report 93-144F-5-1, RWDI, Guelph, Ontario, November 19, 1993.

9. U. S. Department of Agriculture (NRCS) Natural Resources Conservation Service, www.wcc.nrcs.usda.gov/climate/windrose.html

10. Liu, Henry, *Wind Engineering, A Handbook for Structural Engineers*, Prentice Hall, Englewood Cliffs, New Jersey, 1991.